

A novel biomass reactor addressing the people's need for renewable energy in the developing world

*Master of Science Dissertation
in Mechanical Engineering
by D. A. Quan Reyes*

A thesis submitted to the Delft University of Technology in partial fulfillment of the requirements for
the degree of

Master of Science in Mechanical Engineering

by

D.A. Quan Reyes
born in Guatemala

October 2020

Graduation committee:

<i>Supervisor:</i> Professor. dr. Dirk Roekaerts	Delft University of Technology
Asst. Prof. dr. Domenico Lahaye	Delft University of Technology
Asst. Prof. dr. ir. Nijso Beishuizen	Eindhoven University of Technology

Thesis to be defended on October 30th, 2020

Thesis title: *A novel biomass reactor addressing the people's need for renewable energy in the developing world*

Author: Diego Alejandro Quan Reyes

Student number: 4818644

P&E report number: 3033

Department of Process & Energy, Delft University of Technology



Citation: Quan Reyes, D. (2020), *A novel biomass reactor addressing the people's need for renewable energy in the developing world*. Master thesis, Delft University of Technology.

Copyright©2020 by Diego Alejandro Quan Reyes All rights reserved. No part of the material protected by this copyright notice may be reproduced or utilized in any form or by any means, electronic or mechanical, including photocopying, recording or by any information storage and retrieval system, without the prior permission of the author.

Cover design by *Studio DOSIS*

Picture by D.A. Quan Reyes

This thesis is confidential and cannot be made public until 20/10/2022

To the legacy of Isabel Gutiérrez de Bosch

Contents

List of Figures	vii
List of Tables	ix
Abstract	xi
Acknowledgements	xiii
1 Motivation	1
2 Introduction	7
1 The urgent need to replace the fossil fuel based development model	8
1.1 The current world situation	8
1.2 Inequality and climate change	9
2 The energy needs of one third of the world population	11
2.1 A call for new development model	11
3 The current state of biomass cooking technology	15
1 The state of improved cookstoves and the evaluation protocols	16
1.1 Available cooking technologies	16
1.2 General features of improved cookstoves	21
1.3 Performance evaluation protocols	22
1.4 Recent integral protocols	24
2 Emissions: an overlooked and poorly understood problem	25
2.1 Emissions from biomass combustion	25
2.2 The measurement problem	26
2.3 Possible technical solutions	28
2.4 Conclusions	29
4 "The Kulkan", a novel biomass reactor with increased efficiency by heat recovery and combustion optimization	31
1 Kulkan, a novel biomass reactor	32
1.1 Hypotheses	33
2 Validation approach	41
5 The thermochemical phenomena in biomass conversion as an energy source and its mathematical modeling	43
1 Biomass	44
2 Biomass thermochemical conversion	44
3 State of the art in biomass thermochemical conversion modeling	44
4 Modeling of the gas-phase combustion	46
5 Numerical solutions	50
6 Conclusions	50
6 Proving Hypothesis 1: Heat recovery by an air pre-heater	53
1 Algebraic model: Gasifier	56
2 Algebraic model: Combustor and heat-exchanger	59
2.1 Driving force	59
2.2 Combustor analysis	60
2.3 Heat-exchanger analysis	61
3 Algebraic model: Air pre-heater	63
4 Strategy for solving the algebraic model	65
5 Results and discussion	66

7	Proving Hypothesis 2: Premixed laminar flame	71
1	Flame quenching prevention	72
1.1	Flame quenching by heat loss	72
1.2	Flame quenching by stretching.	73
2	Auxiliary hypothesis: feasible laminar flame speed	73
3	2D Model validation	76
3.1	Model reconstruction	77
3.2	Alternative chemical mechanisms	79
3.3	Results and discussion	80
8	3D numerical simulation of heat and flow in the <i>Kulkan</i> reactor	85
1	Mesh.	86
2	Non reactive flow simulation	89
2.1	Turbulence models: <i>k-epsilon</i> vs <i>k-epsilon RNG</i>	89
2.2	Effect of hot-chimney wall	91
3	Reactive flow simulation	94
3.1	System with a secondary air-inlet	94
3.2	System with primary air only	96
9	Argumentation on the hypothesis 3: Alkali fly-ash prevention	101
1	Alternative measure of the harmfulness	102
2	Ultra-fine particle prevention	102
10	Conclusions	105
11	Recommendations	109
A	Appendix	113
1	Solid phase thermochemical conversion of biomass	114
1.1	Drying	114
1.2	Torrefaction	115
1.3	Pyrolysis	115
1.4	Gasification	115
1.5	Solid phase combustion.	116
1.6	Modeling approach for the "fuel bed" processes	117
1.7	Criteria for the best fit model	118
2	2D chemical mechanism comparison.	118
3	Alternative turbulence and combustion models	121
4	Chemical mechanisms	125
4.1	2 steps global syngas mechanism.	125
4.2	21 steps skeletal syngas mechanism	125

List of Figures

1.1	The problem of energy access	2
1.2	Community Based Participatory Research	3
1.3	<i>The hydrogen stove</i>	4
1.4	5 of the 7 top tier technologies investigated	5
2.1	Pathway to carbon neutrality by 2040	8
2.2	CO_2 emissions vs Human Development Index	10
2.3	Scale of energy needs for sustainable development	12
3.1	Open Fire with traditional <i>comal</i> on top	16
3.2	Flat iron top cookstove	17
3.3	Schematic of a Rocket stove	18
3.4	Rocket stove prototypes	19
3.5	Schematic of a Rocket stove	20
3.6	Number of ultra fine particles and particle mass emitted per unit of useful energy	23
3.7	Mass of CO and $PM_{2.5}$ per unit of useful energy	23
3.8	Comparison of emission factors	25
3.9	Particle deposition in the respiratory system	27
3.10	Soot formation process	28
3.11	Emissions number density and aerodynamic diameter from three combustions regimes	29
4.1	Hypothesis map	34
4.2	Kulkan design 1: partially premixed laminar combustion	35
4.3	Kulkan design 2: non-premixed turbulent combustion	36
4.4	Kulkan design 3: non-premixed laminar combustion	37
4.5	Detailed conceptual drawing of the Kulkan's gasifier and burner for laminar combustion	39
4.6	Detailed conceptual drawing of the Kulkan's gasifier and burner for turbulent combustion	40
6.1	Heat balance schematic	55
6.2	Gasifier energy balance schematic	56
6.3	Derivation of the chimney equation	59
6.4	Validation model: flame temperature vs syngas power output	62
6.5	Validation model: flue gas mass flow vs syngas power output	63
6.6	Graphical summary of the inputs and outputs of each sub-system	66
6.7	Efficiency map for different configurations	68
6.8	Comparison of the two models and the experimental data, flame temperature	69
6.9	Comparison of the two models and the experimental data, total mass flow-rate	69
7.1	CO_2 reaction rate according to the Slavinskaya et.al., 2-step mechanism	73
7.2	Laminar Flame Speed	74
7.3	Laminar Flame Speed of updraft syngas at high inlet temperatures	75
7.4	Experimental set-up and geometry for CFD study of (Pundle et al., 2019)	76
7.5	Comparison between reconstructed model and (Pundle et al., 2019)	77
7.6	Comparison between reconstructed model and (Pundle et al., 2019)	78
7.7	Comparison between reconstructed model and (Pundle et al., 2019)	78
7.8	CO mass fraction for a premixed laminar flame, $\phi = 8.5$	80
7.9	Reaction rate of H_2O for a premixed laminar flame, $\phi = 8.5$	81
7.10	Reaction rate of CO_2 for a premixed laminar flame, $\phi = 8.5$	82
7.11	Radially integrated CO mass fraction	82

7.12	Radially integrated distribution along the axis	83
8.1	Geometry and mesh for the <i>Kulkan's</i> 3-D simulation. Plane cut at $y = 0$	87
8.2	Close-up views of the burner	88
8.3	3-D contour plot of velocity magnitude. Plane cut $y = 0$	89
8.4	3-D contour plot of total pressure. Plane cut $y = 0$	90
8.5	3-D contour plot of static temperature. Plane cut $y = 0$	90
8.6	Flat contour plot of density. Plane cut $y = 0$	91
8.7	3-D contour plot of \hat{z} velocity. Plane cut $y = 0$	92
8.8	3-D contour plot of total pressure. Plane cut $y = 0$	92
8.9	3-D contour plot of static temperature. Plane cut $y = 0$	93
8.10	3-D contour plot of density. Plane cut $y = 0$	93
8.11	3-D Contour plot of O_2 Mass Fraction. Plane cuts $y = 0$ and $x = 0$	94
8.12	3-D Contour plot of CO and O_2 Mass Fraction. Pane cuts $y = 0$ and $x = 0$	95
8.13	3-D Contour plot of OH Mass Fraction. Plane cuts $y = 0$ and $x = 0$	95
8.14	3-D Contour plot of temperature. Plane cuts $y = 0$ and $x = 0$	96
8.15	3-D Contour plot of CO_2 reaction rate. Plane cuts $y = 0$ and $x = 0$	97
8.16	3-D Contour plot O_2 and CO mass fractions. Plane cuts $y = 0$ and $x = 0$	97
8.17	Close up of the temperature at the burner. Plane cuts $y = 0$ and $x = 0$	98
8.18	Pressure drop of non-reactive versus reactive flow simulations. Plane cuts at $y = 0$	99
A.1	Axial Velocity	119
A.2	Hydrogen mass fraction	119
A.3	Volumetric emitted radiation	120
A.4	H ₂ O reaction rate	120
A.5	Axial velocity	121
A.6	Temperature	122
A.7	CO ₂ Mass fraction	122
A.8	O ₂ Mass Fraction	123
A.9	Temperature	123
A.10	H ₂ Mass Fraction	124
A.11	CO ₂ Mass Fraction	124

List of Tables

3.1	Biomass cooking technologies	20
3.2	IWA performance Tiers	21
4.1	Specific and common technical aspects of each conceptual Kulkan version	38
6.1	Pressure loss coefficients, area and density ratios	64
6.2	Optimal configuration for fire powers of [2.5 - 4.0] kW	66
6.3	Outputs of the algebraic model	68
7.1	Syngas Composition [% by volume] (Oliveira et al., 2020)	74
8.1	Burner elements and their functions	88

Abstract

The current economic-development system based on fossil fuels can no longer sustain itself and is incapable of satisfying the needs of the global population. Nearly one third are unable to meet even their most basic needs that involve harnessing energy for everyday essential tasks such as maintaining livable shelter and food preparation.

Models of *development* have exacerbated the problem by promoting and subsidizing fossil fuel based solutions that require those struggling to survive to do so at the expense of the environment and other species. This is a self-defeating trap, whereby the urgent needs of the most vulnerable are pitted against climate change and the mass extinction of complex life forms. The only way to break this contradiction is through the creation of a new development system that removes incentives for short-term, destructive profit and puts people and other forms of life at its center. Healthy, sustainable development must be rooted in the fair and democratic allocation of resources. Prioritization of truly life-focused progress would allow for human beings to shape their own destinies through the use of locally available, renewable energy resources that do not contribute to mass extinction or climate catastrophe.

While the downward spiral towards extinction may seem unstoppable, in reality, the biggest obstacle is simply coming to accept that the old view of what constitutes positive development – an extractive, hierarchical philosophy powered by fossil fuels - must be replaced with the new paradigm based on sustainability and cultural realism. Once that understanding has been reached, it is a matter of targeting key areas for change that will make the most difference in the shortest amount of time. The project outlined herein is a contribution to that new development system. My carefully selected target will address the energy needs for clean cooking and heating for the one third of the world population that relies on low-efficiency biomass combustion technology. Although such technology may at first seem too modest to make a difference, the impacts of making this simple change would have profound, world-wide implications. If that vulnerable one third of the world's population could access clean domestic technology, there would be enormous improvements in health and environmental conditions.

The *Kulkan* reactor is a biomass gasifier coupled to a burner that optimizes the combustion process and heat transfer by means of heat recovery using an air pre-heater and partially premixed laminar combustion of the syngas. The novel design was founded on three hypotheses that addressed the optimization of efficiency, pollution minimization by flame quenching prevention, and reduction of ultra-fine alkali particle emissions. The first two were investigated using an algebraic model (0-D), and computational fluid dynamics of reacting flow for 1-D, 2-D and 3-D. The algebraic model predicts an efficiency of [60 – 65%] which is 4-8 times higher than traditional cooking technology and 25% higher than the best improved cookstove ever reported. The 1-D and 2-D simulations show reduction feasibility of laminar pre mixed combustion and a reduction of flame length of up to 50% compared to non-premixed, supporting the idea of more compact combustion chambers and prevention of flame quenching.

The 3-D simulations show essential information on the importance of the pressure drop calculations necessary for the design process of a *Kulkan* reactor, particularly for the burner. Furthermore, arguments for the third hypothesis are presented which invite further investigation to reduce the ultra-fine particles containing highly toxic alkali metals, which are produced during high efficiency biomass combustion.

Acknowledgements

Special thanks to:

Professor Dirk Roekaerts for the incredible mentoring, and for keeping the flame of scientific curiosity lit.

Professor Burak Eral for the unconditional support for all my projects, the *GETI*, emergency ventilator for *COVID-19* patients, among others.

My family for the constant, unconditional support and love, even at the distance.

The *Fundación Juan Bautista Gutiérrez* for believing in my "causes" and supporting me in the process of making them a reality.

The *Quantum Energy Team* for the trust, dedication, and commitment for making this world a more just and beautiful place.

My friends in The Netherlands and around, who made my "Delft" experience so rich and transforming, and to my friends in Guatemala, who allowed me to stay so rooted, a warm and sincere greeting.

Motivation

May all rise up, may all be called,
may no one, not one or two groups
be left behind

Popol Vuh, Mayan - K'iche's sacred book



1

¹Life on Earth is undergoing dramatic, rapid and irreversible change. Human actions such as the use of fossil fuels, deforestation and resource extraction have combined to become the driving force of evolution and extinction. Since 1970, the resultant habitat destruction has wiped out a staggering 60% of vertebrate animal species. People are also being driven from their communities as changes in climate make it impossible for them to farm or gather food. Extractive industries and agricultural corporations exacerbate this problem as they claim and destroy, fields, forests and water sources in the name of *development*.

The Merriam Webster dictionary says that to develop is “to make visible or manifest.” Interestingly, it defines the word *development* as “a tract of land that has been made available or usable.” These two definitions combine to give insight into the privileged perspective of those who profit from the displacement, destruction and extraction that generate what we recognize as development. As defined here, the act becomes an almost biblical duty to take unavailable or unusable land (a development), and make it visible and manifest (develop) in the form of profit. Without the transformative magic of development, millennia of independent subsistence, culture and history of undeveloped societies are invisible and worthless. Developed entities in the position to undertake these noble missions are viewed as heroes working to save the one third of the world’s population trapped unaware in their pitiful state of underdevelopment.

Figure 1.1: The problem of energy access



(a) Kids carrying wood for cooking



(b) A typical house with the roof and walls covered with emissions

While this may have been the popular narrative since European colonization began, we now understand that these actions are transactional, undertaken for profit. If there is local support for development projects, it is usually obtained through assurances that a profit-making enterprise, though potentially disruptive in the short-term, will ultimately benefit the greater population through mechanisms such as increased employment. Nations already claiming the status bring great pressure to bear on those living in under-developed conditions, as many are vulnerable and have difficulty in meeting their most basic needs, like obtaining food, clean water, or energy. In the end, we also know that these enterprises are fleeting. Inevitably, the majority of these profits are extracted from under-developed areas and removed to developed ones. The cycle will be repeated until there is no more profit to be wrung from the land and people.

The current one-sided development model is based on irrational consumption and is heavily reliant on fossil fuels. This scheme depends on the stability of power monopolies, which are maintained by coercion, brute force and war. The entire system has exacerbated irreversible climate change, leaving us in a fundamental contradiction. If the underdeveloped ever hope to become developed, their lands, livelihoods and cultures must be sacrificed for the good of those who seek to strengthen their privileged

¹Only this chapter is written as a personal statement and with little or no references. In the next chapter many facts and statements related to historical trends, current state of affairs and what are the needs of people are addressed again with proper referencing.

statuses.

This is the world into which I was born, and in less than three decades, I have seen the astonishing decay of biodiversity and destruction of the environment. I have also been witness to the injustices imposed by specific classes of society that deny democracy in order to maintain the hegemony of power and wealth. Much like the failed and twisted promise of development, those who control the levers of power self-righteously readily expound that *All human beings are born free and equal in dignity and rights* (Nations, 1948), while working tirelessly to make life, itself, impossible.

The only way to overcome this fundamental contradiction and existential crisis is by creating a new development system that genuinely prioritizes life over power. A system developed by and for people, not consumers. True democracies where one generation's "development" does not compromise the future of those who follow. The question that follows is How? And I believe the answer is through the use of science to transform the current imbalanced reality into a more beautiful and just place for all. That is why I have focused on finding a culturally respectful solution to the energy needs of people living in the developing world through the use of locally available energy resources. Meaningful access to clean, sustainable energy is fundamental for true development. Currently, the nearly one third of the world population unable to meet their basic needs rely on low efficiency combustion technologies for cooking and heating. These methods are responsible large amounts of CO2 emissions, deforestation, millions of pre-mature deaths, poor quality of life. Women and children are disproportionately affected.

Figure 1.1 exemplifies the situation². Moreover, large institutional efforts have been unable to provide meaningful assistance and available technology has failed to create significant improvements in out-of-lab conditions. In most cases, while the ideas and tools may seem good, they fail because they are culturally inappropriate.

My first attempt to tackle the problem was the creation of a hydrogen stove powered with solar energy, developed in collaboration with 125 families from the community 31 de Mayo in the highlands of Guatemala. The project was funded by an Inter-American Development Bank Greenovators grant. My proposal was selected from 784 proposals submitted from all over the continent.

Figure 1.2: Community Based Participatory Research



(a) The road the *Comunidad 31 de Mayo*



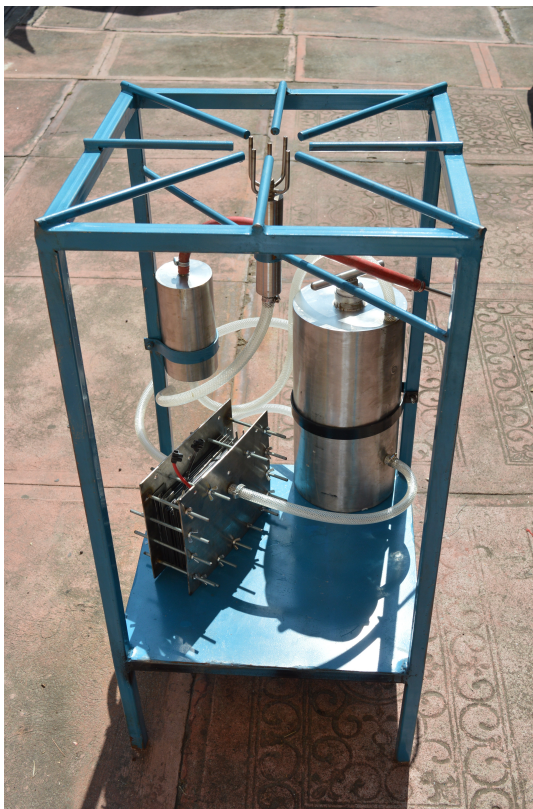
(b) Community meeting to define the research plan

I visited this remote community and then decided to live there for several weeks because the journey from Guatemala City was so dangerous and difficult. It took at least 14 hours by a 4x4 vehicle to reach the area. My decision to use the *Community Based Participatory Research* methodology allowed me to experience, first-hand, the life of these families. I was able to understand the critical importance of cooking. The stove is the glowing center of daily life and only sleeps when the family sleeps.

²Note the color of the roof and walls covered with emissions from the cookstove

My work with this community proved the hydrogen stove to be a technically feasible concept, but the high cost made scaling it up to use impossible. The need for a clean, sustainable cooking method was still unmet so I continued to look for an alternative. I was approached by the largest cooperative in Guatemala *COOSAJO R.L.*, a cooperative community located in one of the poorest regions in the country. This area suffered the loss of 25% of its forest due to deliberate deforestation policies and practices between 2006-2010.

Figure 1.3: *The hydrogen stove*



(a) Final version of the hydrogen stove



(b) "Chico" carrying one of the three stoves to his house

With community input, I designed a study that incorporated 492 people from 10 communities that used fuel as their main source of energy. We first quantified the fuel consumption and emissions. Then, we evaluated the efficiency of their traditional technologies along with those of seven modern commercially available technologies from different parts of the world; two pellet gasifiers with electric fans, two rocket stoves, one induction stove, one electric coil stove, and one solar oven (For details, see (Quan-Reyes, Goel, and Mora, 2020)). These technologies were chosen as the most efficient and cleanest according to the Global Alliance for Clean Cookstoves, the most respected institution in the field.



Figure 1.4: 5 of the 7 top tier technologies investigated
3

From these direct experiences, I was able to grasp the enormous complexity of what at first appeared to be simple problem. It is no wonder that all major efforts to replace low-efficiency technologies have failed.

Major findings:

1. Biomass will continue to be the main energy resource of choice, as it is readily available and accessible. Alternative fuels that could meet the power and energy demand all require large infrastructure and investment (e.g., gas and electricity) that cannot be attained. This is also the tendency in Europe, where it is more than 50% of the energy share (Scarlat et al., 2019).
2. Renewable alternatives cannot affordably meet the demand for power at the times people need it. Solar is a good example of this.
3. Top tier technologies are often developed in a lab without taking into account essential cultural needs. They inevitably fail in out-of-lab scenarios.
4. Since biomass will continue to be the main energy resource, the technical goal should be to optimize its use in order to make it as clean and sustainable as possible.
5. My knowledge at that time was not sufficient solve the problem. I realized I needed to learn the fundamentals of biomass thermochemical conversion, and thus I decided to study for a Masters in Mechanical Engineering at *TU Delft*.

In summary, with access to renewable, sustainable and clean energy (SDG7) people can improve their life quality, reduce emissions, and reduce negative environmental impacts. And by using locally available energy resources, they remain in control, thus making it truly democratic. This same approach can be extended to larger energy scales for other needs when the local economies start to grow. It is sustainable, allowing people to develop as they see fit, without the outside profiteering more commonly known as development.

Introduction

A woman in a red shirt is cooking in a traditional wood-burning kitchen. She is using a whisk to stir something in a large, shallow pan over a fire. The kitchen is filled with steam, and there are several pots and pans on the stove. The scene is dimly lit, with light coming from a window or opening in the background.

2

1. THE URGENT NEED TO REPLACE THE FOSSIL FUEL BASED DEVELOPMENT MODEL

1.1 THE CURRENT WORLD SITUATION

The current global economic-development system based on the use of fossil fuels is no longer sustainable. The amount of greenhouse gases -GHG- emitted by humanity's demand for this energy has altered the earth's climate. The changes taking place make it clear that human activities dependent on this power are the main drivers of this unfolding disaster. These events have led us into a new geological era, the Anthropocene, characterized as the sixth mass extinction. Since 1970, 60% of mammals, birds, fish and reptiles have disappeared due to human activity (Grooten, Almond, et al., 2018).

Climate change is now pushing the limits of the planet's stability to such a degree that should we fail to drastically cut GHG emissions by 2030 (Masson-Delmotte et al., 2018) when the increase of the average temperature of the earth is estimated to surpass 1.5 Celsius, the climate system will become dangerously unstable. At that point, the changes will be unstoppable, mass extinctions will accelerate and the survival of humanity will be uncertain. As shown in Figure 2.1, time is running out and change is urgently needed.

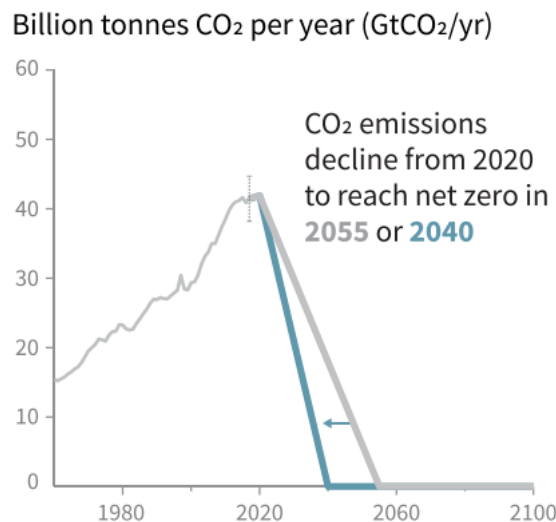


Figure 2.1: Pathway to carbon neutrality by 2040

Figure obtained from (IPCC, 2018)

Aside from the obvious environmental effects, the current global development system threatens our shared existence in other ways. Political institutions are undergoing a qualitative change as growing inequality inexorably destabilizes the current world order. On one hand, there are opportunities for positive change. With the breakdown of the old system, it is possible that we will be motivated towards innovation, to recreate, invent and embrace sustainable ways of organizing and supporting populations. Unfortunately, the alternative scenario is a familiar one, strikingly similar to the milieu that fueled the rise of fascism in the 1930's. Radical politicians control key decision-making points at this critical juncture and these so-called "strongmen" consolidate short-term power by fomenting divisions such as classicism, racism, misogyny, nationalism and trans/ homophobia, at the time when global shared-purpose is most needed. Reason and science, the very tools essential to our collective survival, are vilified as obstacles to their pursuits. Thus, humanity again finds itself at the brink of calamity, but this time the enemy is our own inability to unify and take actions that could prevent mass extinction.

Since 1947, the *Doomsday Clock tended by the Bulletin of Atomic Scientists* has tracked humanity's movement toward atomic or environmental disaster. The clock symbolically measures the time left to

act before reaching midnight - the cataclysmic end of life on the planet as we know it. On January 23, 2020 the minute hand was adjusted for only the 24th time, reducing our action window from 2 minutes to a mere 100 seconds until that midnight. This is mentioned not to discourage, but rather to emphasize the urgency of our situation and the necessity of proposing realistic alternatives that can be implemented within those precious remaining moments.

Current non-renewable, large scale energy systems rely heavily on transportation chains that themselves rely on fossil fuels and military hegemony. This complex infrastructure consumes a vast amount of resources. For example, the United States, the largest emitter of CO_2 , has spent nearly USD 6.4 trillion in wars against Afghanistan, Pakistan and Iraq in pursuit of fossil fuels (Watson Institute for International and Public Affairs, 2020). According to Gen. John Abizaid, former head of U.S. Central Command and Military Operations in Iraq, in 2007 *"of course it's about oil; we can't really deny that"* (Juhasz, 2013).

With the potential to reap enormous profits through destructive and hegemonic purposes, it is no wonder that the US is reluctant to shift to renewables. The cost of converting the US energy matrix completely off fossil fuels is estimated to be USD 4.7 trillion (Groom, 2019). When short-term profitability for a few takes precedence over long-term profit and sustainability for all, it is apparent that the climate crisis is also a political crisis. While the Trump-led US is certainly the most openly egregious example, other world leaders have yet to address even the comparatively modest requirements of the Paris Agreement (Al Jazeera News, 2018). This shared failure is due to lack of political will, not lack of resources, as evidenced by collective global military expenditures which amounted to USD 3.4 million per minute in 2018 (Stockholm International Peace Research Institute, 2018). Clearly, there are adequate resources that could be redirected in order to create a sustainable system that meets the needs of everyone without compromising future generations.

Thus, by acknowledging the problem is not a lack of resources but rather one of political will, we are able to understand that the climate crisis, which is an existential crisis, will only be solved by a political revolution that rebalances the current system so that long-term, collective benefits based in science, equality and justice are prioritized over the short-term gain of a few. The earth can no longer bear the consequences of extractive capitalism.

1.2 INEQUALITY AND CLIMATE CHANGE

It is possible to find an alternative development model, and this must be done without delay as the window to prevent unstoppable climate change is quickly closing. The economic resources to accomplish such a task exist, but they are poorly distributed.

In our time, never has humanity seen such rapid economic growth and wealth production. The general accepted view of these measure is positive, yet, at the same time, never has there been such global inequality and destruction of natural resources. Global health and well-being have become uncoupled from current measures of economic growth to such a degree that a modern booming economy, increased production and generation of wealth are inevitably generated at the expense of humanity and nature. In early 2019, 26 people owned the same amount of wealth as the bottom half of the population (Quackenbush, 2019) and the richest man on Earth, Amazon CEO Jeff Bezos, makes USD 215 million per day (Warren, 2020), yet the company paid zero dollars in federal taxes.

This is not a singularity, the current status systematically benefits the ultra rich at the expense of everyone else, including the environment. In 2018, the wealth of the billionaires increased by 12% (USD2.5 billion per day), while the wealth of the bottom 3.8 billion people, who live with less than USD 5.5 per day (The World Bank, 2018), declined by 11% (Quackenbush, 2019). And the global pandemic has only served to widen these disparities. This is wealth built with heavy reliance on fossil fuels, shown as the coefficient of determination for CO_2 emissions and the Human Development Index -HDI- is of $R^2 = 0.81$ (Costa, Rybski, and Kropp, 2011), see Figure 2.2. (Note this is a log scale, so the CO_2 emissions grow exponentially with the HDI).

The irony of the current political and economical situation is that so-called under-developed and developing countries are expected to become developed. Which, as currently defined, means that they are expected to base their growth on the use of cheap fossil fuels. At the same time these countries are required to forego the use of fossil fuels in order to do their part to mitigate climate change. There is no good way forward as they try to navigate through these contradictions with corrupt methods. To address these issues we must reject outdated concepts that undergird a dying system by redefining growth, wealth, health and development as we hurtle towards midnight.

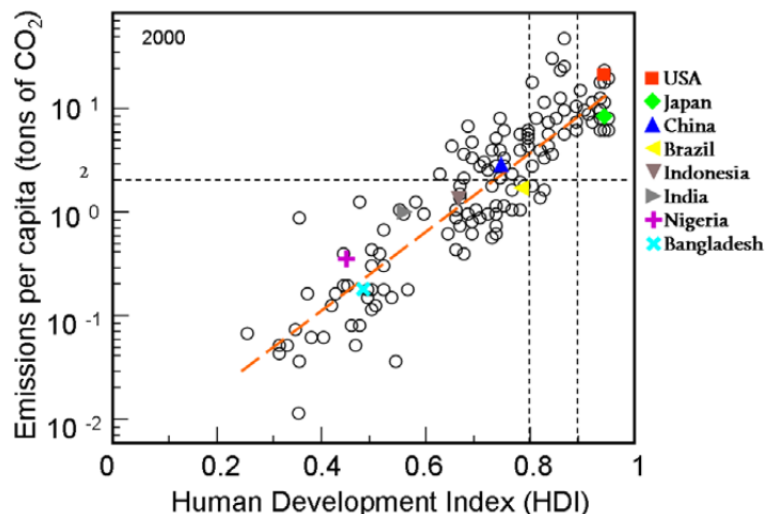


Figure 2.2: CO_2 emissions vs Human Development Index

Figure obtained from (Costa, Rybski, and Kropp, 2011)

WHAT DEVELOPMENT IS NOT

Development is not the same as economic growth, the concepts are related, but not synonymous. Economic growth is defined as, “An increment in the amount of goods and services produced per capita of the population over a period of time (Google Dictionary, 2018), and, “The increase of the GDP per capita minus the inflation” (International Monetary Fund, 2012). According to the Cambridge Dictionary, development is simply, “the process in which someone or something grows or changes and becomes more advanced”. Development and growth are neutral terms. Although both are defined and driven by human action, there is not always a positive correlation with the health or well-being of those subject to a given project or measure.

The United States of America and the United Kingdom are considered developed countries. According to the Human Development Index from the United Nations, the US is ranked 13th ($HDI = 0.924$) and the UK closely follows in 14th ($HDI = 0.922$). By current measures, both have strong economies and are considered world leaders. If economic growth and development were, in fact, the same things, and if mainstream concepts of development were true, it would follow that citizens of these countries would have a better quality of life than all but a dozen others. This is not the case. For example, US maternal mortality is the highest among other so-called developed countries (International, 2010), (Nina Martin, 2017). Women of color are at greater risk. In the UK, Black women are five times more likely to die in childbirth than their white counterparts (Knight et al., 2017). Youth suicide is the second leading cause of death among US teenagers, closely followed by homicide (Population Reference Bureau, 2016). In the U.K. suicide is the leading cause of death among teenagers (Mental Health Foundation, 2018).

2. THE ENERGY NEEDS OF ONE THIRD OF THE WORLD POPULATION

As of 2018, nearly 2.6 billion people rely on biomass as their main source of energy (International Energy Agency, 2019). More than two thirds utilize traditional low-efficiency technologies like open-fires and the other third on basic, improved cooking stoves with benefits which are limited to some minimal improvements (Venkata Ramana et al., 2015).

The pollution from these technologies account for between 2.5 (International Energy Agency, 2019) and 4.3 million premature deaths, and 110 million disability-adjusted years (Venkata Ramana et al., 2015). Women and children are disproportionately affected (M. Thakur, Schayck, and Boudewijns, 2019).

Shared environmental consequences of this system are enormous, the most obvious of which is deforestation, as those who are able to obtain fuel locally will do so until it is no longer feasible. Beyond this, the sustainability of biomass should not be generalized. Methods of production, distribution and consumption will determine its sustainability. For example, biomass is not completely carbon neutral, as there are emissions that are not CO_2 . For example, 25% of the total black carbon emissions are due to poor combustion from cooking technologies (Garland et al., 2017), (Venkata Ramana et al., 2015). Black carbon is considered the second most influential greenhouse gas (GHG) due to its optical properties e.g., increased heat absorption in clouds, reduced snow-albedo in the ice and snow sheets (Bond et al., 2013). Furthermore, biomass consumption results in emissions of CO_2 of between 0.5–1.2 billion metric tons (equivalent to 3% of global annual emissions) (Venkata Ramana et al., 2015).

In terms of economic impact, the median cost of the environmental and direct health effects of this fuel usage are USD 123 billion (idem), and the burden for the national health systems goes between USD 212 billion and 1.1 trillion (Sovacool, 2012). At the family level, the share of annual income directly spent on energy fuels accounts for 20 – 30%, and an additional 20 – 40% is expended on indirect costs such as health care, injury or loss of time (idem). While there are considerable environmental effects, the main negative impact is on public health.

When compared to emissions per capita, the industrialized world emits much more CO_2 than people who rely on the use of biomass. For example, in Bangladesh, where 90% of the population relies in the use of biomass (Mehetre et al., 2017), the CO_2 emissions per cápita in 2014 were 0.474 MT, meanwhile in the U.S.A., (The World Bank, 2014), in line with 2.2.

2.1 A CALL FOR NEW DEVELOPMENT MODEL

A new development model is urgently needed, an approach not based on the use of fossil fuels, nor confused with economic growth, but rather centered around people and other forms of life. It would be a rejection of robotic accumulation at the expense of health, justice or the environment. Within this new paradigm, human rights, civil rights and the rights of Nature are paramount and the economy is grounded in the democratic, rational and sustainable allocation of resources. The use of locally available energy resources would be prioritized until the use of large-scale clean technologies is sustainable. An advantage of using the locally available energy resources is that the environmental footprint of transportation and distribution is minimized.

The energy needs of the people can be categorized in order of magnitude. Such a scale would go from a few watts needed for lighting (with high efficiency LED technology), to the hundreds and thousands for cooking, to thousands and tens of thousands for transportation and various economic activities (see Figure 2.3).

Scales of energy needs for sustainable development

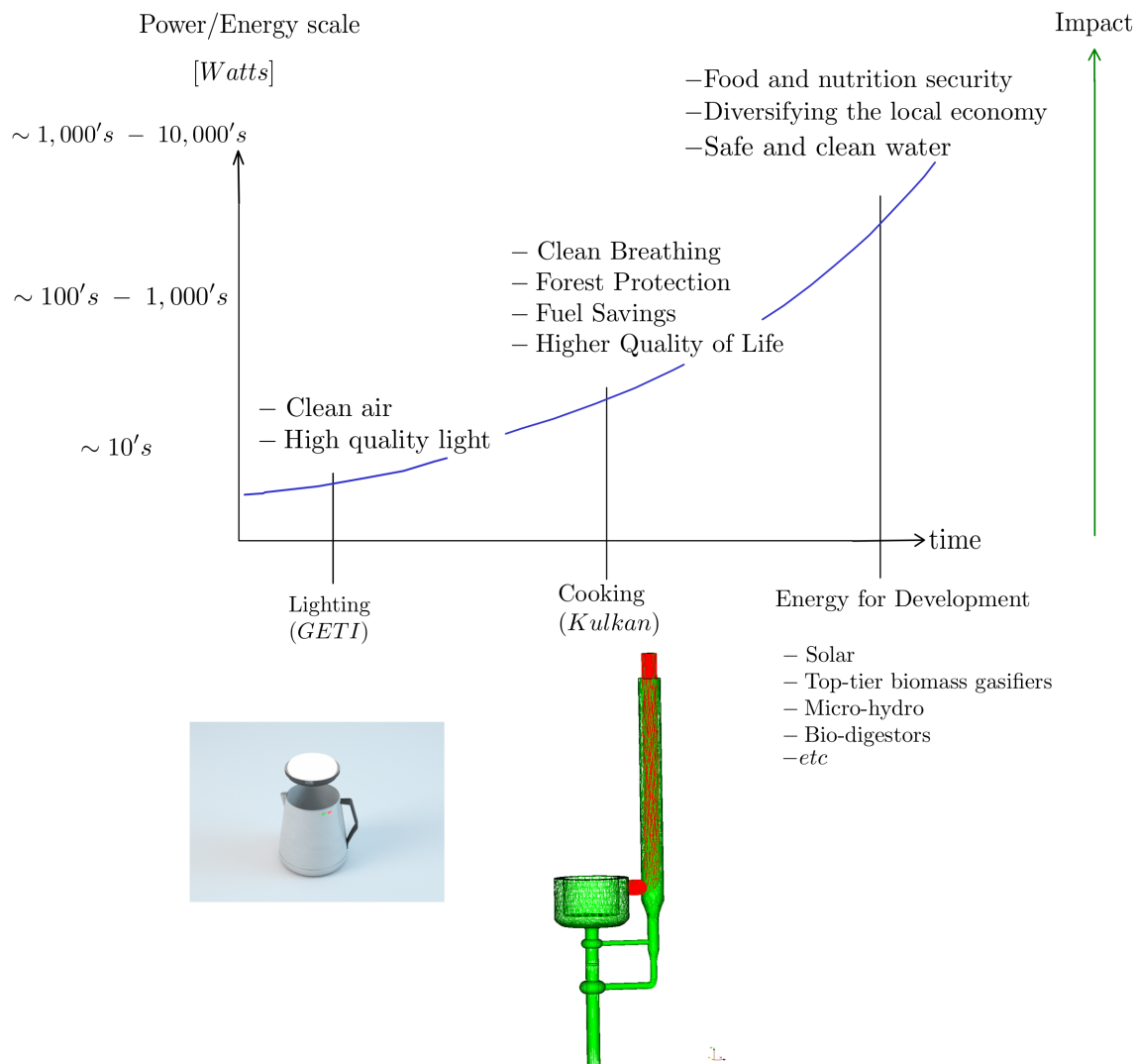


Figure 2.3: Scale of energy needs for sustainable development

Currently, the use of traditional biomass fuels (e.g. wood logs, wood sticks, wood chips, and cow dung) used to fulfill the needs for heat energy (e.g. cooking, boiling water, and temperature regulation) account for over 90% of household energy consumption in the developing world (Urmee and Gyamfi, 2014). Most of these materials are converted to energy through usage of highly inefficient technologies resulting in the previously mentioned negative environmental and health effects.

Replacing the fuel is not viable in most of these countries, as doing so would require significant infrastructural changes and increased reliance on non-renewable energy resources. Biomass, despite the aforementioned problems, is a locally available energy resource that can be renewable if managed properly. In addition to its undervalued cultural-historical significance, it is also a proven method of fulfilling a critical portion of these populations' energy needs. These fundamental considerations are often overlooked by even well-meaning outsiders. With these variables in mind, the use of biomass

could and should be successfully optimized.

Hence, this work will address energy needs in the scale of thousands of watts as needed for cooking with a novel biomass reactor, named the *Kulkan Reactor*. The reactor is intended to optimize the extraction of heat from the chemical potential energy stored in biomass. It is based on an analysis of the fundamental physics of the thermochemical processes of the biomass conversion from fuel to usable heat. It comes to a synthesis after the evaluation of three hypotheses investigated using mathematical models validated with experimental data available from the literature, and detailed computational fluid dynamics -CFD- simulations of reactive flow.

The first hypothesis addresses a new way of controlling the air-fuel ratio by reducing the excessive air draft currently affecting available technologies, while at the same time recovering heat otherwise lost in the flue gas by means of an air pre-heater. The second proposes a new combustion regime that aims to achieve more complete combustion, prevent flame quenching and reduce energy loss through utilization of more compact combustion chambers. The third hypothesis is accompanied by deduction-based arguments for an innovative means of controlling the harmful ultra-fine emissions by primary measures i.e., (by design), another goal that has yet to be reached with existing technologies.

The current state of biomass cooking technology



3

1. THE STATE OF IMPROVED COOKSTOVES AND THE EVALUATION PROTOCOLS

1.1 AVAILABLE COOKING TECHNOLOGIES

The existing biomass cooking technologies can be organized in four categories, in order of increasing efficiency: open-fire $\eta \sim [5 - 17]\%$ (Berrueta, R. D. Edwards, and Masera, 2008) & (Ballard-Tremeer and Jawurek, 1996), iron-top stoves $\eta \sim [7 - 13]\%$ (Berrueta, R. D. Edwards, and Masera, 2008) & (McCracken and Kirk R. Smith, 1998), rocket stoves $\eta \sim [35 - 40]\%$ (Jetter et al., 2012) and gasifiers $\eta \sim [34 - 49]\%$ (Roth, 2011). In the following section the main characteristics of those technologies are presented along with their emissions in terms of carbon monoxide (CO), a poisonous gas product of incomplete combustion, and particulate matter with an aerodynamic diameter less than $2.5\mu\text{m}$, often referred to as "*fine particles*", or "*PM_x*", where "*x*" stands for the aerodynamic diameter in μm . The "*ultra fine particles*" are those with an aerodynamic diameter smaller than $0.1\mu\text{m}$ i.e., *PM_{0.1}*.

OPEN FIRE

Open fire is the oldest, continuously utilized human-created technology. It is the simplest way of extracting useful energy from biomass through combustion. It is also known as the "three stone fire" and it consists of an arrangement of biomass that burns by diffusion of oxygen into the reaction zone. It has one of the lowest energy efficiencies and high emissions $CO \sim 11.2 - 15.1\text{g}/MJ$, and $PM_{2.5} \sim 719, 1350\text{g}/MJ$ in the High Power phase (Jetter et al., 2012). Heat is transferred directly from contact with flames into the cooking objective e.g., corn, or by means of a conducting plate such as a pot or metallic sheet.



Figure 3.1: Open Fire with traditional *comal* on top
Photo by: Diego Quan in the community *31 de Mayo, Quiche*, 2016

FLAT TOP OR CHIMNEY STOVE

Although this stove's thermal efficiency is in the same range as the Open Fire, in some cases it may reduce fuel consumption through improved heat transfer, hence, its position in second place (see Section 1.3), as reported by (Quan-Reyes, Goel, and Mora, 2020). In some studies fuel consumption increased (Sedighi and Salarian, 2017), along with the time required for boiling water. This type of stove is widely used in Mesoamerica and India, an important staple is a type of flat cooked dough e.g., tortillas in Guatemala or masaldosas in India. The stove's defining characteristic is a flat surface where heat is transferred from the combustion zone to the cooking objective. This transfer may be either to the food directly, as in the case of flat breads, or to a cooking vessel.

The stove's reaction zone has a short height, (see Figure 3.2) which results in flame quenching. There is usually an attached chimney designed to reduce indoor pollution by venting flue gas outside the house. However, if the chimney is damaged or ill constructed in a manner that prevents venting, this advantage will be lost as the combustion process, itself, is not improved, as compared to the open fire.

Most importantly, the chimney enhances the draft created by the lower density hot gases inside the reaction zones. This draft increments the amount of air that is coming into the system, to levels which range between [300 – 1250]% of excess air. This results in a "dilution" of the heat, and flame stability problems, as will be explained further in the *thermo-chemical* section.

According to (Jetter et al., 2012), thermal efficiency during the high power stage of the *Water Boiling Test* is of 12.8%, for the popular type *Onil*. The *CO* emissions are of 5.7g/MJ and the PM2.5 of 793g/MJ.



Figure 3.2: Flat iron top cookstove
Photo by Diego Quan in the community *El Zapotalito*, 2016

ROCKET STOVE

This technology is based in 10 principles of construction explained by (M. Bryden et al., 2005). Essentially, and in contrast with the two previously mentioned technologies, it has a taller reaction zone which allows the flames to develop further before quenching, a higher air inlet due to the draft generated by the expansion of the gases in the vertical tube and a better defined reaction zone (See combustion zones in Figures 3.3, 3.4, 3.5). The improved combustion leads to a reduction of the mass of emissions (*which does not necessarily mean less harmful, see Section 2*), both in CO and $PM_{2.5}$, and an increase in the thermal efficiency. According to (Jetter et al., 2012), the emissions are of $5.1g/MJ$ for CO and $478g/MJ$ for $PM_{2.5}$, for the Envirofit G3300 model.

According to (Kshirsagar and Kalamkar, 2015), close to 40% of the total energy is lost via the flue gas in this technology, and according to a recent study by (Pundle et al., 2019), this technology also has extremely large amounts of excess air, specifically, up to ten times more than the required for complete combustion in low fire power ($2kW$), and more than three times in high powers ($5kW$).

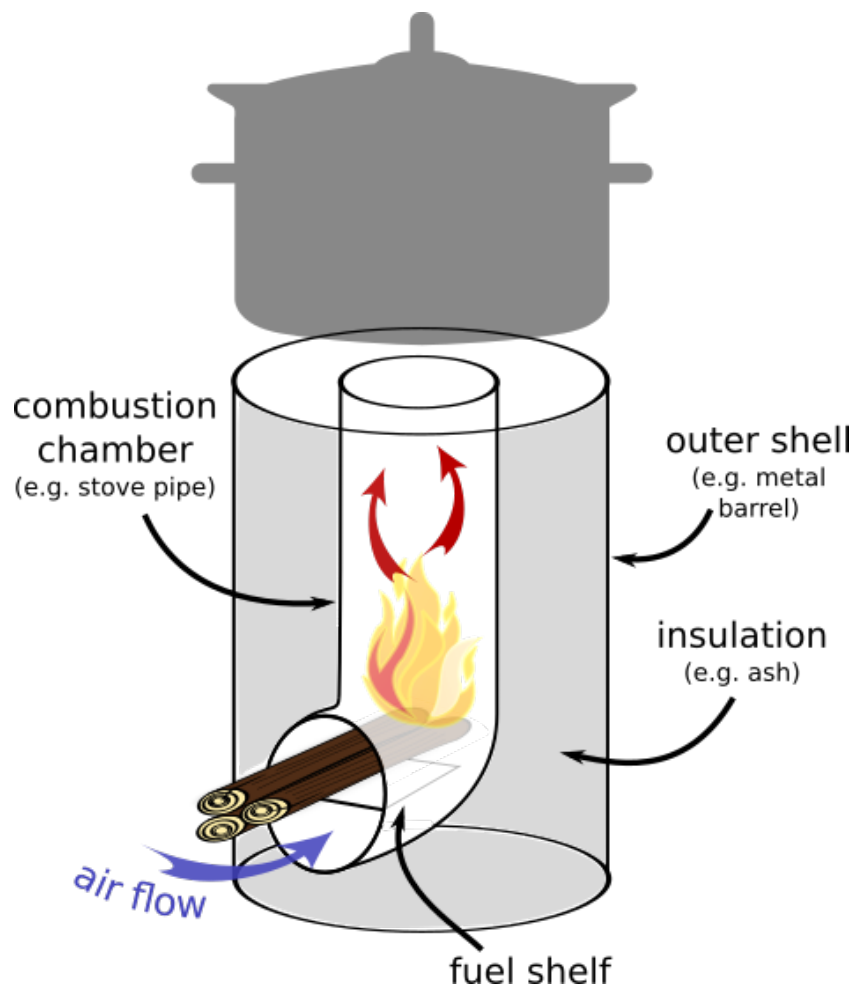


Figure 3.3: Schematic of a Rocket stove

Figure obtained from https://en.wikipedia.org/wiki/Rocket_stove#/media/File:Rocket_Stove.png

GASIFIER STOVES

Gasifier stoves are characterized by having two reaction zones, the first where the solid biomass is gasified into syngas. This syngas then combines with secondary air to be burned in the second reaction zone. Since the combustion takes place in the gas phase, it is generally considered a cleaner method that results in lower emissions and higher efficiency.



Figure 3.4: Rocket stove prototypes
Prototypes by Diego Quan, 2018

According to (Jetter et al., 2012), the emissions are of $0.9g/MJ$ for CO and $1.7g/MJ$, for the StoveTec TLUD, where TLUD stands for Top Lit Up Draft. This type of stove is one of the most recent types and some large companies and universities have developed their own models. For example, one of the top tier stoves in this category is the *Phillips HD4012 fan*, which incorporates an electrically powered fan to increase the air flow.

Although this technology offers substantial increases in thermal efficiency and emissions, it is not necessarily an ideal substitute for traditional stoves, as in many cases the requirements for utilization are culturally inappropriate and/or inaccessible. The stove requires biomass pellets, a luxury not easily accessed by those who need it most, rural people living in poverty. Prohibitive fuel costs and lack of distribution networks render this an unrealistic option.

Some (Sedighi and Salarian, 2017), have also called attention to the lack of power output control, especially in a batch feeding regime. This was found to be an essential determinant of rejection for the families involved in the study by (Quan-Reyes, Goel, and Mora, 2020).

Table 3.1, summarizes the efficiency and emissions of the mentioned technologies. ¹.

¹The efficiency and emissions correspond to the high power cold start of the Water Boiling Test

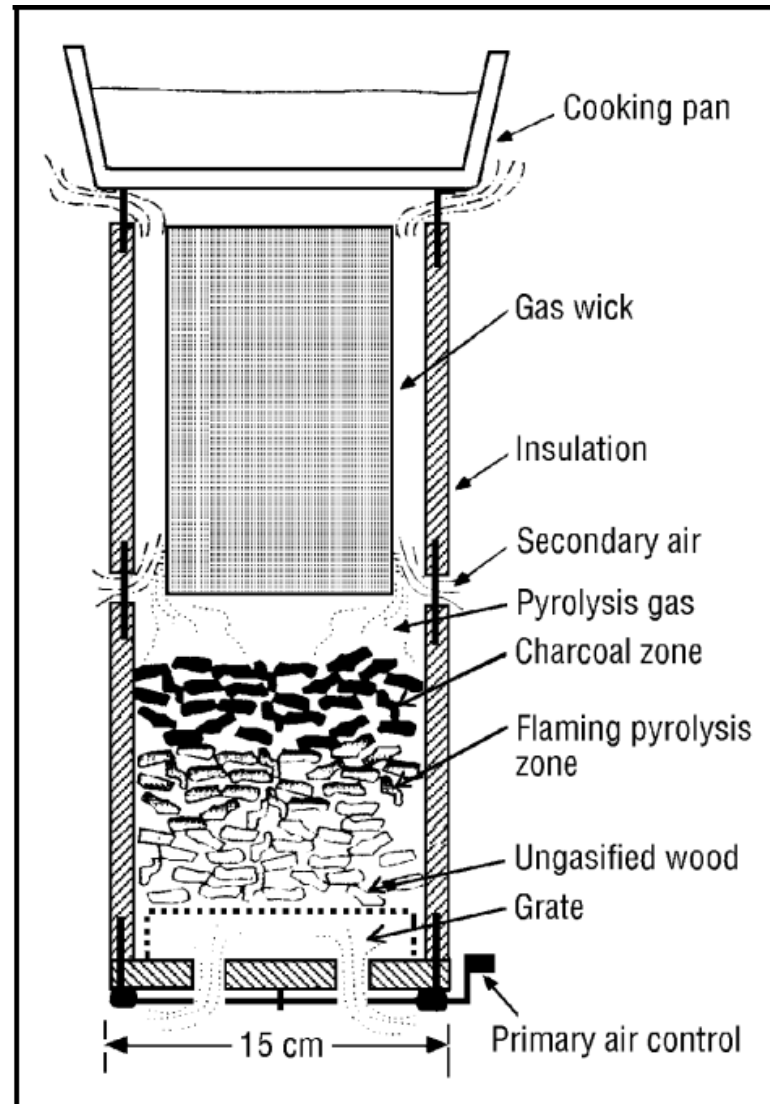


Figure 3.5: Schematic of a Rocket stove
Image obtained from (Reed and Larson, 1997)

Table 3.1: Biomass cooking technologies

Technology	Thermal efficiency	Emissions CO/PM2.5 [g/MJ]	Source
Open Fire	5-17 %	11.2 – 15.1/719 – 1350	(Berrueta, R. D. Edwards, and Masera, 2008) & (Jetter et al., 2012)
Flat top stove	7-13 %	5.1/478	(McCracken and Kirk R. Smith, 1998) & (Berrueta, R. D. Edwards, and Masera, 2008) & (Jetter et al., 2012)
Rocket	35-40 %	5.7/793	(Jetter et al., 2012)
Gasifier	34-49 %	0.9/93	(Roth, 2011) & (Jetter et al., 2012)

Common limitations to all the previously mentioned technologies are:

- little control over the air/fuel ratio.
- non-premixed combustion.

- high excess air, which leads to flame instabilities (See (Monteiro et al., 2010)).
- flame quenching due to direct impingement against surfaces.
- high heat losses in the flue and stove body.
- little knowledge on the fluid dynamics, heat exchange and chemical reactions.

STANDARD TIERS

In recent literature, cookstoves are categorized by "tiers", a structure implemented by the Global Alliance for Clean Cookstoves, developed by the ISO International Workshop Agreement -IWA-.

This metric standardized cookstove performance, ranging from *Tier 0*, for the poorest performing stoves, to *Tier 5*, for the best. Table 3.2 shows the categories and the ranges of thermal efficiency, carbon monoxide emissions, particulate matter emissions, safety scores and durability scores.

Table 3.2: IWA performance Tiers

Tier	Thermal efficiency [%]	CO [g/MJ]	PM2.5 [mg/MJ]	Safety (score)	Durability (score)
Tier 5	≥ 50	≤ 3.0	≤ 5	≥ 95	≤ 10
Tier 4	≥ 40	≤ 4.4	≤ 62	≥ 86	≤ 15
Tier 3	≥ 30	≤ 7.2	≤ 218	≥ 77	≤ 20
Tier 2	≥ 20	≤ 11.5	≤ 481	≥ 68	≤ 25
Tier 1	≥ 10	≤ 18.3	≤ 1031	≥ 60	≤ 35
Tier 0	≤ 10	≥ 18.3	≥ 1031	≤ 60	≥ 35

Reference: <https://www.cleancookingalliance.org/technology-and-fuels/standards/iwa-tiers-of-performance.html>

These voluntary tiers serve as benchmarks for comparison among the different existing cooking technologies. The global alliance for clean cookstoves provides a large catalog of 479 of the existing technologies, including their performance characteristics, price, geographic presence, among other factors. The catalog is available at: <http://catalog.cleancookstoves.org/>

1.2 GENERAL FEATURES OF IMPROVED COOKSTOVES

The literature regarding cookstoves is largely devoted to examinations of performance evaluation based on thermal efficiency, *CO* and *PM* emissions. Most of these studies are based in the Water Boiling Test (see Section 1.3). In this vast array of literature, studies that stand out due to their completeness are those of Nordica MacCarty (eg., (Maccarty et al., 2008), (Nordica MacCarty, D. Still, and Ogle, 2010), (N. A. MacCarty and Kenneth M. Bryden, 2015), (Moses and N. A. MacCarty, 2019)) and particularly the one from Jetter et al., namely *Pollutant emissions and energy efficiency under controlled conditions for household biomass cookstoves and implications for metrics useful in setting international test standards*.

Their group reached some important conclusions including the following:

1. Improved cookstoves reduce the global warming impact compared to traditional stoves or open fire.
2. Rocket stoves reduce the *PM* and *CO* emissions significantly (in terms of mass per unit energy)
3. Rocket stoves and gasifiers reduce fuel consumption significantly compared to traditional stoves or open fire.
4. Gasifiers are the best overall performing biomass technology and the most promising one to achieve Tier 4 performance, especially when using forced air.

These conclusions are well represented in Figures 3.6, 3.7 and in (Nordica MacCarty, D. Still, and Ogle, 2010). Many other authors have arrived at the same conclusions and there is renewed interest in research and development of biomass gasifiers. See for example (Roth, 2011), (J. A. Marchese et al., 2018). In the words of the Global Alliance for Clean Cookstoves, sponsors of the largest initiative to promote clean cooking alternatives to open fires:

- "The potential climate and health benefits of the pellet stove approach those of gas stoves.
- Compared to cooking over a three-stone fire, the pellet stove reduced emission rates by approximately 90% or more for most measured pollutants (black carbon, particulate matter, and carbon monoxide).
- The climate impacts of the pellet stoves are negligible when the pellets are produced from renewable sources, such as gathered wood or agricultural waste, and when using renewable energy to power pellet production.
- Although the pellet stove exceeded the particulate matter emissions target for the World Health Organization indoor air quality guidelines, it neared the interim target, offering drastic improvement over traditional stoves, and the pellet stove met the guideline for carbon monoxide emissions.
- Stove maintenance and customer support programs are critical for ensuring that stoves perform as designed once they are off the shelf and in customers' homes."

These conclusions come from a large study funded by the Global Alliance for Clean Cookstoves (Champion and Grieshop, 2019) and must be read with a great degree of caution as the behavior of devices in laboratory conditions differs markedly from real-life usage (see Figure 3.8). Moreover, cultural variables were not taken into consideration during the design process of these stoves and testing was conducted based on unrealistic assumptions. For example, researchers assumed people would switch to pellets, which, as we have seen, can rarely be obtained. In addition, the functioning of TLUD gasifiers is based upon a batch process that differs radically from the normal semi-continuously fed traditional way. These conditions create fatal flaws in real-life replication, as they ignore behavioral changes and disruptions of cooking processes necessary to re-fuel the system in a manner duplicating lab conditions.

Developing a technology that reduces the emissions, reduces the fuel consumption and has an overall cleaner combustion does not immediately translate into environmental nor health gains. For example, LPG, a cleaner alternative to biomass in simple terms of combustion emissions and efficiency of combustion, is ill-suited for making traditional foods in Mesoamerica (Jeuland and Pattanayak, 2012).

In 2018, the Minimoto stove used for the Alliance's study and other advanced stoves like the Berkley Darfur and the Biolite were tested in real life situations. The study found that women, who are most commonly responsible for cooking in these cultures, did not like gasifiers because of the feeding system. Some families even refused to try them at all because pellets were not available. The notion of removing the cooking pot every time the stove needed new fuel was also impractical and unacceptable (Quan-Reyes, Goel, and Mora, 2020).

These findings will be further discussed in Section 4, including recommendations for addressing the lack of access to energy. Social norms affecting acceptance will be explored in more depth.

1.3 PERFORMANCE EVALUATION PROTOCOLS

Evaluating the performance of a cookstove is not a trivial matter. There are many variables that affect its performance, and the definition of "performance" itself is complex. Aside from the energy variables presented in Table 3.2, there also exists:

- The combustion efficiency, which is approximated by the *Modified Combustion Efficiency -MCE-*: $CO_2/(CO + CO_2)$ (in mole fractions).
- The fuel consumption, which is measured by the specific fuel consumption for a particular food $kg_{fuel}/kg_{particular\ food}$, or by fuel consumption per cooking task.
- The overall efficiency, which is the product of the thermal efficiency η_{th} (heat successfully transferred to the cooking appliance), and the MCE: $\eta = \eta_{th} \cdot MCE$
- Power i.e., (energy per unit time)

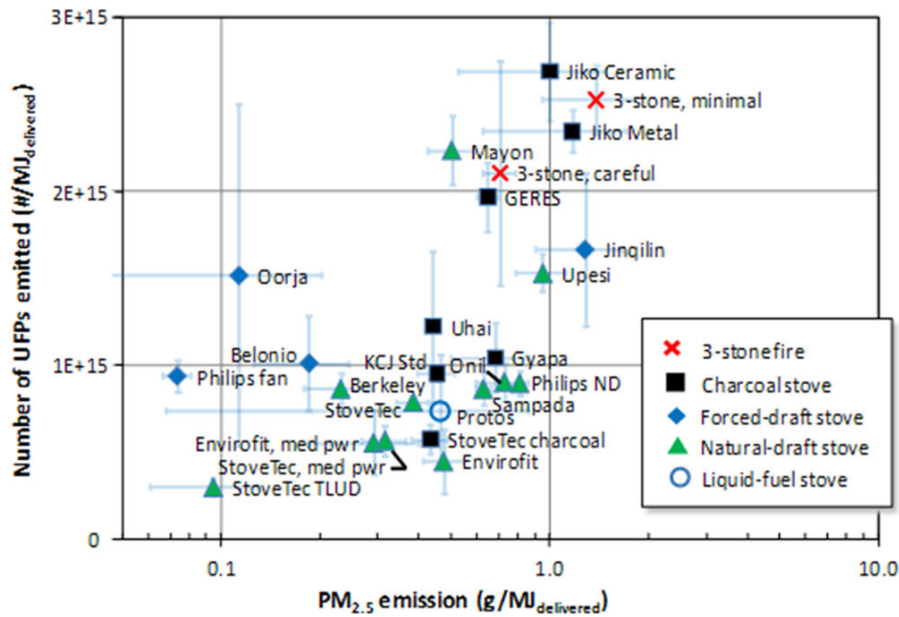


Figure 3.6: Number of ultra fine particles and particle mass emitted per unit of useful energy
Image obtained from (Jetter et al., 2012)

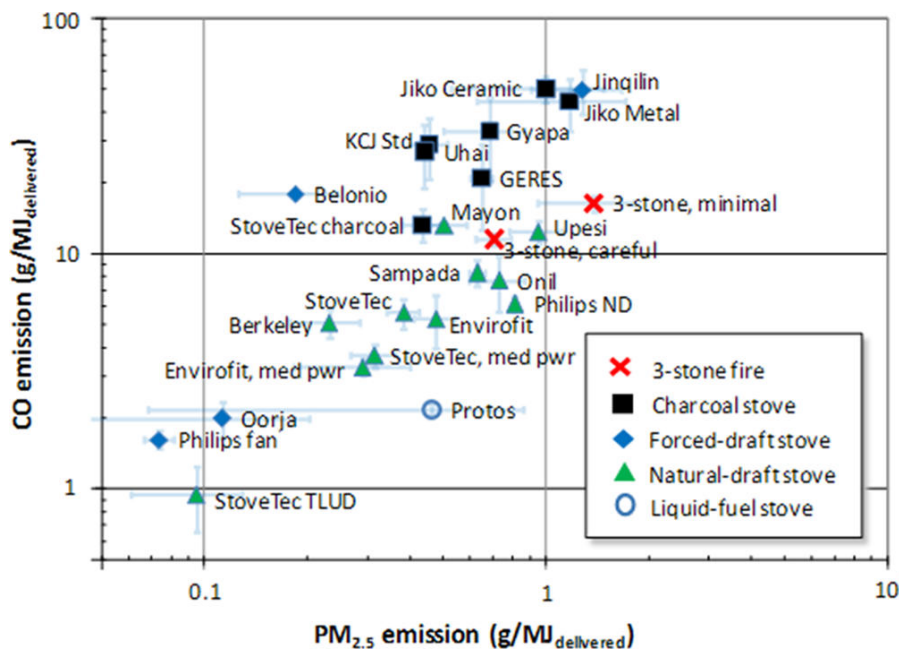


Figure 3.7: Mass of CO and PM2.5 per unit of useful energy
Image obtained from (Jetter et al., 2012)

While it may appear counterintuitive, efficiency and fuel consumption are not strictly related. The user's cooking practices play a critical role and they may not be comfortable with an efficient system or with the type of fuel that would be used. A highly efficient cookstove does not necessarily reduce fuel consumption, and thus quantifying variables is not as straightforward as it would seem. Adding to the complexity is the fact that the physical behavior of fuel is not simple. Unlike other combustion or energy extraction machines, solid biomass goes through different thermo-chemical processes which affect the behavior of the variables. As there is not one measure that truly characterizes a cookstove, it was necessary to develop several measuring protocols.

WATER BOILING TEST -WBT-

The most established testing protocol is the Water Boiling Test, currently at version 4.2.3. It is designed to measure the thermal efficiency and fuel consumption (optionally the emissions) of a cookstove during three phases of combustion: 1) High power (cold start), where the device's body temperature is equal to the ambient, 2) High power (hot start) and 3) Simmering. In the first two phases, the initial temperature of the water is determined and the fuel consumed until the water reaches a boiling point is measured, as well as the time. In the third phase, the amount of fuel required to keep the water at a simmer is calculated. For details see (Committee et al., 2014).

This protocol is one of the most widely used and provides useful information for comparison and understanding of the behavior of the device in controlled conditions. Unfortunately, it does not provide information on the real-world behavior of the device. For that reason, other protocols like the Controlled Cooking Test -CCT-, were developed.

CONTROLLED COOKING TEST -CCT-

The Controlled Cooking Test is designed to compare the consumption of fuel per cooking task of two cooking technologies (usually a traditional versus an improved one) in a more realistic scenario. The evaluation takes place in the field, and the cooking is performed by a local cook who chooses the meal and decides when the cooking process has been completed (Baillis, 2004).

KITCHEN PERFORMANCE TEST -KPT-

This extensive protocol provides a more realistic evaluation of the impact of stove interventions on a household's fuel consumption. Its two main goals are: 1) to assess qualitative aspects of stove performance through household surveys and 2) to compare the impact of improved stoves on fuel consumption. Although this protocol provides more reliable information of the real world performance of the stoves, very few studies have implemented it as it demands significantly more resources than the other two (see (Baillis, Kirk R Smith, and R. Edwards, 2007) for further inquiry).

Most of the stove evaluations limit themselves to the WBT e.g., (Jetter et al., 2012), (Nordica MacCarty, Ogle, et al., 2008), (Yuntenwi et al., 2008), (Nordica MacCarty, D. Still, and Ogle, 2010), (Arora, Jain, and Sachdeva, 2013), (Carbone et al., 2016), among many others. This could lead to un-realistic projections as can be seen, for example, in Figure 3.8, where the emissions factor of PM and CO [g/kg] of the stoves in the field is many times higher than in the labs. Only a handful of studies have been conducted with the KPT. According to the most complete examination on the topic done by (Berkeley Air Monitoring Group and Global Alliance for Clean Cookstoves, 2012), 73 % of the studies comprising the 600 unique sets of performance tests were limited to the WBT and only 5% to the KPT, 12% to the CCT and the rest to other types of tests. This reflects the lack of knowledge of the real-life conditions, particularly on the cultural aspects. Thus, it is highly probable that the majority of studies of technology replacement have provided a distorted analysis of their true effects on health and the environment.

1.4 RECENT INTEGRAL PROTOCOLS

The limitation of the currently available protocols has been identified by other researchers (Orange, Defoort, and Willson, 2012), (Ruiz-Mercado et al., 2011), (Bonan, Pareglio, and Tavoni, 2017), (Moses and N. A. MacCarty, 2019), (Moses, Pakravan, and N. A. MacCarty, 2019). Some seeking to improve the process have proposed the use of alternative protocols that take into account cultural aspects and real-life performance.

N. A. MacCarty and Kenneth Mark Bryden (2016), developed an integral evaluation protocol to determine the various energy technologies as applied to meet specific energy needs in a rural developing village. Their model enables the designer to examine a variety of energy technology components subject to local and global constraints and reports the outcomes in terms of multiple objectives including energy consumption, climate effects, health impacts, cost analyses, and social considerations. It enables accounting for important application factors such as usability, multi-functionality, stacking and incomplete displacement of traditional methods, opportunity costs, effective discount rates, and impact

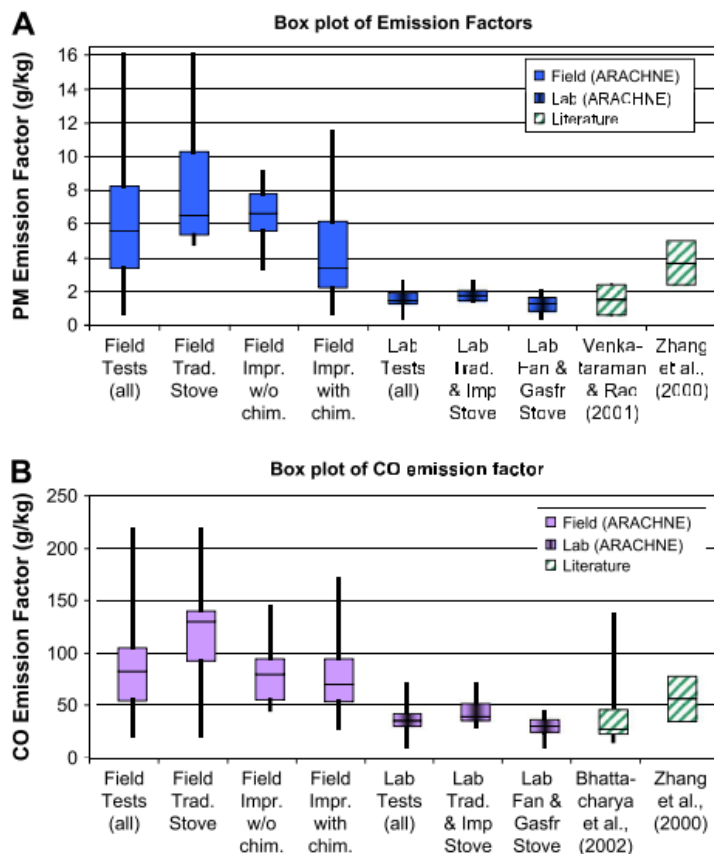


Figure 3.8: Comparison of emission factors
Image obtained from (Roden et al., 2009)

to quality of life.

2. EMISSIONS: AN OVERLOOKED AND POORLY UNDERSTOOD PROBLEM

2.1 EMISSIONS FROM BIOMASS COMBUSTION

Emissions from biomass combustion can be categorized in two, organic and non-organic. All those that contain carbon are organic, and the rest contain the minerals found in biomass like Zn, K, Cl, Na, N , etc. The organic emissions from biomass include soot, which contains organic carbon (adsorbed) and black carbon (solid carbon). The optical characteristics of black carbon make it the second largest most contributing greenhouse gas, with a global warming potential of 900 times that of CO_2 (Bond et al., 2013)². These emissions along with all the others that are not CO_2 pose a potential problem to sustainability of biomass and could create severe health problems.

Biomass residential combustion is the second largest number source of fine particles, especially in China, India and Africa, only preceded by road traffic (Paasonen et al., 2016). It is also the source for 25% of the total black carbon emissions and a major contributor to harmful emissions for the users.

²(See this reference for a detailed study on the effects of black carbon climate forcing, including its interaction with the atmosphere e.g., cloud interaction, snow and ice melting due to albedo reduction, among other key topics

In almost all the literature regarding cookstoves, two variables are generally addressed, low efficiency and harmful emissions e.g., (McCracken and Kirk R. Smith, 1998), (Wilson et al., 2016), (Jetter et al., 2012), (MacCarty et al., 2007), etc. These serve as justification for the development of improved cookstoves. Improvements are measured mainly through the water boiling test (with its already mentioned limitations). Emissions are commonly quantified using the gravimetric approach, which provides information of the emitted *mass*, per unit energy, time, etc..

Studies that address the real impact of these suggested improvements are disappointingly limited. One of the most comprehensive and extensive studies was performed as part of the *RESPIRE* program (*Randomized Exposure Study of Pollution Indoors and Respiratory Effects*) in Guatemala. As of 2018 the most complete study on the impact was the systematic review and metaanalysis by (Megha Thakur et al., 2018).

The researchers found no demonstrable impact on child health outcomes in most of the studies, except for one, which found "a significant reduction of child pneumonia, no significant impact on adverse pregnancy outcomes, no reduction in death due to respiratory disease and no impact on child birth weight". They did, however, find significant reduction of chronic obstructive pulmonary disease (COPD) in women, significant reduction of *PM2.5* and *CO*.

One of the reasons why health outcomes are not as significant as would be desired, is that even though improved cookstoves reduce harmful emissions, they do not completely eliminate them. In fact, the stoves continue to produce emissions at unhealthy levels. Further, the way in which emissions are quantified at this time fails to capture the true negative health impacts, as it will be explained.

2.2 THE MEASUREMENT PROBLEM

The current measurement of emissions in the context of biomass cookstoves is *mass per unit "x"*, almost entirely restricted to particulate matter and carbon monoxide. This is a misleading measurement because it does not include the toxicity of the emissions, and also ignores nitrogen oxides which are harmful for both the health and the environment.

The limits set by the World Health Organization (Johnson et al., 2014) and the ISO-standards (ISO, 2018) are in grams per unit power, and using this measurement, the Global Alliance for Clean Cookstoves, based on the work by (Champion and Grieshop, 2019), which they partially funded, concluded that: *"This analysis suggests that pellet stoves have the potential to provide health benefits far above previously tested biomass stoves and approaching modern fuel stoves (e.g., LPG). Net climate impacts of pellet stoves range from similar to LPG to negligible, depending on biomass source and upstream emissions"*.

This and other similar findings, have shifted the development of cookstoves towards pellet gasifiers (see for example (Morgan Defoort, 2015), (J. A. Marchese et al., 2018)). However, these conclusions should be viewed with caution as the findings assume a correlation between efficiency and health. It has been recently demonstrated that particle emissions from more efficient combustion can be more harmful than those of poor combustion. (Torvela, 2015) performed a large study on the toxicity and morphological features of emissions from biomass combustion at three different combustion conditions, namely smoldering, intermediate and efficient. They found that:

"In near-optimal combustion, when the soot formation was low, the small ash particles remained in the ultrafine particle fraction. This size mode is believed to be potentially dangerous due to the small size, large surface area to mass ratio, deep airway penetration, and ability to be retained in the lung [8]. In incomplete combustion cases the particles were partially "filtrated" into the larger particle fraction. When inhaled, large particles are mainly deposited in the tracheobronchial region of the respiratory tract [33] and, therefore, more easily eliminated by the defence mechanisms of the human body."

This has also been reported by (Mitchell et al., 2019), with the additional emphasis that the fuel composition, moisture, air-fuel ratio, among other variables, also play significant roles.

The higher toxicity of the improved combustion is attributed to the non-organic nuclei that are formed during the pyrolysis process. According to the current theory of particle formation (Warnatz, Maas, and Dibble, 1996), (Poláčik et al., 2018), when gases start to leave the solid fuel, not only "break-up" reactions occur, but also formation reactions, which are responsible for creating soot and other molecules, like benzene and other aromatics, leading to soot molecules. The focus here is on the non-organic emissions, particularly on Zinc, as it is considered to be the most harmful (Torvela, 2015) and one of the most abundant (Sippula, 2010).

As the temperature raises and reaches the vaporization point of the alkali compounds present in the fuel (which are necessary for the plant's growth), small particles are released. In poor combustion, the air-fuel ratio and temperature, allow for the nuclei to grow via condensation and coagulation, and further into accumulation. Figure 3.10 by (Poláčik et al., 2018), depicts the particle growth process.

During efficient combustion, the particle formation process stays in the nucleation side and does not grow, hence, the aerodynamic diameter of the particles remains smaller, (See Figure 3.11), which allows the particles to penetrate deeper into the lungs (See Figure 3.9. So, although the total emitted mass is reduced, giving the impression of reducing the harmfulness of the emissions, the change in aerodynamic properties and chemical composition, changes the harmful potential.

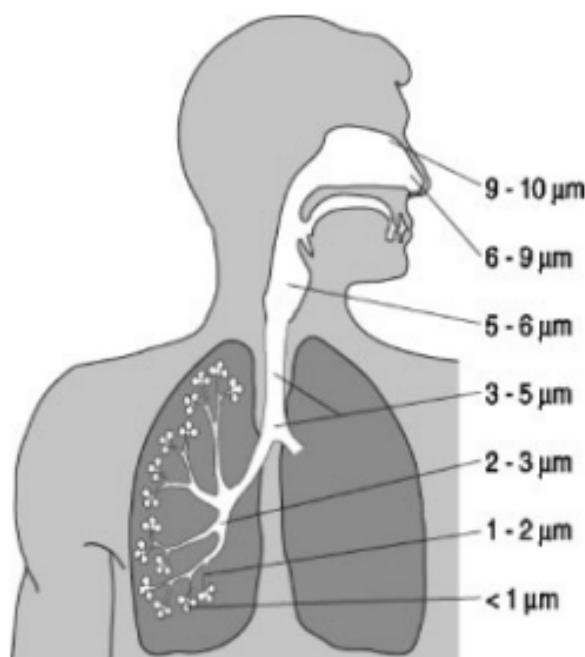


Figure 3.9: Particle deposition in the respiratory system
Image obtained from (Hertzberg and Blomqvist, 2003)

Recent in-vivo and in-vitro studies have demonstrated that the particles emitted from high efficiency combustion are more toxic than those from poor combustion (O. J. Uski et al., 2012), (O. Uski et al., 2014), (Dilger et al., 2016), (Huff, Carlsten, and Hirota, 2019). And the number of particles remains high (Shen et al., 2017), (Mitchell et al., 2019).

These findings regarding the increase in toxicity should not be misinterpreted, because despite the increase in toxicity, the overall emissions are reduced (Leskinen et al., 2014), (Kelz et al., 2010), (O. Uski et al., 2014). Another important remark is that the methods they have used to compare the toxicity are misleading in some cases. For example, (Happo et al., 2013), performed a test in lung cells

on a mass basis exposure. Here again, the comparison is ill-posed as the toxicity of each substance is different, and the real-life exposure would vary and be influenced by the aerodynamic diameter, among other parameters.

Clearly, more research should be conducted for better understanding of the health effects of high-efficiency combustion, preferably in real-life scenarios, in order to better determine what is the best solution to the current situation and to be able to compare the different technologies and fuels. For example, with Eq. Eq. 9.1, the emissions from LPG, open fire and gasification technology could be compared qualitatively and quantitatively to determine the best option. With the current measuring system, LPG and gasification technology are considered clean, but still LPG also emits significant amounts of ultra fine particles, specifically, $1.6 \cdot 10^7 \text{ particles/cm}^3$ and firewood $4.9 \cdot 10^7 \text{ particles/cm}^3$ both for PM_{10} (Shen et al., 2017). Hence, the criteria for "cleanness" is not clear.

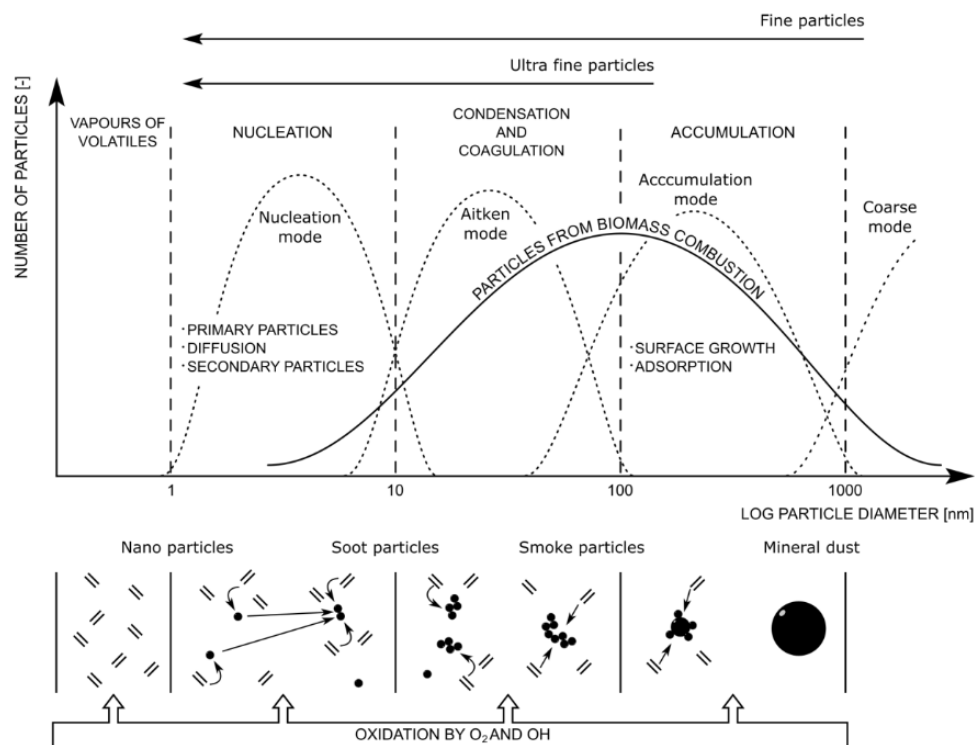


Figure 3.10: Soot formation process
Image obtained from (Poláčik et al., 2018)

2.3 POSSIBLE TECHNICAL SOLUTIONS

The emissions from biomass combustion can be addressed in two ways, during their genesis, presented in Figure 3.10 (primary measures i.e., by design), or at the exit once they have been formed (secondary measures).

Two possible secondary measures are the use of filters and the use of electrostatic precipitators. (D. K. Still et al., 2018) found an 80% reduction of $PM_{2.5}$ using simple filters. (Intra, Limueadphai, and Tippayawong, 2010) used a "simple and inexpensive" electrostatic precipitator with a collection efficiency of 70% for fine particles. Other studies that have treated this topic are (Migliavacca et al., 2014), (Lind et al., 2003), (Bologa, Paur, and Koerber, n.d.), and (Talukder, Park, and Rivas-Davila, 2017). The last one designed a low-cost portable electrostatic precipitator tailored for rural households and found significant reduction.

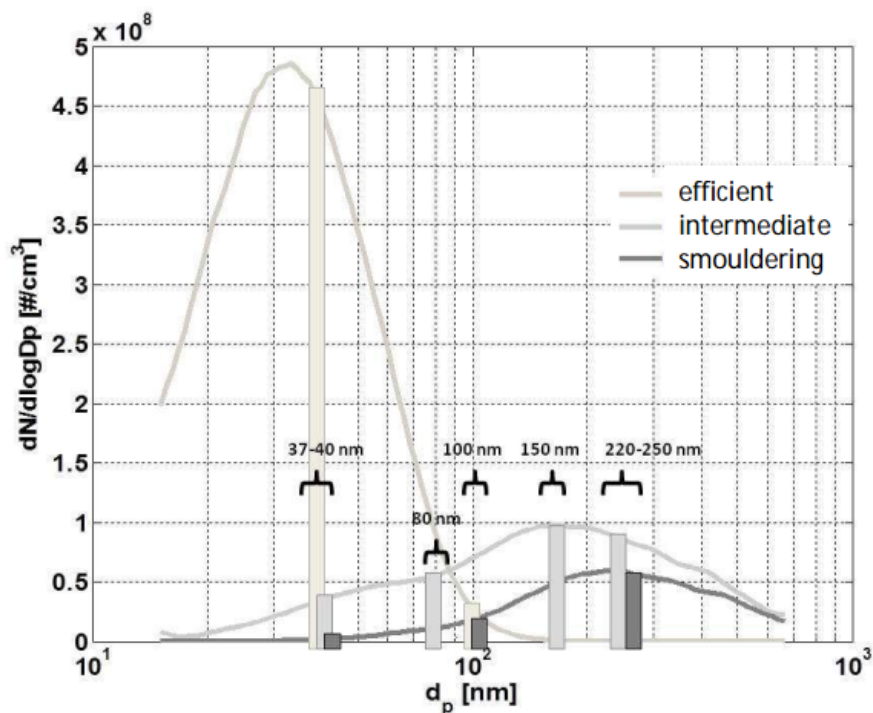


Figure 3.11: Emissions number density and aerodynamic diameter from three combustions regimes
Image obtained from (Torvela, 2015)

It is obvious that the use of secondary measures implies an increase in complexity and cost. Costs are not described here but since the goal of these research is to address the energy needs of people with highly limited resources, reduction of cost at in the design phase is preferred.

Obernberger et al. developed a new approach for biomass combustion using an updraft gasifier directly coupled with a burner with the purpose of minimizing the emitted particles from a large scale installation (2017). They report a reduction of 2 orders of magnitude by primary measures.

2.4 CONCLUSIONS

1. People in developing countries striving to meet their most basic energy needs (cooking) find current available technologies are inefficient and highly polluting. While efforts to create improved technologies have reported higher efficiencies in laboratory tests, real-life scenarios have failed to duplicate these results as in these settings, efficiencies decrease and emissions increase by several folds.
2. The currently available technologies have common problems, like high energy losses in the stove body and hot-flue, poor control over the air-fuel ratio, flame quenching, poor mixing of fuel-oxidizer, excessive air in the system due to draft, and cultural and technical unattended barriers.
3. The most recently promoted technology by the largest cookstove institution -the Global Alliance for Clean Cookstoves-, is called the TLUD stove. It relies on the availability of biomass pellets, which are mostly out of reach for people living in poverty. Also, the power control is challenging to use and the batch feeding process clashes with the traditional semi-continuous feeding of tra-

ditional technologies.

4. Most of the evaluations of the performance of improved cooking technologies are limited to the *Water Boiling Test*, which fails to capture the cultural variables. The largest study on stove evaluations found that out of 600 cases, 73% were limited to the WBT, and only 5% did the more realistic KPT test. This points out to the huge failure in understanding and addressing the cultural implications (and needs) of biomass cooking technology replacement.
5. The current way of measuring the cleanliness of a stove is vaguely defined. Methods of measuring the amount of pollution generated by a cooking technology fail to address the toxicity, exposure time, and penetration depth of the molecules, and is mostly restricted to only two parameters i.e., *CO* and *PM*. Furthermore, there is the general assumption that less emitted mass means less harmful emissions, when in reality the number of particles, chemical composition and exposure time determine the harmfulness of the emissions. Attention should be focused here because high efficiency combustion leads to smaller aerodynamic diameter of the emitted particles, higher particle number and more toxic composition due to the alkali nuclei which evaporates from the biomass.

"The Kulkan", a novel biomass reactor with increased efficiency by heat recovery and combustion optimization

A silhouette of a person standing on a hill, looking out over a city at sunset. The sky is a gradient of orange and blue, and the city lights are visible in the distance.

4

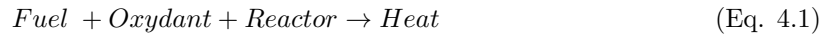
1. KULKAN, A NOVEL BIOMASS REACTOR

As it has been shown, the task of replacing traditional cooking technology is neither trivial nor simple. Finding a solution necessitates a holistic approach because it is the energy core of one third of the world's population. Daily life, economically, socially, culturally, and environmentally, revolves around the quest to secure and convert an energy supply. Social variables are thus determinant in the processes of replacing the current technologies.

During the design phase, the needs of the populations, their cooking habits, and locally available energy resources must be taken into account, and not merely the technical ones. Implementation and follow-up phases cannot be limited to delivering products and returning months afterwards. The lessons from (Simon et al., 2014), (Sedighi and Salarian, 2017), and (Gifford, 2010) should be taken into account.

To address these issues, a clear conceptual division between a *reactor* and a *cookstove* is proposed. The *reactor* is the apparatus wherein fuel reacts and, as a consequence, releases heat (conceptually in Eq. 4.1). The *cookstove* is the device that can be used for the user activities (conceptually in Eq. 4.2), like cooking, boiling water, drying grains, etc. The reason for this division is that the reactions that produce the heat are governed by physics, and to a lesser extent by human intervention, only through fuel feeding rate, choice of fuel and air flow rate via opening control. Further, it is in the reactor where the thermochemical processes occur and hence the formation (or absence of) particulate matter occurs either the vaporization of alkali nuclei or the growth and agglomeration of organics that lead to the formation of polyaromatic hydrocarbons -PAH-. Hence, it is in this domain that the physics can be controlled by geometrical design and the efficiency can be maximized and the harmful products minimized.

It is important to notice that the reactor and the cookstove must remain coupled in certain parameters that are common to the "integrated" system, for example, the type of fuel, feeding process, scales (dimensions, power output).



Once the geometry of the reactor is tailored such that the thermochemical behavior is optimized so most of the heat is extracted and delivered on a surface where the application will take place, then the design of the cookstove can begin, taking into consideration the user's input, subject to certain geometrical constraints that should not be in contradiction with the users behavior and habits e.g., top feed pellet gasifiers or using fuel that is not available.

This approach is based on the arguments presented in Section 2, and driven by the conclusion therein that there is an urgent need to replace the current development model and the energy systems that power it. The design of the reactor should also take into account the locally available resources.

Other researchers have arrived at similar conclusions. For example, (Sedighi and Salarian, 2017) conducted an extensive literature review of the technical aspects of biomass cookstoves. Their top recommendations for future research are:

- "Research should develop an algorithm for cookstove and cookware design using technical (operating, material and geometric variables), social (cooking habits and local fuel resources) and economic (market demand and economic justification) considerations [6]. Before construction and evaluation of a prototype, mathematical and numerical modeling and optimization methods are necessary to provide insight into cookstove and cookware function to improve performance.
- A cookstove should be developed based on social and cultural considerations such as cooking habits, which differ according to ethnic and geographical issues and local fuel resources. In addition to international standards and protocols, local standards and protocols should be developed to better assess cookstove performance as in Arora [sic] et al."

Based on the literature review, field experience, and the works by (Sedighi and Salarian, 2017), (Jetter et al., 2012), (Quan-Reyes, Goel, and Mora, 2020), (Karl, 2014), a biomass reactor is proposed, with three variations for different combustion conditions.

The reactor comprises three reaction zones instead of the typical one or two, and a separation of the gasification and combustion zones, which should allow continuous feeding. In turn, this should relax the computational expense for simulations as the homogeneous and heterogeneous phases could be "decoupled", mostly due to the radiation of the coming from the homogeneous combustion of the pyrolysis gas, not reaching the fuel bed (See (Galgano and Di Blasi, 2006) for details).

Another expected feature of the decoupling of the gasification and combustion zones, is that this would allow for multi-fuel usage, as the syngas-gas composition differences are negligible for the combustion process (Chanphavong and Zainal, 2019) when the gasification occurs in high temperatures (Sedighi and Salarian, 2017). Although this seems to require further investigation for the type of application needed here, therefore, the study will focus only on solid biomass, particularly wood.

In the combustion zone, it is also proposed to use a flame stabilizer (burner) to minimize the formation of soot due to quenching of the flames on the sides and on to the pot surface (see 3.2). The idea is to allow the flames to complete the combustion reaction without disturbing the flame by strain or wall quenching.

The essence of the Kulkan reactor is based on the following hypotheses.

1.1 HYPOTHESES

- 1. Heat recovery by an air pre-heater:** The draft created by the expansion of hot gases in the inner side of the chimney is sufficient to pull air via the annular region of the chimney, which recovers heat from the flue gas (See 4.1 (1)), without the use of auxiliary equipment e.g., (electric fans). This air is later used in the pre-mixing of syngas. The air pre-heater increases the flow resistance and in turn reduces the excessive amount of air (See (Prapas et al., 2014)), thus allows to have an air-fuel ratio closer to the stoichiometric point, hence improving the combustion and allowing higher efficiency.
- 2. Flame quenching prevention:** Stabilizing a partially pre-premixed flame in a laminar regime, allows the flame to fully develop and prevents quenching (See 4.1 (2)), thus it reduces the formation of soot and the amount of unburned hydrocarbons, in turn reducing pollution and increasing efficiency.
- 3. Alkali fly-ash prevention:** By using a burner, and increasing the resistance to the flow upstream, the flow velocity at the fuel bed is reduced, in turn, the skin friction is reduced, which allows for ultra-fine alkali particles to fall as bottom ash, instead of being entrained as fly ash (See 4.1 (3))

Hypotheses visual summary

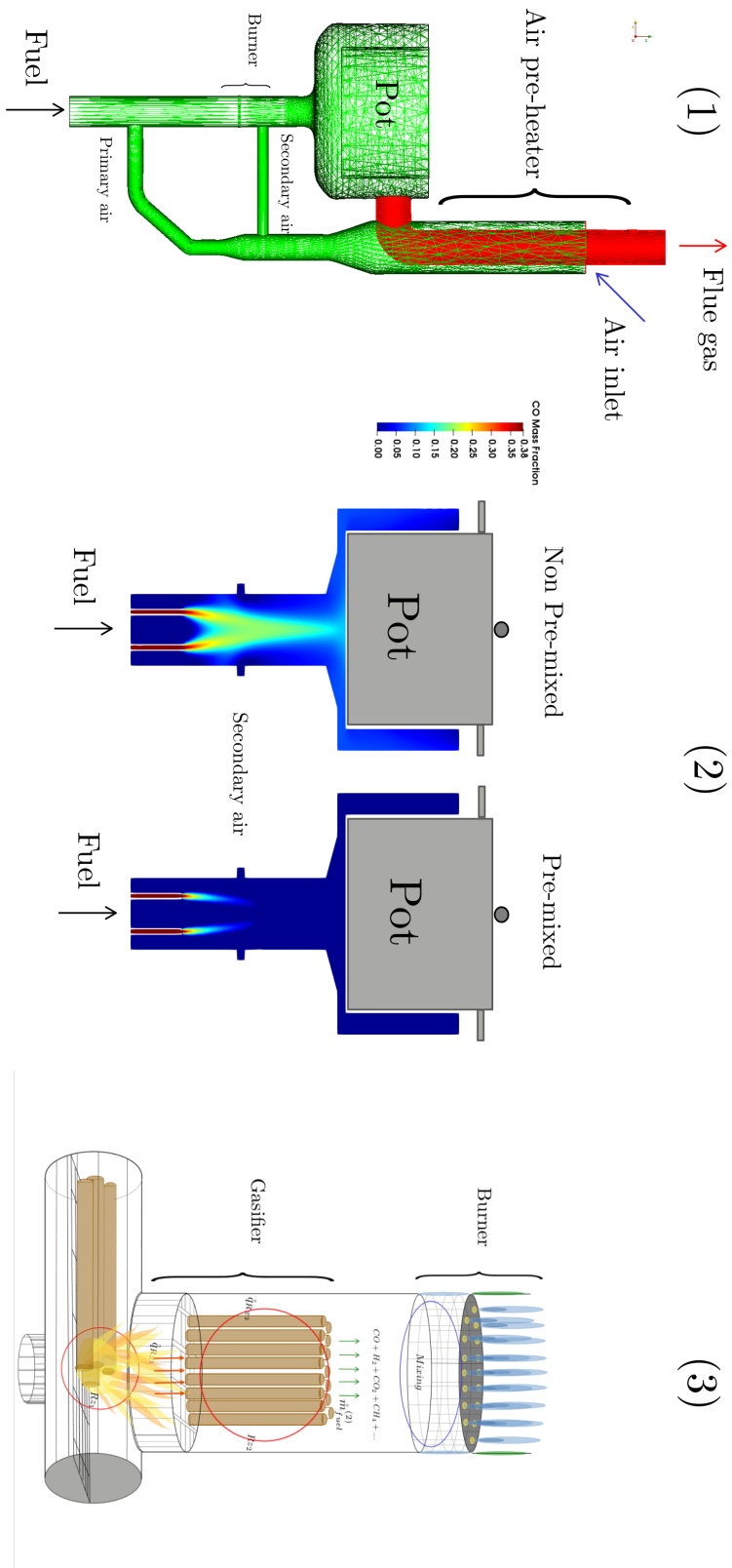


Figure 4.1: Hypothesis map

Hypothesis 1:
Heat recovery by an air pre-heater

Hypothesis 2:
Flame quenching prevention

Hypothesis 3:
Alkali fly-ash prevention

Biomass Reactor Design 1: Partially premixed laminar combustion

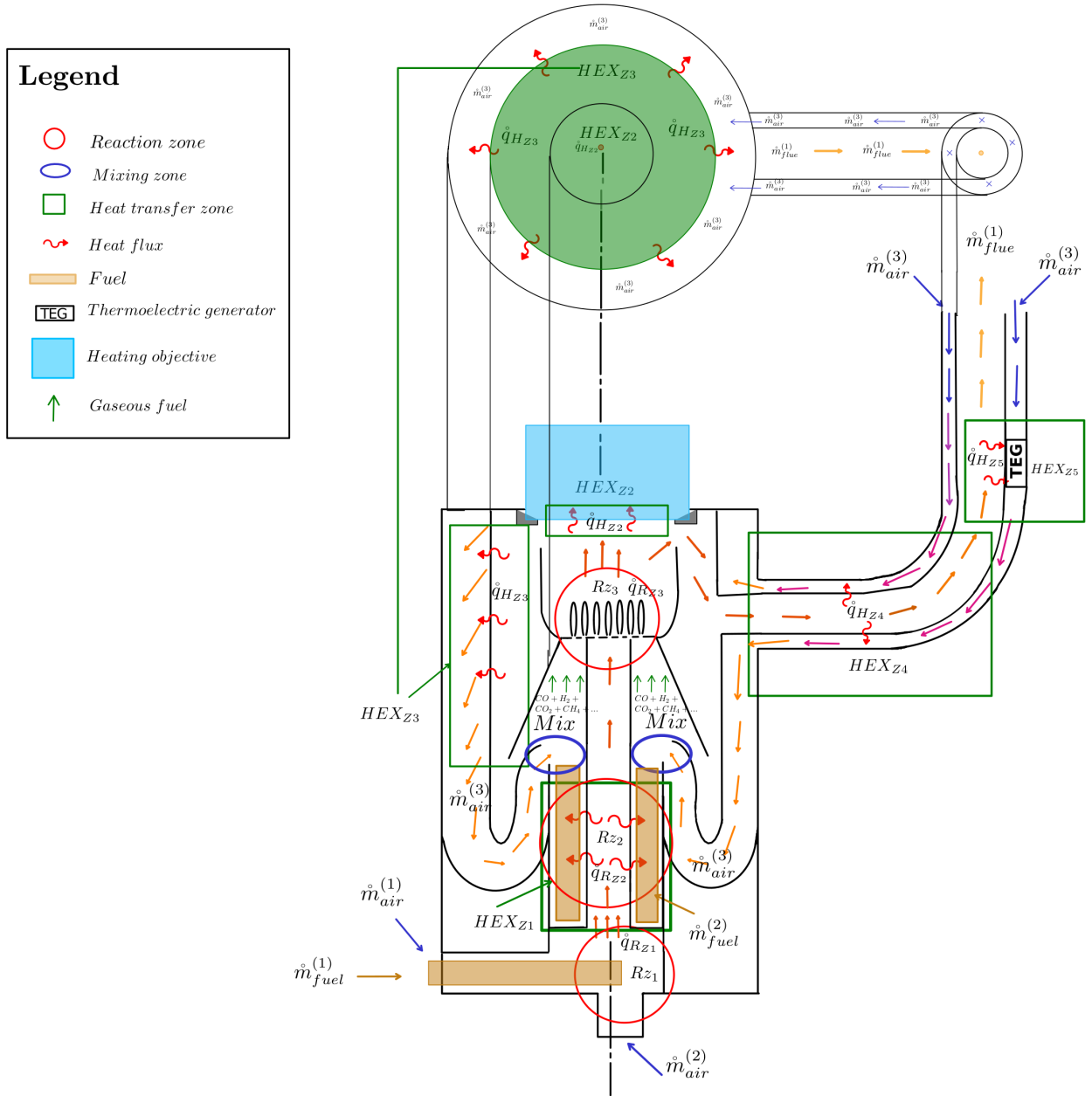


Figure 4.2: Kulkan design 1: partially premixed laminar combustion

In the design presented in Figure 4.2, Fuel $\dot{m}_{fuel}^{(1)}$ is fed at the bottom of the system, it is partially burned in the **Reaction Zone 1** (R_{z1}), with the primary air $\dot{m}_{air}^{(1)}$ and $\dot{m}_{air}^{(2)}$, the heat released (q_{z1}) is partially distributed to the second fuel $\dot{m}_{fuel}^{(2)}$. The heat absorbed by this fuel (q_{z2}) in the **Heat Exchange Zone 1** (HEZ_{z1}), powers the endothermic gasification reaction in the **Reaction Zone 2** (R_{z2}). The product gas is mixed at the mixing zone with incoming preheated air $\dot{m}_{air}^{(3)}$. This mix is then burned in the **Reaction Zone 3** (R_{z3}), where the flames are stabilized in a burner, and allowed to fully burn to prevent flame quenching by direct impingement. The heat released by the flames (q_{z3})

Biomass Reactor Design 2: Turbulent combustion

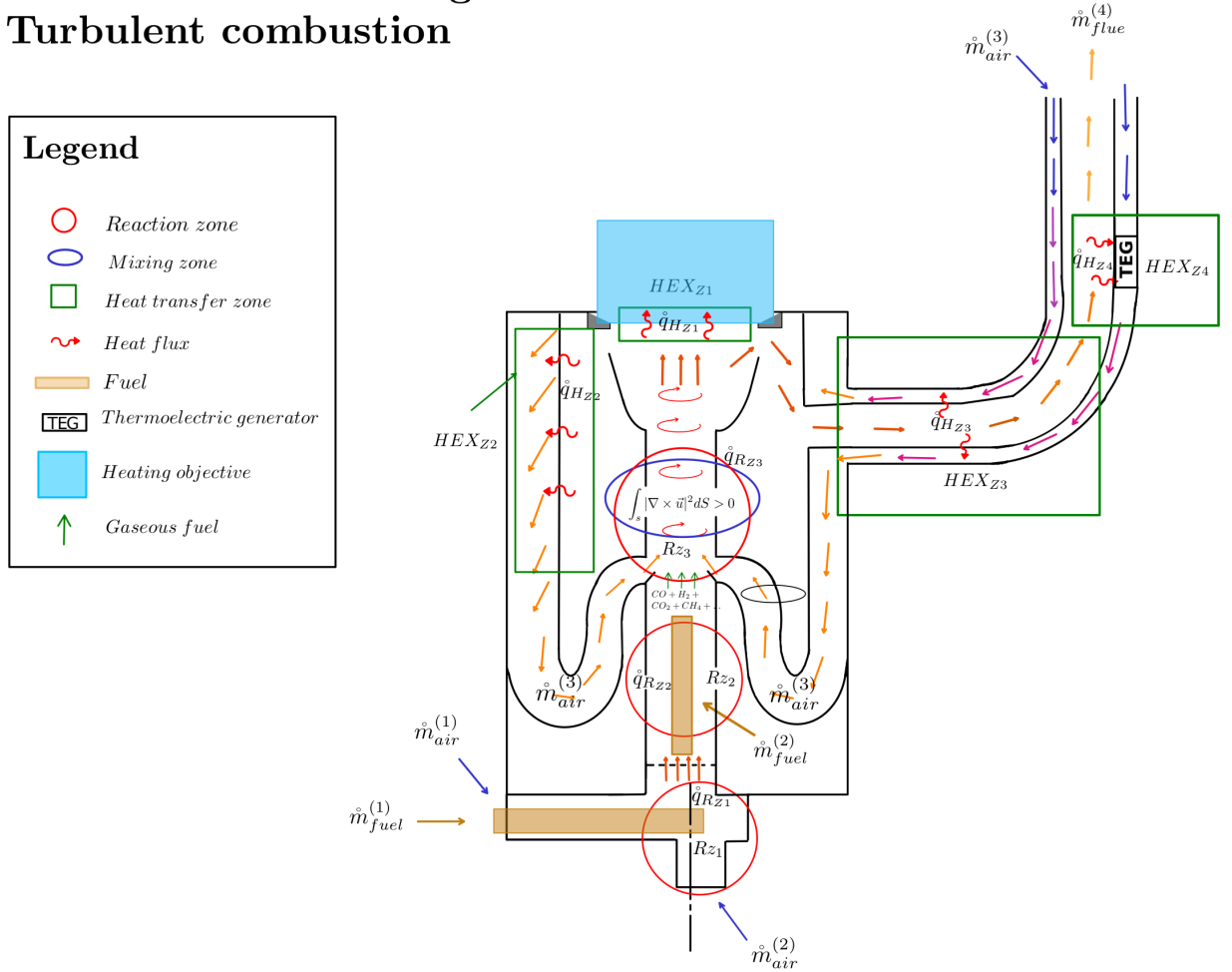


Figure 4.3: Kulkan design 2: non-premixed turbulent combustion

is then focused on the heating objective placed on the **Heat Exchange Zone 2**.

Common for all reactors is that a part of the heat (\dot{q}_{z3}) (which before was a loss (14–42)% (Sedighi and Salarian, 2017)) will now be recuperated in the **Heat Exchange Zone 3**, and used to pre-heat the $\dot{m}_{air}^{(3)}$ used for the pre-mixing. The hot gases will be forced to pass very close to the top before they can exit through the concentric pipes where previously heat was lost (22–39%) (idem)) **Heat Exchange Zone 4** will now be used to start pre-heating the $\dot{m}_{air}^{(3)}$. A thermoelectric generator could be placed at a specific region to make use of the thermal gradient to produce electrical energy to power a fan (for the start-up phase), and then to generate electricity for illumination and other electrical needs.

In the design presented in Figure 4.3, the main difference with the previous one is that the gaseous fuel coming from the **Reaction Zone 2** is burned in a turbulent regime. The trajectory of the flow changes and also the time in which the reactants are in the reaction tube. This would ensure enough reaction time to reach a complete combustion.

The other difference is that the $\dot{m}_{fuel}^{(2)}$ is exposed directly to the upcoming gases from the partial combustion at the **Reaction Zone 1**, instead of being exposed only to the heat by conduction across

Biomass Reactor Design 3: Diffusive combustion

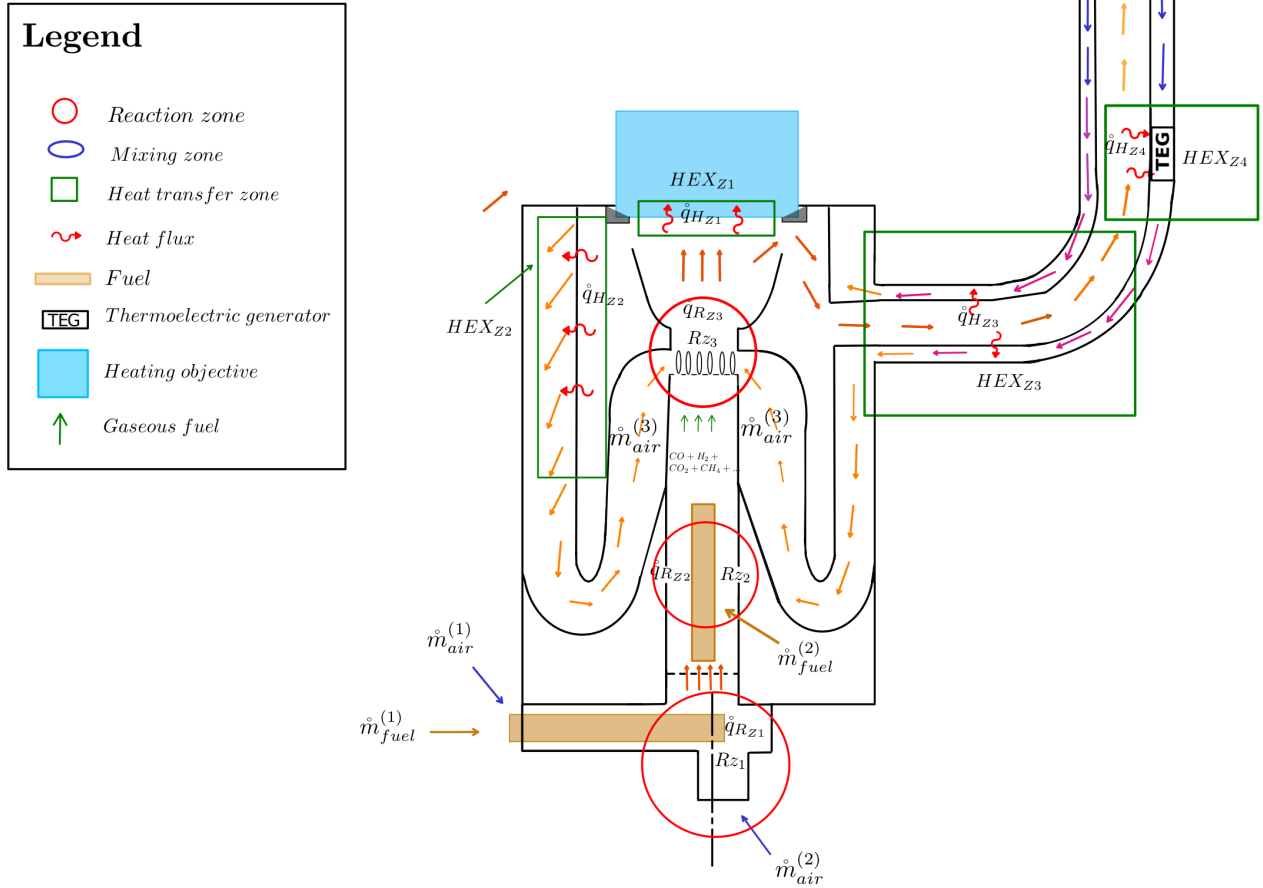


Figure 4.4: Kulkan design 3: non-premixed laminar combustion

the wall as in the previous design. This could ease the ash extraction and reduce the construction complexity, although this will be evaluated later on.

The design presented in Figure 4.4 is a combination of the previous two. The idea is that the $\dot{m}_{fuel}^{(2)}$ is exposed directly to the upcoming gases from the partial combustion at the **Reaction Zone 1**, but they are burned in a stabilized diffusive flame at the **Reaction Zone 3**.

Detailed conceptual drawings are presented in Figure 4.5 and 4.6, which serve as visual aid to understand the main phenomena that can be expected to be present in the gasification and combustion zones. It is important to notice that the dimensions presented there are simple first guesses based on experience and logic. No detailed studies had been performed at the moment and the real geometrical parameters are determined in the upcoming chapters.

A summary of the specific and common technical aspects of each one of the conceptual designs is presented in Table 4.1.

Table 4.1: Specific and common technical aspects of each conceptual Kulkan version

Combustion regime	<i>Partially premixed laminar</i>	<i>Turbulent non-premixed</i>	<i>non-premixed laminar</i>
Specific aspects of each design	1. The syngas coming from the solid biomass premixes with hot air before reaching the burner, where it ignited and stabilizes. 2. The flow regime is expected to be in the low Reynolds number.	1. Since there is no burner, less resistance to the flow is expected, and in turn higher flow speed, and thus higher Reynolds number. The fuel is burned in a non-premixed way with hot air coming from the air pre-heater. 2. Another remark of not having the burner is that the radiation from the flames would reach the fuel bed, and could not be de-coupled like in the cases with a burner.	It is similar to the partially premixed case in terms of flow regime, but it differs in such that the fuel and the oxidizer are not premixed. Longer flame lengths and more unburned hydrocarbons could be expected.
Common aspects to all designs	The largest fraction of the fuel is gasified with the energy supplied by the reaction zone 1. The phenomena driving the flow is the draft caused by the expansion of the gases. An air pre-heater adds resistance to the flow, reducing the excessive amount of air to values closer to the stoichiometric ratio. An "air jacket" is added as an insulator around the gasification and combustion zones.		

Detailed diagram of Design 1 and 3 (Laminar)

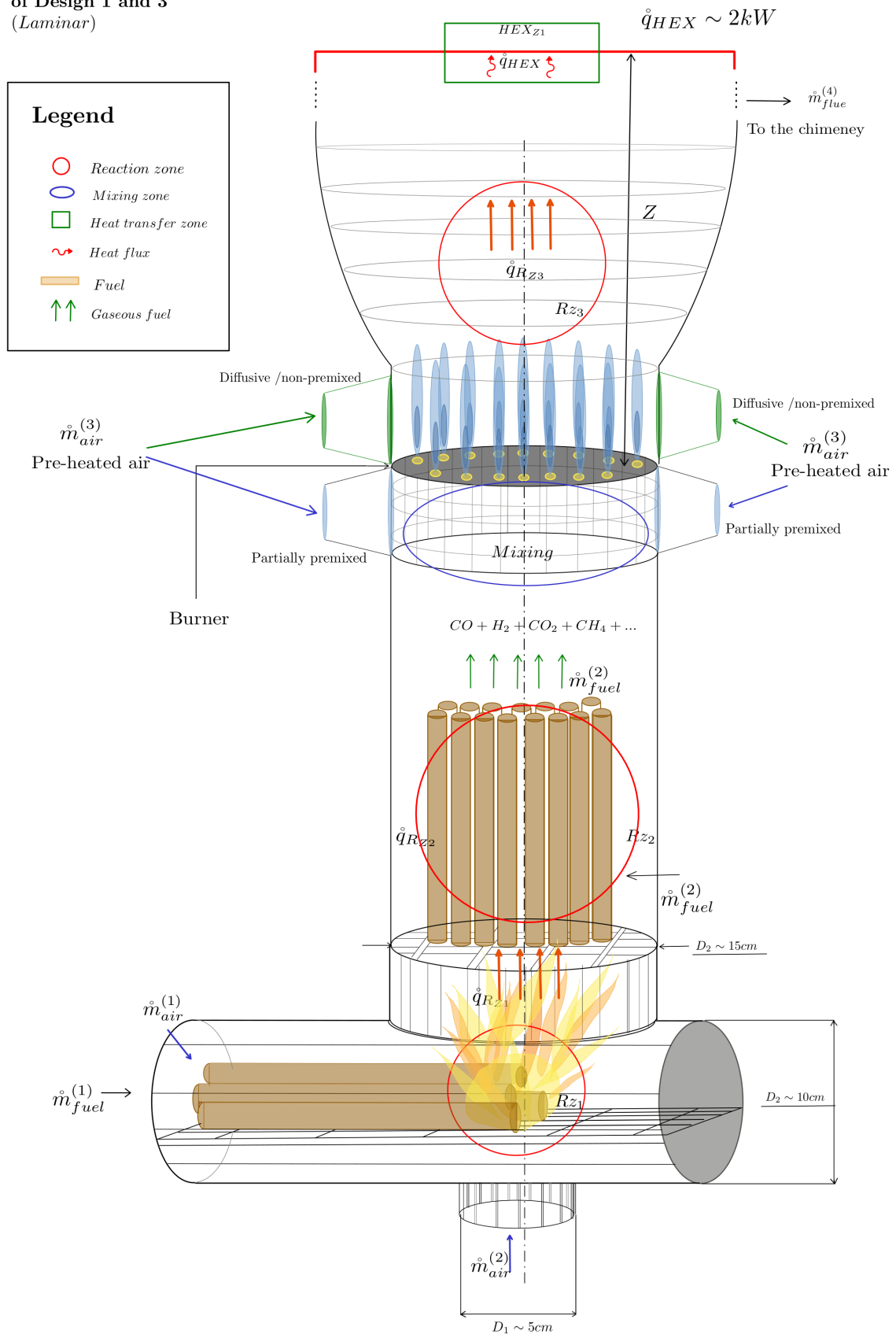


Figure 4.5: Detailed conceptual drawing of the Kulkan's gasifier and burner for laminar combustion

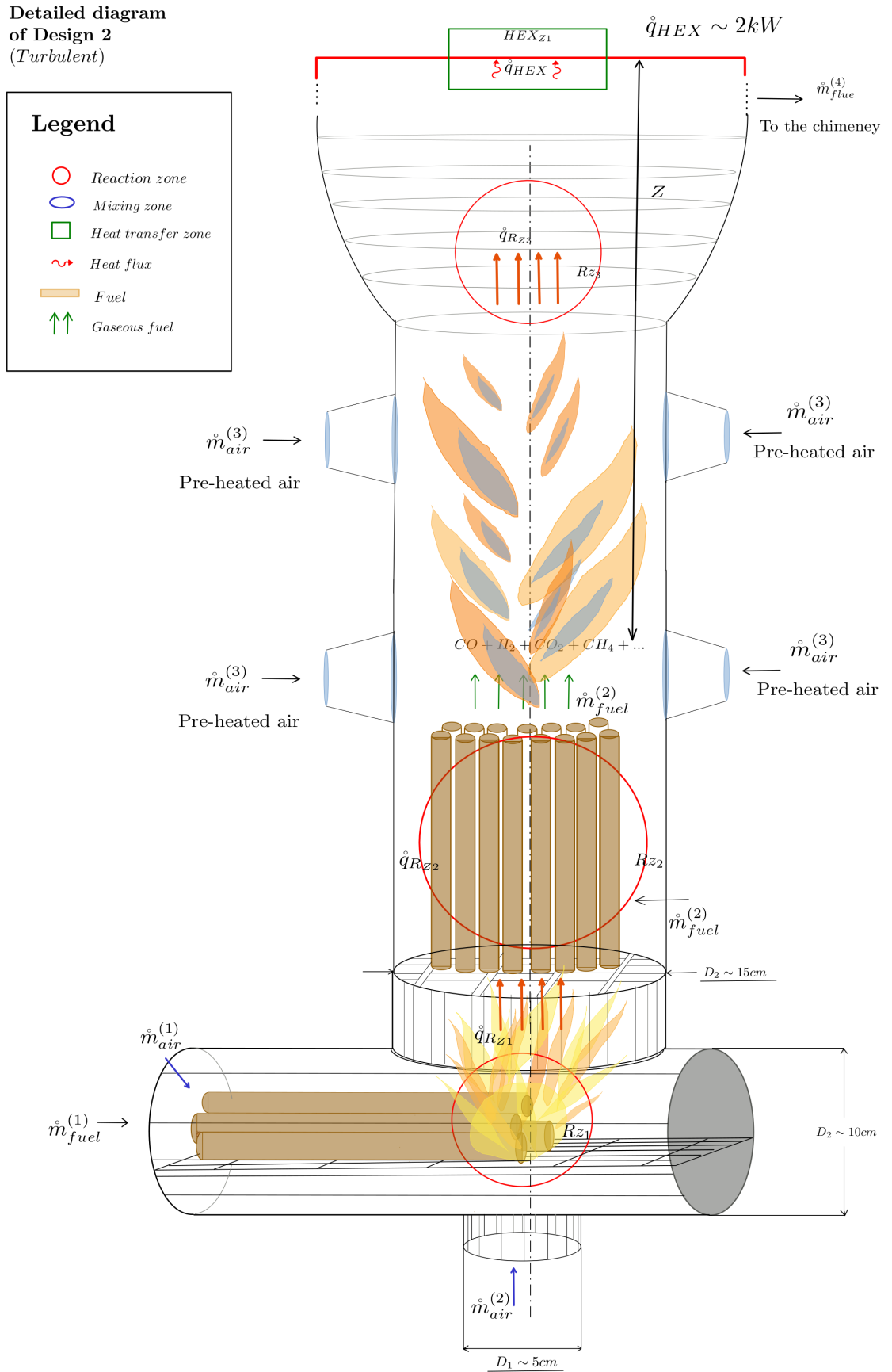


Figure 4.6: Detailed conceptual drawing of the Kulkan's gasifier and burner for turbulent combustion

2. VALIDATION APPROACH

Out of the three different conceptual designs, the *partially premixed laminar combustion* allow the three hypothesis to be tested. The non-premixed cases (laminar and turbulent) would only allow for hypothesis 1 and 2 to be tested, therefore, the first design was further studied.

The hypotheses were tested by different mathematical approaches, namely an algebraic model (0-D, 1, 2 and 3D detailed models computational fluid dynamics -CFD- simulations of reacting flow. The models were limited to the homogeneous phase, as it was the one of most interest. The results were validated with experimental data before being applied to the new proposed reactor. No own experiments could be carried out due to constraints imposed by the COVID-19 pandemic. Nevertheless, the models are considered to be sufficiently accurate to provide insight into the validity of the hypotheses and to guide future research.

For the **Hypothesis 1**, a general "0-D" model was initially constructed based on similar approaches found in literature. Here, the combustion was modeled as a *perfectly stirred reactor*, discretization in the form of "zones" was performed and empirical correlations for the heat-transfer were utilized. Furthermore, the model was extended to include the chimney which was modeled as a plug-flow pipe. This model allowed the first rough optimization of the geometrical parameters of the reactor, which then were used for more detailed studies.

For the **Hypothesis 2**, "1-D" and "2-D" simulations were carried out to understand some of the limiting factors of the pre-mixed laminar case, particularly in terms of the flame speed. Extensive validation of a 2-step chemical mechanism compared with a 24-step one were carried out to determine the accuracy of the more economic one.

In addition, several "3-D" detailed simulations of the homogeneous reaction parts were performed, for non-reactive hot flow and reactive flow cases in order to understand the main physical phenomena and the flow behavior. Different geometrical variations of a full-scale Kulkan reactor were used.

For the **Hypothesis 3**, no experiments were suitable to be performed, and the currently available soot formation models are limited. Therefore, logical arguments were presented which support the hypothesis and guidance on how to test it are presented.

The thermochemical phenomena in biomass conversion as an energy source and its mathematical modeling

5



1. BIOMASS

Biomass is the organic matter generated by a biological process. Here, the focus will be on vegetable biomass which is produced by *plantae*, via photosynthesis.

The three most abundant organic components found in biomass are: 1) cellulose, which is a homopolysaccharide $C_6H_{10}O_5$ and constitutes the main part of the cell walls of plants, it is the world's most common biopolymer. 2) hemicellulose, which are heteropolysaccharides of C_5 and C_6 sugars and it is associated with the cellulose, it serves as a frame cementing material in plant cell walls, holding together the cellulose micelles and fibers. 3) Lignine, which is an amorphous polymer constituted of complex and heterogeneous three-dimensional networks of aromatic substructures, they form the woody cell walls and they give the plant its structural strength (De Jong and Van Ommen, 2014).

Biomass also contains inorganic material which is essential for the growth process. The most relevant essential plant nutrients are (in descending order of mass percentage): N, K, P, Ca, Mg, S, Cl, B, Fe, Mn, Zn, Cu, Mo.

The complex bonds of biomass require energy to be formed, this energy comes from the incident radiation of a light source (typically the sun) which is transformed into chemically bonded energy, or stored energy for practical terms.

Such energy can be used by increasing the entropy or "degrading" it in two ways, namely, the biochemical or the thermochemical routes. Here, attention will be put to the thermochemical pathway, which is divided in sub-processes: drying, pyrolysis, gasification, combustion and liquefaction (Basu, 2010) The first four processes are of interest in this study, as combustion is the focus and drying, pyrolysis and gasification are its precursors.

From here on, special attention will be put to the gasification and combustion of wood, as it by far the most used form of biomass energy in the world ([Clean Cooking Alliance 2020](#)), (FAO, 2019).

2. BIOMASS THERMOCHEMICAL CONVERSION

The extraction of energy from the chemical bonds of biomass by means of thermochemical conversion is a complex 3-dimensional time dependent process that involves multiphase flow, thousands of chemical reactions and variability of the phenomena due to fuel composition and operating conditions and a broad spectrum of time scales, going from the relatively fast combustion reactions and the slow drying and pyrolysis ones.

The thermochemical conversion of biomass, in general, does not include high pressure nor use of liquids like in super-critical gasification or liquefaction, and in the following it is restricted to the case of atmospheric pressure.

In the Appendix, a detailed description of the thermochemical processes which make solid biomass turn into "synthetic gas" a.k.a., "syngas" is presented. This includes drying, torrefaction, pyrolysis and gasification. Mathematical models available in the literature which have been used and validated with experimental data are presented, with the intention of providing a guide for future modeling. From here, focus will be in the thermochemical processes regarding the gaseous phase (homogeneous), and its modeling, because the essence of the Kulkan's hypotheses concern the combustion of the syngas coming from the solid biomass.

3. STATE OF THE ART IN BIOMASS THERMOCHEMICAL CONVERSION MODELING

The modeling of biomass thermochemical conversion is a useful tool that provides fundamental understanding of the physical phenomena, which then enables the optimization of parameters for desired

purposes.

Several efforts have been developed through history for modeling the complex physics of the thermochemical conversion, from the most basic ones assuming no spacial differentiation of the domains (0-D), restricted to sets of algebraic equations, to the most complex ones like in 3-D spatial and temporal discretization schemes using computational fluid dynamics -CFD- of reactive flow governed by partial differential equations. Each type of model provides information at different scales, with varying computational cost. For example, the less complex ones are capable of providing useful insight of the "bulk" variables, like average temperatures, flow speed, air-fuel ratios, and efficiency, at a relatively low computational cost and mathematical complexity. The more complex ones are capable of providing information on the specific details of the fluid and thermodynamics, as well as the chemical reactions. All the models are based on three physical principles, mass, momentum and energy conservation.

The two most accurate 0-D models done to this day are the works of (Shah and Date, 2011), where they modeled the steady-state behavior of a buoyancy driven rocket stove divided in four zones. Each zone was modeled as a well-stirred reactor taking into account chemical kinetics of char and volatile burning. They model bulk flow velocity using the Bernoulli equation (which they call "*momentum balance*"). The energy conservation follows heat balances using the three modes (conduction, convection and radiation). And their model is capable of providing useful information of the relationship between control parameters (geometrical characteristics, fuel moist, heat losses) and the overall efficiency of an experimental stove.

The second most complete work is that of (Kshirsagar and Kalamkar, 2015). Here, they also modeled a buoyancy driven rocket stove. Their approach is similar to the one of the previous authors in such that they did "zonal" discretization and the reaction zone was assumed to behave as a perfectly stirred reactor (although not explicitly mentioned). They also used the Bernoulli equation and calculated the pressure losses due to viscosity by the so called "discharge" coefficient. Their model was remarkably accurate when compared to experimental data for the bulk parameters, temperatures, flow speed, flow rate. They validated against the experimental data of (Agenbrood et al., 2011a), (Agenbrood et al., 2011b) studies which served as the foundation for their work. This latter author is one of the first ones to provide a mathematical model of the behavior of a stove, and as they point out "*Simplified theories for understanding the behavior of this unexpectedly complex combustion system, along with practical engineering tools to inform its design, are markedly lacking*".

If simplified theories were lacking, more complex models for cookstoves are even more scarce, despite many studies having been conducted on the modeling of biomass combustion using CFD, but only for larger applications.

Zero of the 127 studies analyzed in the extensive review on CFD of biomass thermochemical conversion done by (Dernbecher et al., 2019) were related to cookstoves. On the review by (N. A. MacCarty and Kenneth M. Bryden, 2015), there were only three studies which used CFD to study a cookstove, restricted to pure description, and one which used artificial intelligence for optimizing a geometry, not only describing.

The general structure of the existing CFD models is divided in some or all of the following three sections: 1) the fuel-bed where heterogeneous reactions happen, in this part of the domain is where drying, pyrolysis, gasification and char smoldering combustion occur. The reactions in this region are considerably slower than those of the gas phase, the heat transfer in this part is dominated by conduction; 2) the gas or homogeneous phase is where combustion of the incoming gases from the bed takes place, the heat transfer is dominated by convection and radiation, the later one is coupled with the solid phase reactions as they provide a significant part of the energy required for the endothermic reactions; 3) Additional models to take into account pollutant formation (Dernbecher et al., 2019).

Besides the previous reviews, there is the remarkable work by (J. A. Marchese et al., 2018) where they investigated a pellet fed gasifier stove, which seems to be the most profound in terms of physics and modeling of biomass cookstoves because of the level of detail and depth of their numerical and

experimental methods. Other works from this group have provided valuable knowledge, for example the work by (Morgan Defoort, 2015), (Orange, Defoort, and Willson, 2012), (Tryner, Volckens, and A. J. Marchese, 2018), among others.

Three other works worth mentioning are the one by (Prapas et al., 2014), where they investigated the influence of the draft caused by the expansion of gases in the chimney of a biomass cookstove, using CFD and experimental validation. They found, similarly to (Pundle et al., 2019), that the draft created by the expansion of gases, leads to an excessive amount of air coming into the system, of between [300 – 1250]% higher than the stoichiometric, the third one is that of (Daniel David, 2011), which was the first one to do a 3-D coupled solid-gas, unsteady simulation using *LES* with soot-formation, although under-predicting this last phenomena with great error, to be expected as the Moos and Brookes soot model was developed for mostly methane, and syngas contains less than 10% of it, which according to the author, could have influenced the under-prediction.

The most recent studies are:

- (Pande, Kshirsagar, and Kalamkar, 2018), which is a continuation of the (Kshirsagar and Kalamkar, 2015), where they use CFD to investigate the new parameter defined in their previous work, namely the "Inlet Area Ratio", the second is that by (Husain et al., 2019), divided in two parts (only the first one has been published) where they use CFD to investigate the "hydrodynamics" and homogeneous combustion of a biomass cookstove and optimized the geometry.
- (Pundle et al., 2019) where they investigated a rocket stove using detailed chemistry of the homogeneous phase. They found that there is an excessive amount of air coming into the system, between three times the stoichiometric requirement for high-power (5kW) and higher than ten times for the low power (2kW). They limited themselves to a 2D axis-symmetric simulation.
- The most recent one is that by (Scharler et al., 2020), which although not focused on a cookstove but a heating stove, remains relevant due to the similar physics, and the analysis of the difference in turbulence between the standard $k - \epsilon$ and the $k - \epsilon$ *RNG*, also because it claims to be the first transient study of the combustion of wood. In addition, they coupled the fuel bed reactions with the homogeneous ones. It is important to mention that all of the previously mentioned works have utilized the *Discrete-Ordinates method* for the radiation modeling.

Hence, although there has been work done in the field of cookstove modeling using CFD, the field is still in its early stage, and can prove to be a useful tool for geometry optimization. Moreover, the field of detailed soot formation modeling is still incipient, as the phenomena is not yet well understood.

4. MODELING OF THE GAS-PHASE COMBUSTION

Combustion is characterised by presence of fast exothermic chemical reactions, these reactions require three fundamental ingredients, namely, a fuel, an oxidizer and heat. In this study, the fuel is limited to "syngas" coming from the pyrolysis and gasification of solid biomass from an bottom-lit updraft gasifier, the oxidizer is air and the heat comes from the reaction itself, after it has been ignited.

The study of combustion requires the fundamental principles of classical mechanics, mass conservation, momentum conservation and energy conservation. These laws capture the physics, and allow for mathematical representation.

These laws are represented in the following equations (using Einstein's notation) (Roekaerts, Bohlin, and Rao, 2020):

Mass conservation:

$$\frac{\partial}{\partial t} \rho + \frac{\partial}{\partial x_i} \rho u_i = 0 \quad (\text{Eq. 5.1})$$

Momentum conservation:

$$\frac{\partial}{\partial t} \rho u_j + \frac{\partial}{\partial x_i} \rho u_i u_j = -\frac{\partial p}{\partial x_j} + \frac{\partial \tau_{ij}}{\partial x_i} + \rho g_j \quad (\text{Eq. 5.2})$$

Energy conservation:

$$\frac{\partial}{\partial t} \rho e + \vec{\nabla} \cdot \rho e \vec{u} = -\vec{\nabla} \cdot (\vec{q}_{\text{conduction}} + \vec{q}_{\text{interdiffusion}}) + s_e \quad (\text{Eq. 5.3})$$

Where:

- \vec{u} = velocity vector
- x_i = Cartesian directional vector
- τ = viscous stress tensor
- g = body accelerations
- e = total energy
- s = energy source term e.g., radiation

Radiation plays an essential role in high temperature heat transfer, as is the case here. The modeling of radiation takes into account the composition, temperature and optical properties.

One of the models for the radiation source term is the *Discrete Ordinates Method* -DOM-:

$$s_e = -\vec{\nabla} \cdot \vec{q}_{\text{radiation}} = an^2 \frac{\sigma T^4}{\pi} - (a + \sigma_s) I(\vec{r}, \vec{s}) + \frac{\sigma_s}{4\pi} \int_0^{4\pi} I(\vec{r}, \vec{s}') \Phi(\vec{s} \cdot \vec{s}') d\Omega' \quad (\text{Eq. 5.4})$$

Where:

- $an^2 \frac{\sigma T^4}{\pi}$ = emission term
- $(a + \sigma_s) I(\vec{r}, \vec{s})$ = absorption term
- $\frac{\sigma_s}{4\pi} \int_0^{4\pi} I(\vec{r}, \vec{s}') \Phi(\vec{s} \cdot \vec{s}') d\Omega'$ = scattering term

All the studies relevant in the literature have demonstrated that the DOM is the best solution method for radiation in terms of combination of accuracy and acceptable computational cost.

The change in species is due to chemical reactions i.e., some species transform into others, there is the need for another mass conservation equation.

Species mass conservation:

$$\frac{\partial}{\partial t} \rho Y_i + \vec{\nabla} \cdot \rho Y_i \vec{u} = -\vec{\nabla} \cdot \rho Y_i \vec{U}_i + M_i \omega_i \quad (\text{Eq. 5.5})$$

Where:

- Y_i = species "i" mass fraction
- \vec{U}_i = diffusion velocity
- M_i = molar mass of species "i"
- ω_i = production rate of species "i"

The species diffusive flux requires an approximation, which is often done by the *Fick's* law of diffusion.

$$\vec{J}_i \equiv \rho_i \vec{U}_i = -\rho D \vec{\nabla} Y_i \quad (\text{Eq. 5.6})$$

Different models for the diffusive coefficient D exist e.g., binary, between two component; multicomponent, where one species is considerably more abundant and the others are independent of each other;

mixture diffusivity, where the diffusivity depends on all species. Even more general than Eq. Eq. 5.6 is the case of general multicomponent diffusion when the fluxes depend on the gradients of all species and possibly temperature

Similar to the to the species (mass) diffusivity treatment, the momentum and heat diffusion also require special treatment.

For momentum diffusion:

$$\tau_{xy} = -\nu \frac{\partial}{\partial x} \rho u_y \quad (\text{Eq. 5.7})$$

For heat diffusion:

$$q_x = -\alpha \frac{\partial}{\partial x} \rho C_p T \quad (\text{Eq. 5.8})$$

At last to fully describe the state of the system based on the physical parameters, that is the relationship between pressure, temperature and volume, is covered by the equation of state. Typically, the ideal gas law is used.

$$P = \frac{\rho}{M} RT \quad (\text{Eq. 5.9})$$

With this, the enthalpy of the system can be calculated, defined as:

$$h = \Delta_f^0 + \int_{T_0}^T C_p(T') dT' \quad (\text{Eq. 5.10})$$

Re-writing the energy equation (Eq: Eq. 5.3) in terms of the enthalpy:

$$\frac{\partial}{\partial t} \rho h + \vec{\nabla} \cdot \rho h \vec{u} = -\vec{\nabla} \cdot \vec{j}_q + \Phi_{\text{viscous}} + \frac{Dp}{Dt} + s_e \quad (\text{Eq. 5.11})$$

With:

$$h = e_t - \frac{1}{2} \vec{u} \cdot \vec{u} + \frac{P}{\rho}$$

$$\Phi_{\text{viscous}} = \tau_{ij}$$

$$\frac{\partial u_i}{\partial x_j} \tau_{ij} = -\frac{2}{3} \mu \frac{\partial u_k}{\partial x_k} \delta_{ij} + \mu \left(\frac{\partial u_i}{\partial x_j} + \frac{\partial u_j}{\partial x_i} \right)$$

$$\delta_{ij} = \text{Dirac's delta}$$

These equations relate all the interested physical parameters of interest, however, they are expressed in a differential way. The interest here is to have such parameters as temperature, velocity or pressure, defined for all the domain i.e., a solution. Nevertheless, a problem exists and it is the seemingly impossible integrability of Navier-Stokes equations Eq. 5.2. These equations although deterministic, they seem to not have a stable solution for all conditions, that means, that two identical systems given the same boundary conditions and an initial state, can lead to different behaviors throughout time, a concept known as *deterministic chaos*, and in fluid dynamics called *turbulence*.

This remains an unsolved problem of classical mechanics, however, there are several ways of approximating solutions with sufficient accuracy for the purpose of this study, from here it will only be limited to classical statistical approach, that of Osborne Reynold completed by Komogorov, Spalding and Launder, based on the hypotheses of Boussinesq and Prandtl.

In essence, the turbulence is understood as an energy cascading process with phenomena occurring mainly in two scales, the macro scale governed by instabilities leading to eddy break up, and thus energy cascading; and the micro-scale, where they dynamics are damped by the viscosity. Since the eddy break-up is a random, exponentially growing problem, studying each eddy is impossible, thus dividing

the velocity into a mean value \bar{u}_i and a fluctuation u'_i preferred.

$$\bar{u}_i = \bar{u}_i + u'_i \quad (\text{Eq. 5.12})$$

The average operator must meet the *Reynolds conditions*, and thus it is not the typical arithmetic averaging, but the so called *ensemble average* (See (Nieuwstadt, Boersma, and Westerweel, 2016) for details) and the *density weighted average* or *Favre average*.

Ensemble average, where f is any quantity:

$$\bar{f} \equiv \langle f \rangle = \frac{1}{n_{\text{samples}}} \sum_{n=1}^{n_{\text{samples}}} f_n \quad (\text{Eq. 5.13})$$

Favre average:

$$\tilde{f} = \frac{\langle \rho f \rangle}{\langle \rho \rangle} \quad (\text{Eq. 5.14})$$

With such definition, the governing equations become:

Averaged mass conservation:

$$\frac{\partial}{\partial t}(\bar{\rho}) + \frac{\partial}{\partial x_i}(\bar{\rho}\bar{u}_i) = 0 \quad (\text{Eq. 5.15})$$

Averaged Navier-Stokes:

$$\frac{\partial}{\partial t}(\bar{\rho}\bar{u}_j) + \frac{\partial}{\partial x_i}(\bar{\rho}\bar{u}_i\bar{u}_j) = \left[-\frac{\partial \bar{p}}{\partial x_j} + \frac{\partial \bar{\tau}_{ij}}{\partial x_i} + \bar{\rho}g_j \right] - \frac{\partial}{\partial x_i}(\bar{\rho}\tilde{R}_{ij}) \quad (\text{Eq. 5.16})$$

Where:

$$\tilde{R}_{ij} = \text{Reynolds stress tensor}$$

Averaged scalars ϕ :

$$\frac{\partial}{\partial t}(\bar{\rho}\tilde{\phi}_k) + \frac{\partial}{\partial x_i}(\bar{\rho}\tilde{\phi}_k\bar{u}_i) = \left[-\frac{\partial}{\partial x_i}(\bar{J}_{k,i}) + \bar{\rho}\tilde{S}_k \right] - \frac{\partial}{\partial x_i}(\bar{\rho}\tilde{F}_{ki}) \quad (\text{Eq. 5.17})$$

With:

$$\tilde{F}_{ki} = \text{Turbulent scalar flux}$$

This procedure results in a *closure* problem for the following terms:

Reynolds stress tensor:

$$-\bar{\rho}\tilde{R}_{ij} \equiv -\overline{\rho u'_i u'_j} = -\overline{\rho u''_i u''_j} \quad (\text{Eq. 5.18})$$

Turbulent scalar flux:

$$-\bar{\rho}\tilde{F}_{kj} \equiv -\overline{\rho \phi'_k u'_j} = -\overline{\rho \phi''_k u''_j} \quad (\text{Eq. 5.19})$$

And the mean source term:

$$\overline{\rho S_k} = \bar{\rho}\tilde{S}_k \quad (\text{Eq. 5.20})$$

There are several ways of closing these terms, only the standard $k - \epsilon$ model will be treated here, and one variation, the *RNG $k - \epsilon$* for the Reynolds stress tensor and the scalar flux. The RNG model was derived using the *re-normalization group theory*, which allows systematic investigation of physical phenomena at different scales. The *RNG $k - \epsilon$* allows to capture the phenomena better for swirling motion and close to the walls (Poinsot and Veynante, 2005), (Scharler et al., 2020), although, at higher computational cost and with more difficulties for finding convergence (Cable, 2009). For the closure of the chemical mean source term combustion modeling comes into play (Poinsot and Veynante, 2005), (Warnatz, Maas, and Dibble, 1996).

Most of the models which capture the chemical source term are based on a comparison between the limiting factors of the reactions, be it the reaction rate itself, or the mixing rate. The ones based on kinetics, are based on experimentally determined chemical mechanisms with hypothetical reactions which are capable of capturing the natural development of chemical species with sufficient accuracy. These models often are composed of tens or even hundreds of reactions e.g., the *GRI-3.0* with 53 species and 325 reactions, or the *DLR-LS-full* with 55 species and 459 reactions. These mechanisms often can be reduced to capture only the parameters of relevance, and thus reducing the computations cost.

Other commonly used models assume the reactions to be limited by the mixing, which is related to the flow. A typically used model is the *Eddy dissipation model* which calculates the mean chemical source term based on the mass fractions of the flue, oxidizer and products, and depends on the turbulent mixing scale (See (Poinot and Veynante, 2005)). This model was later extended by the *Eddy dissipation n concept*, which also takes into account detailed reactio mechanisms in combination with a stirred reactor model to represent reactive zones.

5. NUMERICAL SOLUTIONS

All the ingredients for the full description of the homogeneous phase combustion have been presented, now the question that arises is "how to solve it?". Since the model is described by partial differential equations which are non-integrable i.e., no exact solution can be found with the currently available mathematics, then, numerical approximations are made.

The three most common numerical schemes used for solving partial differential equations are finite differences, finite volumes and finite elements. As their name suggest, the essence of the models is transform the problem from an infinitesimally small domain (differential), to the finite one.

The mathematics of the models will not be addressed in detail here, the following literature is suggested (Wesseling, 2009), (LeVeque et al., 2002), and (Kan, Segal, and Vermolen, 2005).

In essence, the equations are discretized and re-written in a finite form and solved for a discretized domain. The finite volume method is preferred over the finite difference as it is better at conserving quantities near discontinuities because it is formulated in the integral form, in contrast to the finite differences. In the finite volume method, quantities are approximated as the integral over a "cell" volume (hence the name), instead of discrete points over a grid.

To reach a good approximation, it is necessary to capture the physics of the phenomena at different scales, as it was previously explained, the fluid dynamics are composed of different behavior at different scales and regions. Some of there regions of particular interest and importance are the ones close to walls, where gradients (thermal and velocity) are large do to viscosity and or thermal behavior e.g., a "hot" or "cold" wall.

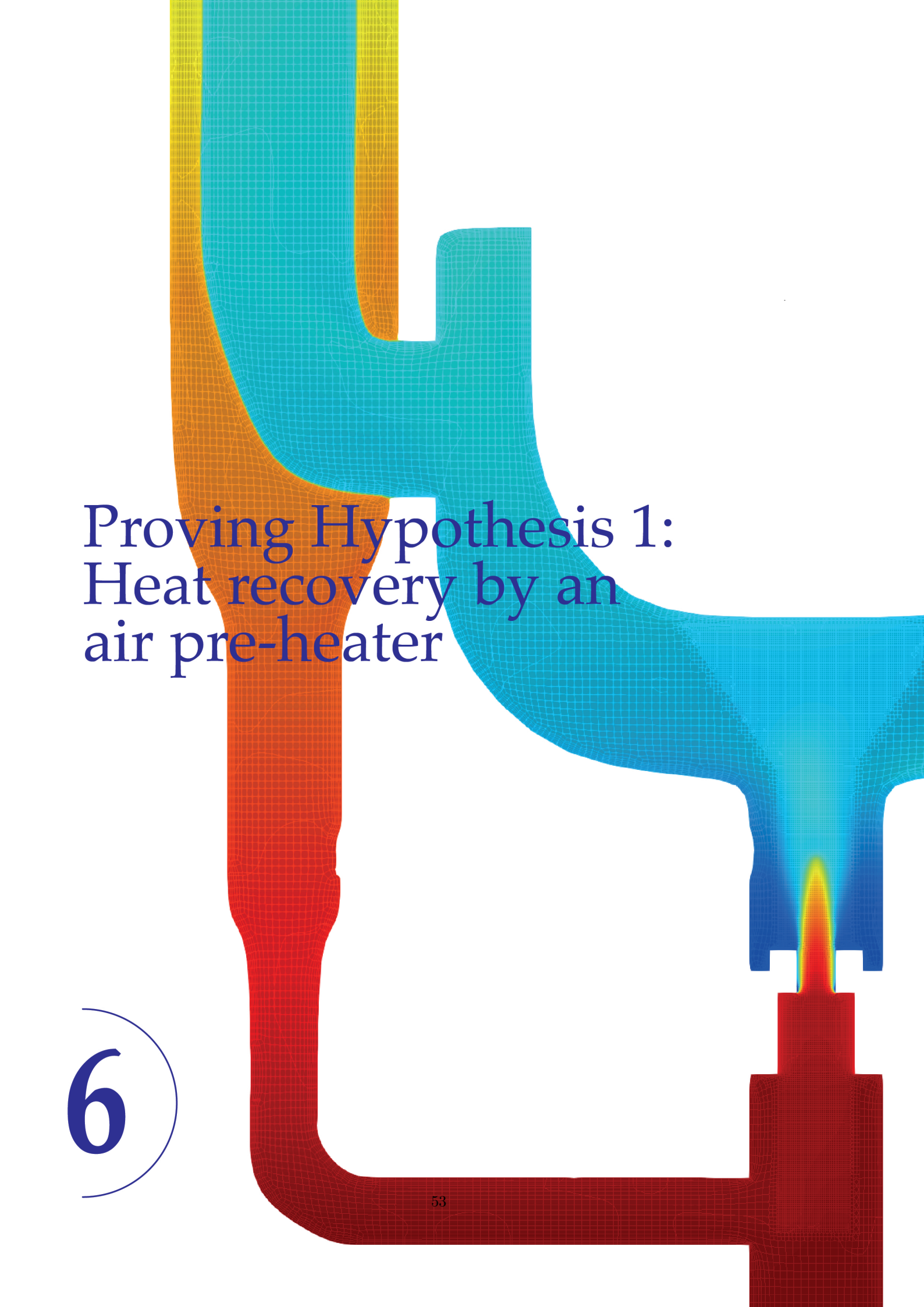
Thus in the computational domain, it is desired to have grids which are designed in such a way that they can capture the physics that are corresponding to that region. That is, the resolution of the information prediction (the model) must be fine enough to capture the small phenomena present in these regions.

6. CONCLUSIONS

1. The thermochemical conversion of biomass from a solid product of *plantae* into useful energy in the form of heat, is composed by complex physical phenomena which includes reacting multiphase flow at different scales. Modeling of such physics can be restricted to "bulk" calculations using sets of algebraic equations or detailed using partial differential equations which require computational power for solving them.

2. Although hundreds of studies have been done in the modeling of the thermochemical conversion of biomass, very few have been dedicated to cookstoves, even though one third of the world population relies on them. From the vast literature reviewed here, by 2015, only four studies had been done, none of them was included in the largest review done by Dernbecher et al. Since then three more studies have been done in the field specific, three of them between 2018-2019 ¹. This can be due to lack of interest and or the high-complexity of such systems, but it is positive that there is more interest in the recent years.
3. The detailed modeling of the heterogeneous and/or homogeneous is complex and requires high computational power due to the complexity of the mathematics that describe the physics. It is thus important to find a practical balance between the less complex, fast models, like 0-D/algebraic and the higher complexity like CFD of reacting flow. Since both can provide useful information at a corresponding effort.
4. Most of the works done in the study of biomass have utilized the standard $k - \epsilon$ model, or a variation of it, with high accuracy, and has been experimentally validated in some cases. This provides a good starting point for future works.

¹It is possible that there are more studies that were not included in this review



Proving Hypothesis 1:
Heat recovery by an
air pre-heater

6

In order to prove this hypothesis, the reactor was analyzed from its essential nature, meaning, by understanding the fundamental physics which dictate the behavior of the phenomena present. These phenomena are: reacting flow dynamics, heat and mass transfer, which are mostly influenced by the geometrical characteristics of the reactor. Only by understanding the essence of the driving forces of the phenomena, an optimal design could be proposed.

In other words, *Kulkan reactor* is, in essence, a geometrical construction of space and materials which determine the reactions, flow and heat transfer characteristic; which in turn determine the efficiency and pollution. Hence, the technical goal is to find the configuration which allows the optimal behavior according to one's goal i.e., high efficiency and low emissions. Here a 0-D (algebraic) model will be formulated. It describes the flow and heat transfer using overall characteristics and empirical correlations, but has the advantages that it can readily be solved for many different possible geometries and other parameters.

This model consists of algebraic sets of equations which are focused on the "bulk" variables, based on the heat and mass balance for the whole reactor, it can be divided in zones and each zone can be modeled with the desired detail. A schematic of the heat balance is shown in Figure 6.1. The syntax of the parameters follows this format:

$$X_{\alpha}^{(\beta,\gamma)} \quad (\text{Eq. 6.1})$$

Where¹:

X = variable
 α = type
 β = region it corresponds to
 γ = gain or loss

The analysis of the system is based on divisions into seven zones, which correspond to the gasifier (Zones 1 and 2), burner (Zone 3), heat-exchanger with the pot (Zone 4, 5 and 6) and the air pre-heater (Zone 7). These zones are categorized in three sub-systems, namely the **gasifier**, the **combustor and heat exchanger**, and the **air pre-heater**.

¹**Note:** except for the syngas \dot{m}_{sg} , which does not have the indicator β , as it is produced in zone 2 but burned in zone 3. This might lead to confusion, hence its not used

Heat balance schematic

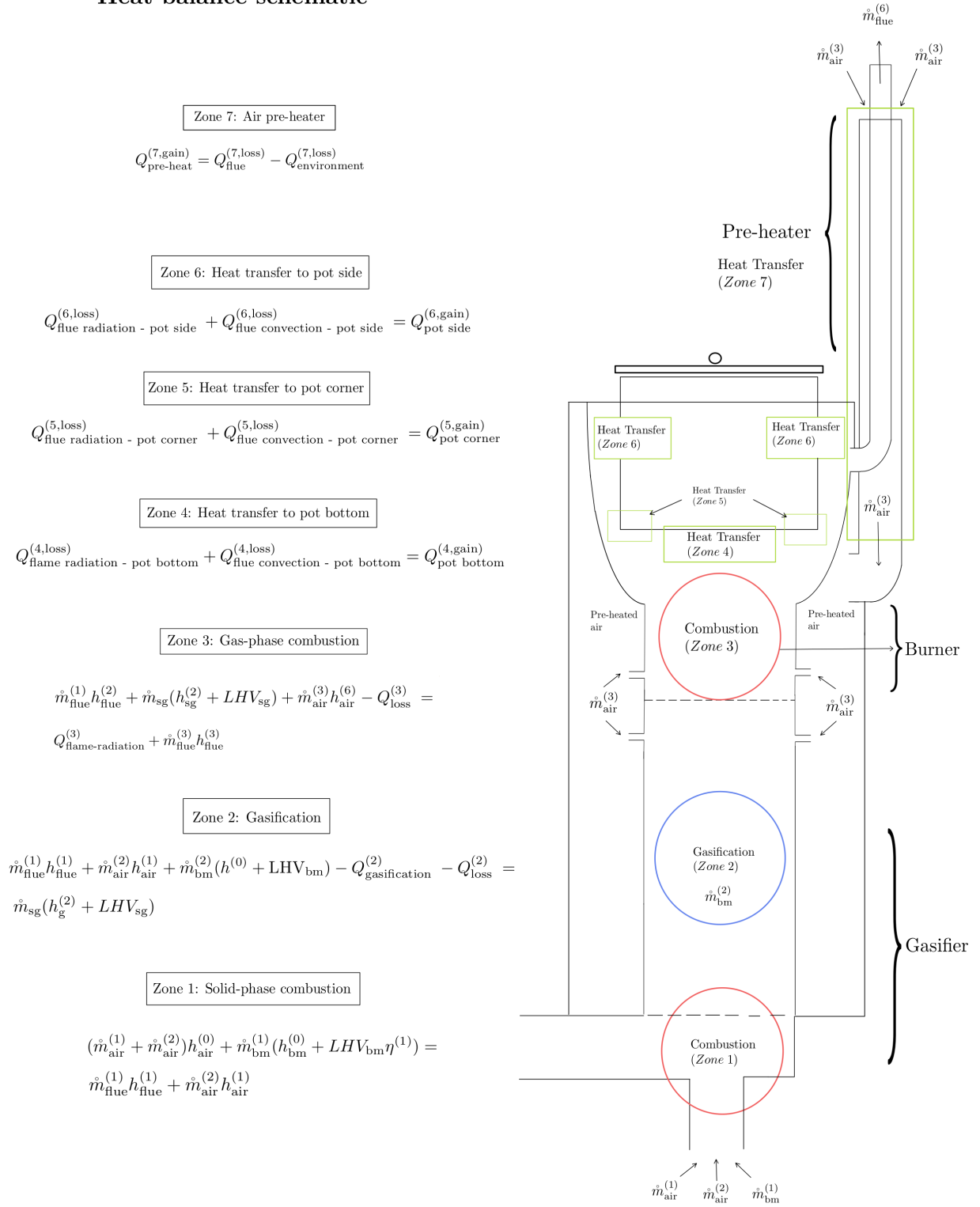


Figure 6.1: Heat balance schematic

1. ALGEBRAIC MODEL: GASIFIER

A bottom-lit updraft gasifier is a type of fixed bed biomass reactor which transforms solid fuels into gaseous fuels. In this case, the reactive layers travel upwards, the thermal gradients make the produced gas and the gasifying medium (in this case air) to also travel upwards while the fuel bed travels downwards to allow for continuous operation.

The construction of the model presented here is based on the methodology used by (Basu, 2010), which is a standard book on gasifier design. There are some particular ways of the author to describe certain parameters that are different from the combustion or chemistry literature e.g., he makes a distinction between lower heating value and the chemical and thermal enthalpies which result from the conversion of raw biomass into products and heat. For consistency, the syntax of the author was used.

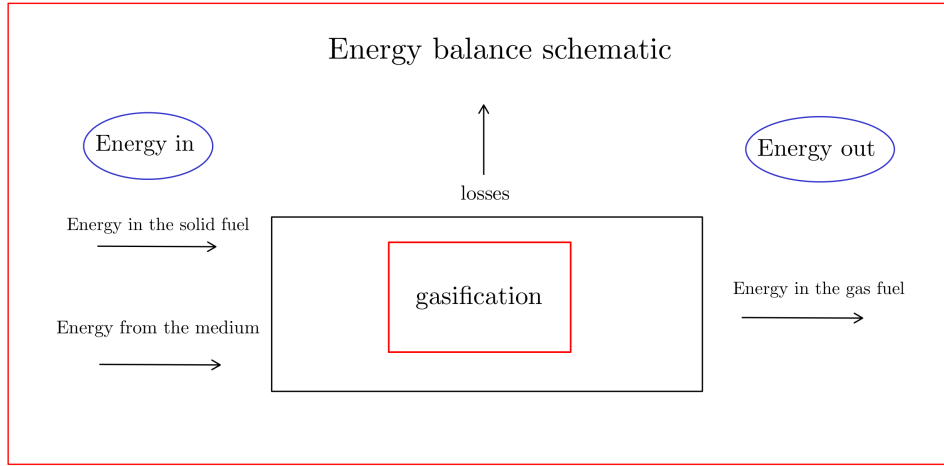


Figure 6.2: Gasifier energy balance schematic

Figure 6.2 represents the energy balance for the gasifier (Zone 2), the other zones follow the same logic.

$$\text{Energy in} = \dot{m}_{\text{flue}}^{(1)} h_{\text{flue}}^{(1)} + \dot{m}_{\text{air}}^{(2)} h^{(1)} + \dot{m}_{\text{bm}}^{(2)} (h^{(0)} + \text{LHV}_{\text{bm}}) - Q_{\text{gasification}}^{(2)} - Q_{\text{loss}}^{(2)} \quad (\text{Eq. 6.2})$$

$$\text{Energy out} = \dot{m}_{\text{sg}} (h_{\text{g}}^{(2)} + \text{LHV}_{\text{sg}}) \quad (\text{Eq. 6.3})$$

In detail, **Zone 1** is where the solid fuel $\dot{m}_{\text{bm}}^{(1)}$ and $\dot{m}_{\text{air}}^{(1)}$, with their respective incoming enthalpies $h_{\text{air}}^{(0)}$ and $h_{\text{bm}}^{(0)}$ burn in the solid phase, providing the heat $\dot{m}_{\text{flue}}^{(1)} h_{\text{flue}}^{(1)}$ required to drive the gasification process $Q_{\text{gasification}}^{(2)}$ of the biomass $\dot{m}_{\text{bm}}^{(2)}$ and air $\dot{m}_{\text{air}}^{(2)}$ taking into account the losses $Q_{\text{loss}}^{(2)}$ and the heat to raise the enthalpy of $\dot{m}_{\text{flue}}^{(1)} h_{\text{flue}}^{(1)}$ and $\dot{m}_{\text{air}}^{(2)} h^{(1)}$.

The heat balance of these **Zone 1 and 2** is given by Eq. 6.4 and Eq. 6.5 respectively. Note that in this analysis, the *lower heating values* were used, differently than the author, this was done for simplicity as the contributions of steam were neglected as they represent less than 5% of the total energy of the system (Kshirsagar and Kalamkar, 2015).

$$(\dot{m}_{\text{air}}^{(1)} + \dot{m}_{\text{air}}^{(2)}) h_{\text{air}}^{(0)} + \dot{m}_{\text{bm}}^{(1)} (h_{\text{bm}}^{(0)} + \text{LHV}_{\text{bm}}) = \dot{m}_{\text{flue}}^{(1)} h_{\text{flue}}^{(1)} + \dot{m}_{\text{air}}^{(2)} h_{\text{air}}^{(1)} \quad (\text{Eq. 6.4})$$

$$\dot{m}_{\text{flue}}^{(1)} h_{\text{flue}}^{(1)} + \dot{m}_{\text{air}}^{(2)} h^{(1)} + \dot{m}_{\text{bm}}^{(2)} (h^{(0)} + \text{LHV}_{\text{bm}}) - Q_{\text{gasification}}^{(2)} - Q_{\text{loss}}^{(2)} = \dot{m}_{\text{sg}} (h_{\text{g}}^{(2)} + \text{LHV}_{\text{sg}}) \quad (\text{Eq. 6.5})$$

To determine the amount of fuel required for both zones $\dot{m}_{\text{bm}}^{(1,2)}$, its necessary to know the composition, (ultimate and proximate analysis) the gasifying agent, the operating parameters (temperature

and pressure), and the required gas composition.

The process begins by defining the required volumetric flow \dot{V}_{sg} rate calculated from the required energy output and the lower heating value of the gas coming from the gasifier, which for updraft gasifiers is between $3.7 - 5.1 MJ/m^3$ (Monteiro Magalhaes, 2011), (Chomiak, Longwell, and Sarofim, 1989).

$$\dot{V}_{sg} = \frac{Q}{LHV} [m^3/s] \quad (\text{Eq. 6.6})$$

With the volumetric flow rate, knowing its composition, and with an equation of state, the mass flow \dot{m}_{sg} can be determined (All calculations in this section are at standard conditions).

$$\rho_{sg} = M_{sg}/\nu_{ig}^M \quad (\text{Eq. 6.7})$$

Where:

$$M_{sg} = \sum_k x_k M_k; \text{ g/mol for all } k \text{ elements}$$

$$\nu_{ig}^M = 0.0224 m^3/mol; \text{ ideal gas molar specific volume}$$

From mass conservation, it's known that the mass of syngas will be equal to the mass of biomass used for gasification $\dot{m}_{gasification}$ and the mass of the gasifying agent, in this case, air \dot{m}_{air} , under the assumption of total conversion of the solid biomass into gaseous fuel.

$$\dot{m}_{sg} = \dot{m}_{air}^{(2)} + \dot{m}_{bm}^{(2)} \quad (\text{Eq. 6.8})$$

The amount of oxidizer, which in this case is air *Air Fuel Ratio -AFR-* is determined with the following equation (Basu, 2010, p.82).

$$AFR_{st} = 0.1153C + 0.3434(H - \frac{O}{8} + 0.043S) \text{ kg/kg of dry fuel} \quad (\text{Eq. 6.9})$$

For this case $AFR_{st} = 5.67 \text{ kg/kg}$ of dry fuel. Using the general composition of biomass recommended by (Monteiro Magalhaes, 2011). This value is close to that used by (Prapas et al., 2014) of 6.1 kg/kg , but in their case they were performing complete combustion and a different type of biomass. Since here, the desire is to gasify, the real air/fuel ratio must be smaller, typically of around 25% of the stoichiometric ratio, hence:

$$AFR = 0.25 \cdot AFR_{st} = 1.4175 \text{ kg/kg of dry fuel} \quad (\text{Eq. 6.10})$$

With equations Eq. 6.8, Eq. 6.9 and Eq. 6.10 the amount of fuel for gasification is determined as follows:

$$\dot{m}_{bm}^{(2)} = \frac{\dot{m}_{sg}}{1 + AFR} \quad (\text{Eq. 6.11})$$

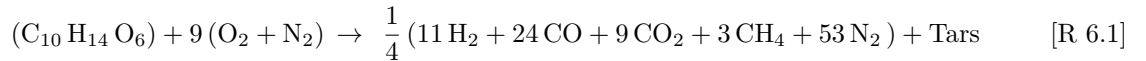
It is essential to know the amount of useful energy that the fuel can provide, represented by the *Lower heating value -LHV-*, which is determined as the difference between the higher heating value minus the contribution of condensation of steam, arising from biomass moisture and formed by combustion. Typical values of biomass moisture used for cooking is Y_{moist} 15 – 20%, on a mass basis, thus from (Basu, 2010).

$$LHV_{bm} = HHV - 20,300 \cdot Y_H - 2260 \cdot Y_{moist} \quad (\text{Eq. 6.12})$$

The higher heating value HHV_{bm} of biomass is of about $HHV = 21 MJ/kg$ (Viana et al., 2018). In large samples, a relatively constant atomic ratio of $C_{10}H_{14}O_6$ is found (Monteiro Magalhaes, 2011), also used by (Oliveira et al., 2020), (Monteiro et al., 2010) and similar to that reported by (Chomiak, Longwell, and Sarofim, 1989). The use of a generalized composition of biomass is supported by the fact that in reality, the biomass used will vary from place to place, as well as the local conditions -humidity, geometry, cooking style, among other-. Nevertheless, as stated by (Chanphavong and Zainal, 2019):

[...] "influence of different biomass types in the gasification process has no significance on the combustion properties of PG such as flame speed, adiabatic flame temperature, Wobbe Index, flame stability, and extinction limits. Although there are changes in the compositions of PG [producer gas i.e., syngas], similar combustion properties have been found."

It follows to determine the amount of energy required to carry out the gasification, which requires a design temperature. For an updraft gasifier, it is of around $900C^\circ$ (Basu, 2010). With this data, the enthalpy of reaction $Q_{\text{gasification}}^{(2)}$ is calculated based on a hypothetical one step reaction. This reaction predicts the composition of the products and can be solved via stoichiometric models, Gibbs energy minimization or from experimental data (idem). In this case, experimental composition of the syngas is used based on the data provided by (Bridgwater, 1995) $U\text{pdraft syngas} = 11H_2 + 24CO + 9CO_2 + 3CH_4 + 53N_2$, with the previously mentioned biomass composition, the hypothetical gasification reaction would look like this:



Neglecting the heat of formation of the tars and preserving the molar composition of the syngas, the heat of the reaction can be calculated as:

Heat of reaction = heat of formation of products – heat of formation of reactants

$$\Delta H_0^T = \sum \left(A'_k H_0^{298} + \int_{298}^T A'_k C_{p,k} dT \right)_{\text{products}} - \sum \left(\alpha'_k H_0^{298} + \int_{298}^T \alpha C_{p,k} dT \right)_{\text{reactants}} \quad (\text{Eq. } 6.13)$$

Where A' and α correspond to the stoichiometric coefficients of any element k in the products and reactants, respectively.

For this case, the heat of reaction is determined by the heat of reaction formation of each species. The heat of formation and the correlations for the specific heat are obtained from (Basu, 2010). The gasification temperature T_g was chosen to be $1100K$, slightly lower than the 1173° . The heat of formation of biomass is taken from (Burnham, 2010).

$$\Delta H_{H_2} : 11 \int_{298}^{T_g} 27.71 + 0.0034T dT = 265.423 \text{ kJ/kmol} \quad (\text{Eq. } 6.14)$$

$$\Delta H_{CO} : 24(-110.5 + \int_{298}^{T_g} 27.62 + 0.005T dT) = 596.249 \text{ kJ/kmol} \quad (\text{Eq. } 6.15)$$

$$\Delta H_{CO_2} : 9(393.5 + \int_{298}^{T_g} 43.28 + 0.0114T dT) = 355.433 \text{ kJ/kmol} \quad (\text{Eq. } 6.16)$$

$$\Delta H_{CH_4} : 3(-74.8 + \int_{298}^{T_g} 22.35 + 0.048T dT) = 134.275 \text{ kJ/kmol} \quad (\text{Eq. } 6.17)$$

$$\Delta H_{N_2} : 53 \left(\int_{298}^{T_g} 27.21 + 0.0042T dT \right) = 1,281.377 \text{ kJ/kmol} \quad (\text{Eq. } 6.18)$$

$$\Delta H_{\text{Biomass}} : (19.7 \cdot y_C - 278.2 \cdot y_H + 29 \cdot y_N - 50 \cdot y_S - 108 \cdot y_O) = -1,198.280 \text{ kJ/mol} \quad (\text{Eq. } 6.19)$$

Hence the heat of reaction of the gasification process from 1mol of biomass $Q_{\text{gasification}}$ is:

$$Q_{\text{gasification}}^{(2)} = \frac{1}{4} H_{\text{syngas}} - H_{\text{biomass}} = 1,856.47 \text{ kJ/mol}_{\text{biomass}} \quad (\text{endothermic}) \quad (\text{Eq. } 6.20)$$

The enthalpy of the air, flue gas and syngas h_{air} , h_{flue} and h_{sg} respectively, are calculated based on their heat capacities $C_{p_i}(T)$ which were determined using the *JANAF polynomials* (NASA, 1999).

2. ALGEBRAIC MODEL: COMBUSTOR AND HEAT-EXCHANGER

Next the sub-system where the combustion in the gas-phase takes place is considered, it is also where heat is transferred to the pot. Most of the heat is released here as the larger part of the total fuel is burned. This part is of essential importance as it is here where control over the stoichiometry can happen and thus control on the organic emissions.

2.1 DRIVING FORCE

It is buoyancy that drives the dynamics of the system, which is caused by the change in density of the gases due to the increase in temperature during combustion, this phenomena is often referred as the "*stack effect*". By assuming the hot gas to have a constant temperature, the buoyant force can be calculated as in Figure 6.3. This approach is used both by (Prapas et al., 2014), and (Kshirsagar and Kalamkar, 2015) which were taken as references, however, there seems to be an error in the equation by the first one, therefore, it was re-derived here.

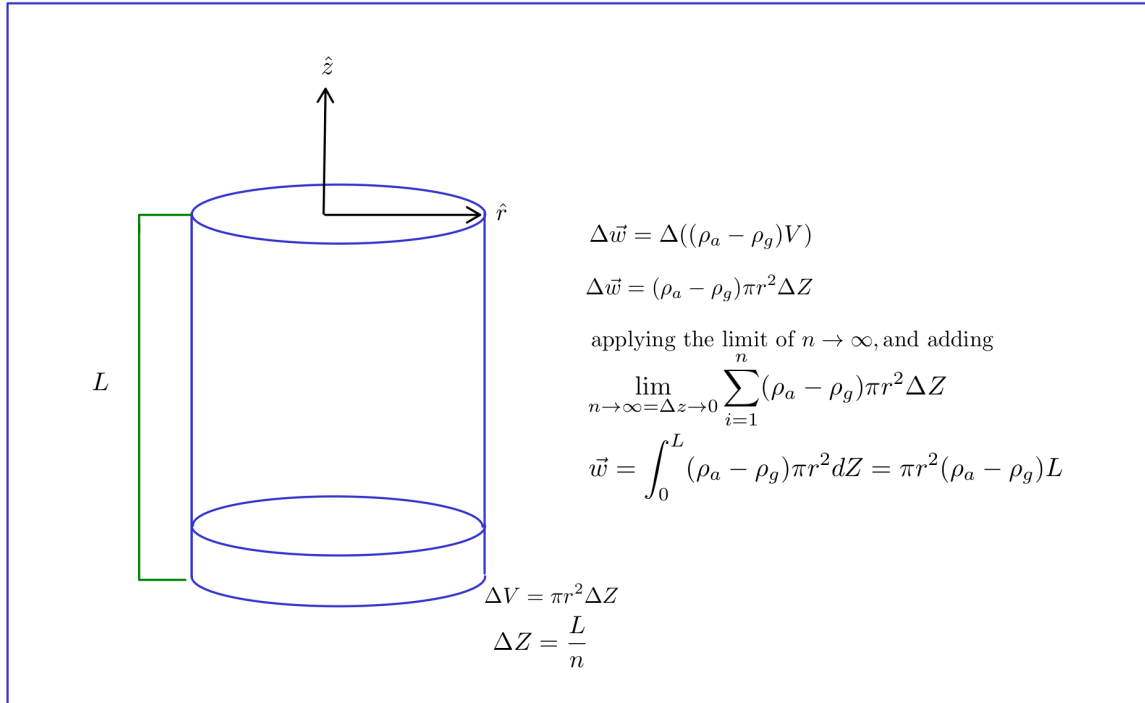


Figure 6.3: Derivation of the chimney equation

Where:

$$\begin{aligned} \vec{w} &= \text{buoyant force} \\ \rho_a &= \text{atmospheric density} \\ \rho_g &= \text{density of hot gas} \end{aligned}$$

And with that, the static pressure is calculated:

$$P = \frac{\vec{w}}{A} = \frac{\pi r^2(\rho_a - \rho_g)gL}{\pi r^2} = (\rho_a - \rho_g)gL \quad (\text{Eq. 6.21})$$

Since the system is open to the environment, the pressure gradient will produce movement, assuming no heat losses and incompressibility (they will be taken care of later), then the pressure will create a final velocity, assuming zero pressure gradient at the exit, then:

$$(\rho_a - \rho_g)gL = \frac{1}{2}\rho_g\vec{u}^2 \quad (\text{Eq. 6.22})$$

Assuming ideal gas behavior.

$$\vec{u} = \sqrt{2gL \left(\frac{\rho_a}{\rho_g} - 1 \right)} \quad (\text{Eq. 6.23})$$

$$\rho = \frac{P}{R_u T} \quad (\text{Eq. 6.24})$$

Where R_u is the ideal gas constant divided by the molar mass, assumed to be the same for both. Re-writing:

$$\vec{u} = \sqrt{2gL \left(\frac{\frac{P_a}{T_a}}{\frac{P_g}{T_g}} - 1 \right)} \quad (\text{Eq. 6.25})$$

Since the difference in temperature is much larger than the difference in pressure i.e., $P_a \simeq P_g$ then it simplifies to Eq. 6.26, which is the equation of the theoretical velocity equation used by (Kshirsagar and Kalamkar, 2015), although they don't explicitly mention the low pressure difference assumption.

$$u_{th} = \sqrt{2gL \left(\frac{T_g}{T_a} - 1 \right)} \quad (\text{Eq. 6.26})$$

To adjust this equation to more a more realistic scenario where there are pressure losses and temperature reduction in the hot gas do to exchange with the environment, the so called *discharge coefficient* C_d is introduced, according to (idem), this parameter ranges between 0.35 – 0.42 (This will be treated with more detail further in section 3).

2.2 COMBUSTOR ANALYSIS

Zone 3: In this zone, the syngas \dot{m}_{sg} is burned in the gas-phase in combination with the pre-heated air $\dot{m}_{air}^{(3)}$. The combustion results in heat released in the form of radiation from the flame $Q_{flame}^{(3)}$, and losses through the wall $Q_{loss}^{(3)}$. The heat balance if this zone is given by Eq. 6.27. The radiation from the hot gases is approached using the mean beam length model, convection is determined using correlations adequate to each case, based on the dimensionless numbers of Reynolds, Grashof and Nusselt.

$$\dot{m}_{flue}^{(1)} h_{flue}^{(2)} + \dot{m}_{sg} h_{sg}^{(2)} + \dot{m}_{sg} LHV_{sg} \eta^{(3)} + \dot{m}_{air}^{(3)} h_{air}^{(6)} = Q_{flame}^{(3)} + Q_{loss}^{(3)} + \dot{m}_{flue}^{(3)} h_{flue}^{(3)} \quad (\text{Eq. 6.27})$$

The $Q_{flame}^{(3)}$ is obtained using a well stirred furnace model (Ragland and Kenneth M Bryden, 2011).

$$Q_{flame}^{(3)} = \sigma A (\varepsilon_g T_g^4 - \alpha_g T_p^4) \quad (\text{Eq. 6.28})$$

With:

$$\varepsilon_g = e^{(A+B \ln(0.2 \cdot 3.6 \frac{V_m}{A_m}))} \quad (\text{Eq. 6.29})$$

$$\alpha_g = \varepsilon_g \cdot \left(\frac{T}{T_s} \right)^{0.5} \quad (\text{Eq. 6.30})$$

$$A = 0.848 + 9.02 \cdot 10^{-4} T \quad (\text{Eq. 6.31})$$

$$B = 0.9589 + 4.8 \cdot 10^{-6} T \quad (\text{Eq. 6.32})$$

$$(\text{Eq. 6.33})$$

Where:

$$\varepsilon_g = \text{effective emissivity of the medium} \quad (\text{Eq. 6.34})$$

$$\alpha_g = \text{effective absorptivity of the medium} \quad (\text{Eq. 6.35})$$

$$V_m = \text{Volume of the medium} \quad (\text{Eq. 6.36})$$

$$A_m = \text{Area of the medium} \quad (\text{Eq. 6.37})$$

$$(\text{Eq. 6.38})$$

And where, in the case of a long cylindrical combustion chamber, is lost to the environment Q_{loss} is:

$$Q_{\text{heat loss}}^{(3)} = \frac{(T_g - T_a)}{\frac{1}{(h_{ci} + h_{rfl})A_0} + \frac{ln(D_o/D_i)}{2\pi z k_t} + \frac{1}{(h_{co} + h_{ro})A_0}} \quad (\text{Eq. 6.39})$$

With:

$$h_{rfl} = \frac{\sigma (\varepsilon_g T_g^4 - \alpha_g T_{wi}^4)}{(T_g - T_{wi})} \quad (\text{Eq. 6.40})$$

$$h_{ro} = \sigma \varepsilon_o (T_{wo}^2 + T_a^2) (T_{wo} + T_a) \quad (\text{Eq. 6.41})$$

$$h_{co} = \frac{k}{z} 0.59 Ra_z^{0.25} = \frac{k}{z} 0.59 (Gr_z Pr)^{0.25} \quad (\text{Eq. 6.42})$$

$$(\text{Eq. 6.43})$$

Where:

$$D_o = \text{Outer diameter of the cylinder} \quad (\text{Eq. 6.44})$$

$$D_i = \text{Inner diameter of the cylinder} \quad (\text{Eq. 6.45})$$

$$k_t = \text{Thermal conductivity of the wall} \quad (\text{Eq. 6.46})$$

$$T_{wo} = \text{Temperature of the outer wall} \quad (\text{Eq. 6.47})$$

$$T_{wi} = \text{Temperature of the inner wall} \quad (\text{Eq. 6.48})$$

$$k = \text{thermal conductivity of the fluid} \quad (\text{Eq. 6.49})$$

$$z = \text{characteristic length, in this case, combustion chamber height} \quad (\text{Eq. 6.50})$$

2.3 HEAT-EXCHANGER ANALYSIS

Zone 4, 5, and 6 are where the heat is transferred to the pot by radiation and convection, through the walls, corner and bottom. These heat transfers are respectively described in the following equations:

$$Q_{\text{flame radiation - pot bottom}}^{(4,\text{loss})} + Q_{\text{flue - pot bottom}}^{(4,\text{loss})} = Q_{\text{pot bottom}}^{(4,\text{gain})} \quad (\text{Eq. 6.51})$$

$$Q_{\text{flue radiation - pot corner}}^{(5,\text{loss})} + Q_{\text{flue convection - pot corner}}^{(5,\text{loss})} = Q_{\text{pot corner}}^{(5,\text{gain})} \quad (\text{Eq. 6.52})$$

$$Q_{\text{flue radiation - pot side}}^{(6,\text{loss})} + Q_{\text{flue convection - pot side}}^{(6,\text{loss})} = Q_{\text{pot side}}^{(6,\text{gain})} \quad (\text{Eq. 6.53})$$

To compute the heat transferred by radiation from the flue gas in equations [Eq. 6.51](#), [Eq. 6.52](#), [Eq. 6.53](#) and [Eq. 6.61](#) are calculated in the same way as in [Eq. 6.28](#), with its respective area A_i , gas temperature T_{g_i} and gas properties ε_i and α_i with their respective geometrical adaptations for the hydraulic and equivalent diameters. The heat transferred to the pot bottom by convection (Kshirsagar and Kalamkar, 2015) recommend the following correlation for an impinging jet taken from (Zuckerman and Lior, 2006).

$$Q_{\text{flue convection - pot side}}^{(6,\text{loss})} = h_{\text{bottom}} A \left\{ \left(\frac{T_g + T_e}{2} \right) - T_p \right\} \quad (\text{Eq. 6.54})$$

$$Nu_{\text{bottom}} = 0.424 \text{Re}_D^{0.57} \left(\frac{H_i}{D} \right)^{-0.33} \quad (\text{Eq. 6.55})$$

$$h_{\text{bottom}} = \frac{k_{\text{bottom}}}{D} 0.424 \text{Re}_D^{0.57} \left(\frac{H_i}{D} \right)^{-0.33} \quad (\text{Eq. 6.56})$$

To validate this model, the results for the flame temperature and the total mass flow rate with varying firepower were compared with those from (Agenbrood et al., 2011b), referenced in (Kshirsagar and Kalamkar, 2015). The error bars were set at 10%, as suggested by the authors. A value for the discharge coefficient Cd of 0.383 was used, as the reference in (Agenbrood et al., 2011a). After validation, of the replicated model, a discharge coefficient corresponding specifically to the Kulkan was calculated (See section 3). This model is called *Validation Model*, not to be confused with *Complete Model*.

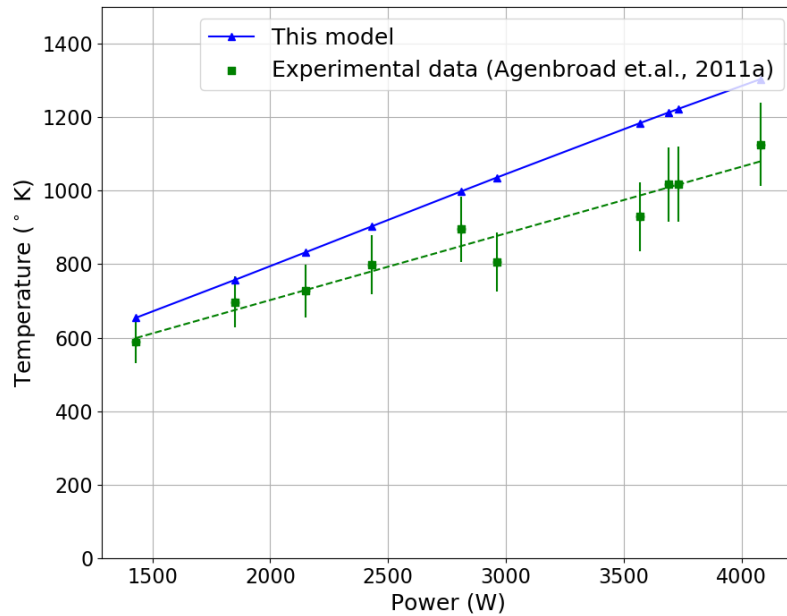


Figure 6.4: Validation model: flame temperature vs syngas power output

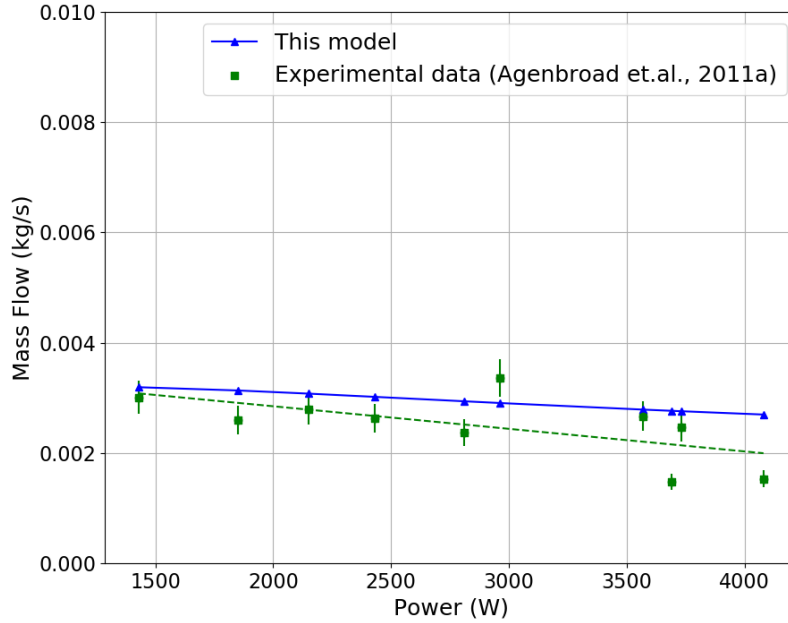


Figure 6.5: Validation model: flue gas mass flow vs syngas power output

In Figure 6.4, it can be noticed that the tendency of the temperature to increase with power is shown properly. Nevertheless, with higher values than the reference. This is to be expected as the \mathbf{q}_{char} is not present as the combustion happens in the gas phase. According to (Kshirsagar and Kalamkar, 2015), the char radiation represents 10% of the total energy.

3. ALGEBRAIC MODEL: AIR PRE-HEATER

Since the Kulkarni incorporates more resistances to the flow, as well as an air pre-heater which reduces the amount of draft and "cools down" the flue gas, it would be unrealistic to assume a value of the discharge coefficient. Hence, it was added to the model as follows:

$$C_d = C_{viscous} \cdot C_{heat} \quad (\text{Eq. 6.57})$$

(Kshirsagar and Kalamkar, 2015) propose a value for friction enhancement due to heat transfer effects $C_{heat} = 0.95$

The viscous losses are calculated according to the geometry of the flow path, so from conservation of energy (idem):

$$\frac{1}{2}\rho_g u_r^2 = \frac{1}{2}\rho_g u_{th}^2 - \frac{1}{2}\rho_g u_r^2 \left(\sum K_{l_i} \frac{\rho_g}{\rho_a} \left(\frac{A}{Al} \right)^2 \right) \quad (\text{Eq. 6.58})$$

$$ur = \frac{u_{th}}{\left(1 + \sum K_{l_i} \frac{\rho_g}{\rho_a} \left(\frac{A}{Al} \right)^2 \right)^{\frac{1}{2}}} \quad (\text{Eq. 6.59})$$

Hence,

$$C_{viscous} = \frac{1}{\left(1 + \sum K_{l_i} \frac{\rho_g}{\rho_a} \left(\frac{A}{Al} \right)^2 \right)^{\frac{1}{2}}} \quad (\text{Eq. 6.60})$$

The pressure loss coefficients K_{l_i} , Area ratios $\frac{A}{Al}$, and density ratios $\frac{\rho}{\rho_i}$ are presented in Table 6.1, obtained from (Kshirsagar and Kalamkar, 2015).

Table 6.1: Pressure loss coefficients, area and density ratios

Type of loss	Loss coefficient (K_{l_i})	ρ/ρ_i	A/A_i
Friction loss in elbow length	$K_{l_1} = \frac{f_e L_e}{D_h}, f_e = \frac{64}{Re_c}, D_h = \frac{4A_r \cdot A}{d(\pi - \theta + \sin \theta)}$ $\theta = (-2.29 \cdot A_r^2 + 1.24 \cdot A_r + 1.53)$ Correlated from the results obtained from expression: $A_r \cdot A = \frac{D^2}{4} \left(\pi - \theta \frac{\sin 2\theta}{2} \right)$	$\frac{T_g + T_a}{2T_g}$	$\frac{1}{A_r}$
Expansion to chimney	$K_{l_2} = [1/(A_r - 0.5) - 1]^2$	1	1
Fuel bed resistance (viscous and inertial)	$K_{l_3} = 3.5 \cdot H \frac{(1 - \varepsilon)}{d_p} \cdot \frac{\rho_b}{\rho_g} + \frac{300 \cdot H \cdot \mu}{d_p^2 \cdot \rho_g \cdot V} \cdot \frac{(1 - \varepsilon)^2}{\varepsilon^3}$ $\varepsilon = \text{bed voidage} = 0.69$ $H = D/4$	1	1
Friction loss in the chimney	$K_{l_4} = f \cdot h/D$ $f = (0.79 \ln(Re)_D - 1.64)^{-2}$	1	1
Loss due to bend at pot bottom	1	1	1
Loss due to friction in the pot gap zone	$K_{l_5} = \frac{4f(d_p - d)}{D_h}$ $f = \frac{24}{Re}$ $D_h = w_1 + w_2$	$\frac{T_c + T_e}{2T_g}$	$\frac{d^2}{(d + d_p)(w_1 + w_2)}$
Loss at the outlet	1	1	1
Loss at the burner ²	5	1	1

The losses due to the draft caused by the increase in temperature of the air are also taken into account using the same equations as for the buoyancy force of the flow, since it is the same phenomena, but in the opposite direction (See Section 3). With the relationships between the mass flow and the temperature determined, only the relationships of the heat transfer are needed.

The previous model does not consider the incorporation of a chimney for the exhaust gases after the contact with the pot, nor a pre-heater, which are novel features of the Kulkan. These are approximated as plug-flow behaviour heat exchangers localized in **Zone 7** divided in n sections. According to (Kshirsagar and Kalamkar, 2015), up to up to 40% of the total energy is lost through the flue for updraft rocket stoves, so the objective here is to optimize the heat recovery for efficiency and combustion quality improvement.

The essential objective of the complete model is to find the optimal geometrical and material properties for both chimneys, and combustion chamber, to ensure the best draft range for stable operation and optimal stoichiometry of the combustion. Since the driving force of the system is buoyancy, only a certain amount of heat $Q_{pre-heat}^{(7, \text{gain})}$ can be recovered, else the draft will reach too low values and the system will suffocate.

²This is an assumed value, taken to be large as a conservative first approximation. It should be numerically or experimentally calculated, based on the type of burner

The heat exchange in this region is characterized by the following equation:

$$Q_{\text{pre-heat}}^{(7,\text{gain})} = Q_{\text{flue}}^{(7,\text{loss})} - Q_{\text{environment}}^{(7,\text{loss})} \quad (\text{Eq. 6.61})$$

It is also known that the heat loss through the flue gas is equal to the heat across the wall between the flue and the air, also the heat lost to the environment is equal to the heat across the air pipe wall.

$$\dot{Q}_{\text{flue}}^{(7,\text{loss})} = \dot{Q}_{\text{flue-side wall}} = \dot{Q}_{\text{flue-air wall}} = \dot{Q}_{\text{air-side wall}} \quad (\text{Eq. 6.62})$$

$$\dot{Q}_{\text{air-side wall}} = \dot{Q}_{\text{air-environment wall}} = \dot{Q}_{\text{environment-side wall}} = Q_{\text{environment}}^{(7,\text{loss})} \quad (\text{Eq. 6.63})$$

$$\dot{Q}_{\text{flue}}^{(7,\text{loss})} = \frac{(T_f - T_a)}{\frac{1}{(h_{c,\text{flue}} + h_r)A_f} + \frac{l_n(D_a/D_f)}{2\pi z k_t} + \frac{1}{(h_{c,\text{air}})A_0}} \quad (\text{Eq. 6.64})$$

$$\dot{Q}_{\text{flue-side wall}} = \frac{(T_f - T_{wf})}{\frac{1}{(h_{c,\text{flue}} + h_r)A_f}} \quad (\text{Eq. 6.65})$$

$$\dot{Q}_{\text{air-side wall}} = \frac{(T_{wa} - T_a)}{\frac{1}{(h_{c,\text{air}} + h_{r,\text{air}})A_a}} \quad (\text{Eq. 6.66})$$

And the heat lost to the environment is defined in the same way with the hot side being the air side and the cold side the environment.

There are missing equations to complete the system, which are the enthalpy equations that relate the mass and energy of the flue and air in each of the n sections.

$$\dot{m}_{\text{flue}}(h_{\text{flue}}^{(n+1)} - h_{\text{flue}}^{(n)}) = Q_{\text{flue}}^{(7,\text{loss})} \quad (\text{Eq. 6.67})$$

$$\dot{m}_{\text{air}}(h_{\text{air}}^{(n)} - h_{\text{air}}^{(n+1)}) = Q_{\text{flue}}^{(7,\text{loss})} - Q_{\text{environment}}^{(7,\text{loss})} \quad (\text{Eq. 6.68})$$

With the previous relations, the algebraic model of the stove is completed, which results in a system of non-linear simultaneous equations which require a numerical solution algorithm and computing power. The solution took around 2 seconds for one iteration to complete on a computer with a Intel Core i7-7700HQ, CPU @2.80GHz, 16Gb of RAM, running on Linux-Ubuntu 18.04 distribution.

4. STRATEGY FOR SOLVING THE ALGEBRAIC MODEL

The essence of the algebraic model relies on a heat and mass balance, whose behaviour is determined by the geometrical parameters of the reactor and the chemical composition of the fuel. Since the chemical composition of the fuel is fixed based on experimentally determined data obtained from literature, only the geometrical parameters are to be optimized. This geometrical parameters will dictate the speed (see Eq. 6.26), which will in turn determine the flow regime, and thus the convective heat transfer coefficients. They will also influence the heat transfer (see Eq. 6.39).

Nonetheless, all these relationships depend on the temperature, and this depends on all of these relationships. In other words, the heat exchange capacity of the system influences the temperature, and the temperature influences the heat exchange capacity. Hence, the system is coupled.

$$f : T \rightarrow \mathbb{R} \quad (\text{Eq. 6.69})$$

To solve the system, the open-source mathematics library *SymPy* from *Python* was used, for its symbolic capabilities. And the full system was coded using the following logic.

```

define function(symbolic_T, parameters):
    output = mathematical_operations(symbolic_T, parameters, other_functions)
    return(output)

```

By defining all the mathematical relations as function in *Python* in terms of the symbolic variables, the code was simplified and the chances of typos minimized. Moreover, for similar phenomena e.g., the sections in the chimney, *dictionaries* of symbolic variables and mathematical relations were constructed, which allowed for automatization of the variable definition process.

5. RESULTS AND DISCUSSION

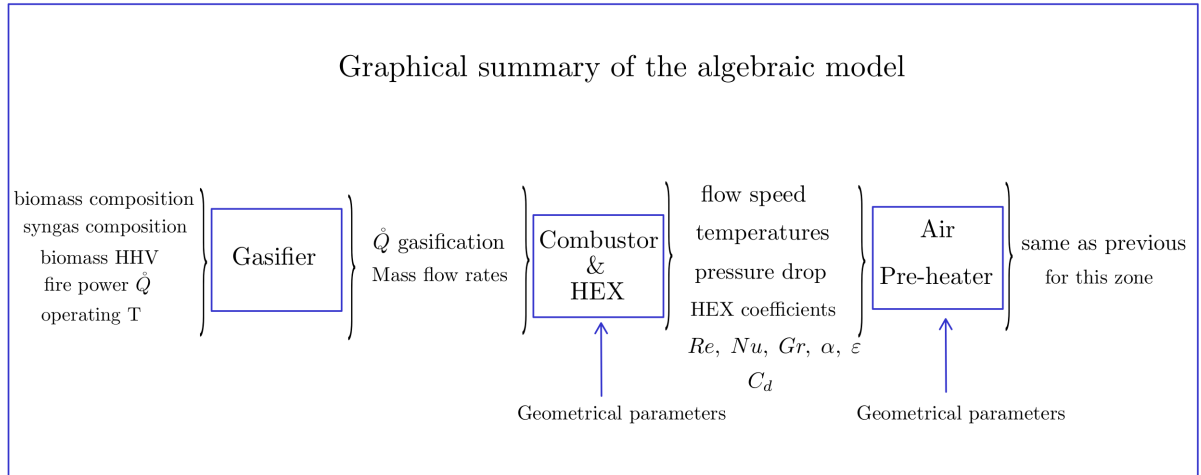


Figure 6.6: Graphical summary of the inputs and outputs of each sub-system

Table 6.2: Optimal configuration for fire powers of [2.5 - 4.0] kW

Chimney Inner Diameter (Flue-side)	Air-side	Wall thickness	Combustion chamber height [m]	Chimney length [m]	Combustion Chamber Diameter [m]	Efficiency η	Stoichiometric ratio ϕ
0.1 [m]	0.18 [m]	0.001 [m]	0.15	1.00	0.07	[57 – 68]%	[0.50 – 0.99]

1. A complete algebraic (0-D) model for the *Kulkan* has been developed and solved using open source software. It allows to estimate the behavior of essential design variables for 7 zones (See Table 6.3) as functions of geometrical parameters, fuel composition and operating conditions. It comprises 46 simultaneous non-linear equations which were solved for more than 8,000 different configurations, varying the chimney and combustion chamber height, the combustion chamber diameter, the discharge coefficient based on literature data and the wall material. From this, it was found that the most influential parameter on the efficiency (defining efficiency as in Eq. 6.70) is the discharge coefficient C_d .

$$\eta = \frac{\text{Total heat transferred to the pot}}{\text{Total fuel} \cdot LHV} \quad (\text{Eq. 6.70})$$

2. To make the model more accurate, the C_d calculated specifically for the *Kulkan* is obtained using equation Eq. 6.60. With this new definition, 810 different configurations were compared, for which the maximum average efficiency at 4 different firepowers (2.5, 3.0, 3.5, 4.0)[kW] resulted in $\bar{\eta} = 63\%$. The geometrical parameters are shown in Table 6.2. It is important to notice that not all configurations reached convergence, and not all of them had real roots, although some had extremely small imaginary parts, in the order of 10^{-30} , for which their real part was filtered out

and conserved, as the solution made logical sense when compared to the converged real solutions from parameters close to this ones.

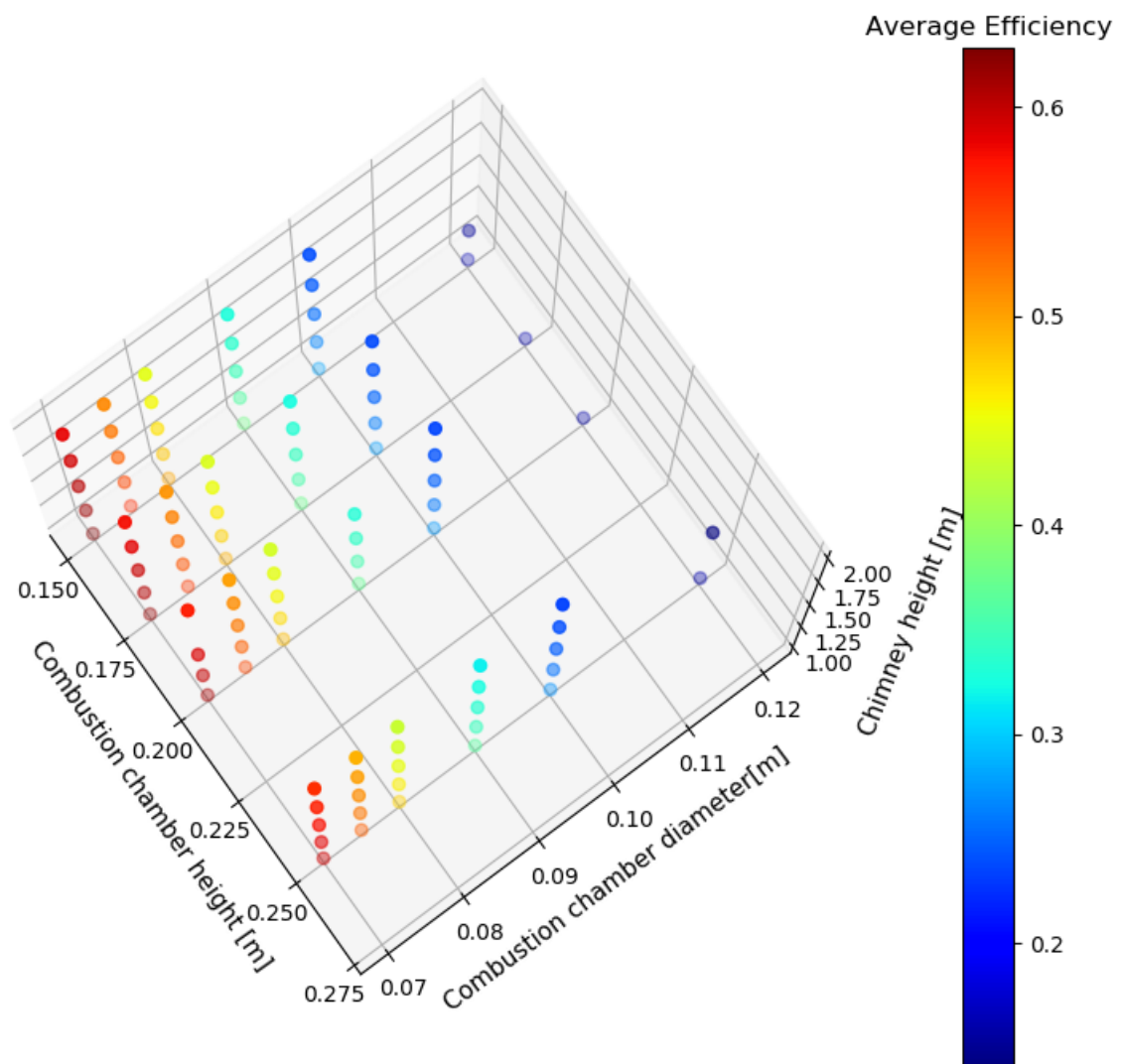
3. In Figures 6.8 6.9, the comparison between the validation model and the experimental data which were obtained from a rocket stove are compared with the complete model which includes the features of air pre-heating and optimized geometry. It can be seen that there is a significant increase in the flame temperature, reaching values close to the stoichiometric flame temperature, at a stoichiometric ratio of $\phi = 1.02$ which shows the consistency of the model.
4. After the parametric optimization of the geometry of the reactor, configurations with a theoretical efficiency of $\sim 60\%$, which is 4-8 times higher than open fires and 25% higher than the most efficient ever reported, which used an electric fan (See (Jetter et al., 2012)). This was achieved by means of heat recovery via an air pre-heater which surrounds the chimney and extracts heat from the flue gases. It has been shown that the draft created by the expanding gases is sufficient to pull air in via the outer tube covering the chimney. This in turn, increases the resistance to the flow, reducing the excess air to values closer to the stoichiometric point, instead of the 300% – 1250% excess reported by (Prapas et al., 2014).
5. From the 4-Dimensional plot shown in Figure 6.7, it can be seen that that the most influential geometrical parameter is the combustion chamber diameter. This is because the area increases with the square of the radius, which leads to higher heat losses to the surroundings. Also, having a wider combustion chamber diameter leads to lower speeds, which in turn reduce the heat transfer coefficients. The second most influential parameter is the chimney height, which influences the draft caused by the system, and thus the speed. Lastly, the least influential parameter is the combustion chamber height ³
6. From Figure 6.7, it can also be seen that for some geometries no results are displayed. This is because for those configurations convergence was not reached, particularly those with "high losses" and "high draft". This makes sense as a configuration with a large combustion chamber would lose significant amounts of heat and would probably not allow the flow to go through the chimney, which could suffocate the fire. These are interesting remarks that could be further explored, to understand the limitations of this algebraic mode.
7. From Figures 6.7, 6.8 and 6.9, it is possible to see that there seems to be a limit on the efficiency that this model can reach, which is between 60–65%. This can be understood by noticing that the smaller the combustion chamber, the lower the losses are, and the higher temperature reached. However, this also implies a reduction in the mass flow rate. At the optimal configuration, a stoichiometric ratio of $\phi \simeq 1$ was reached, with a tendency to increase i.e., reduce the air. This means that there would be a deficit of oxidizer, and that the combustion would not be complete, and thus the combustion efficiency would go down, together with the overall efficiency.

The algebraic model is capable of providing the results shown in Table 6.3. A graphical summary of the inputs and outputs of each sub-model is shown in Figure 6.6:

³Note that this model does not take into account the reactions chemistry, for which the combustion chamber height is influential due to flame quenching, this will be addressed in the next chapter.

Table 6.3: Outputs of the algebraic model

In each zone	Entire system
Convective heat transfer coefficient	Air-fuel ratio i.e., stoichiometric ratio
Conductive heat transfer coefficient	Efficiency
“Radiative” heat transfer coefficient	Recovered heat
Heat transfer	
Flow velocity	
Temperature	
Dimensionless number (Re, Nu, Gr, etc)	
Pressure drop	
Gas emissivity	
Gas absorptivity	

**Figure 6.7:** Efficiency map for different configurations

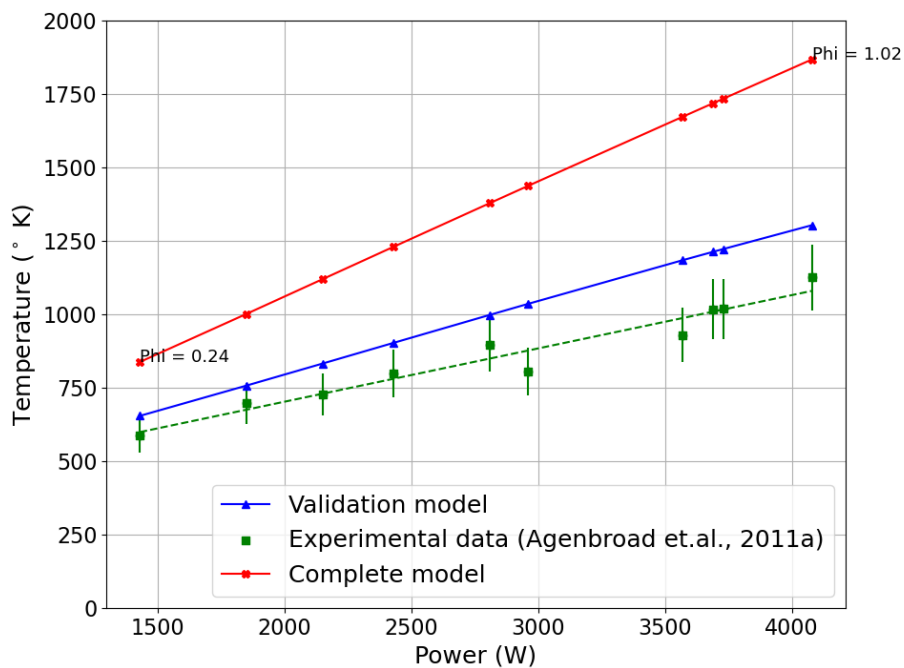


Figure 6.8: Comparison of the two models and the experimental data, flame temperature

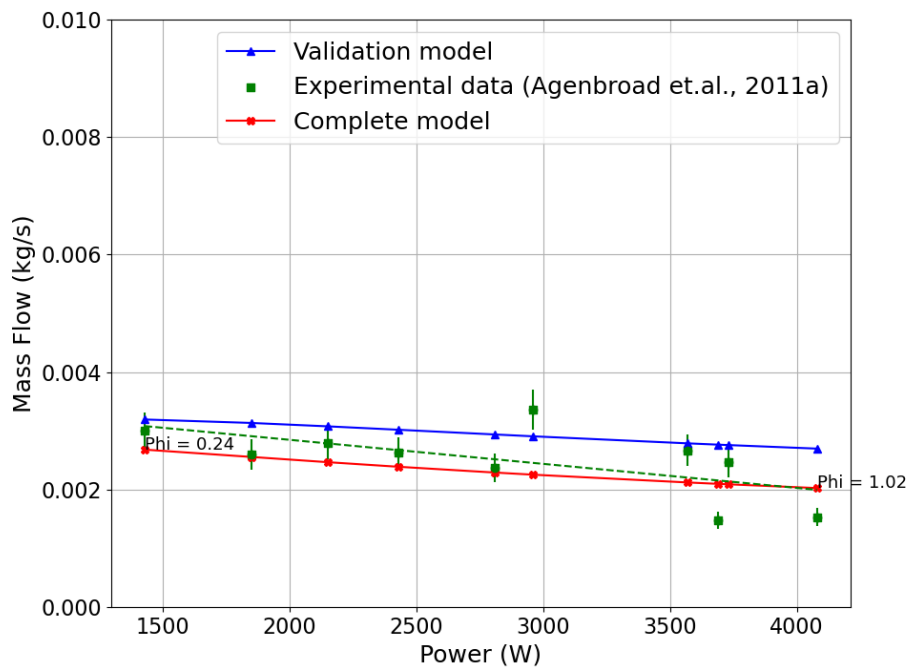
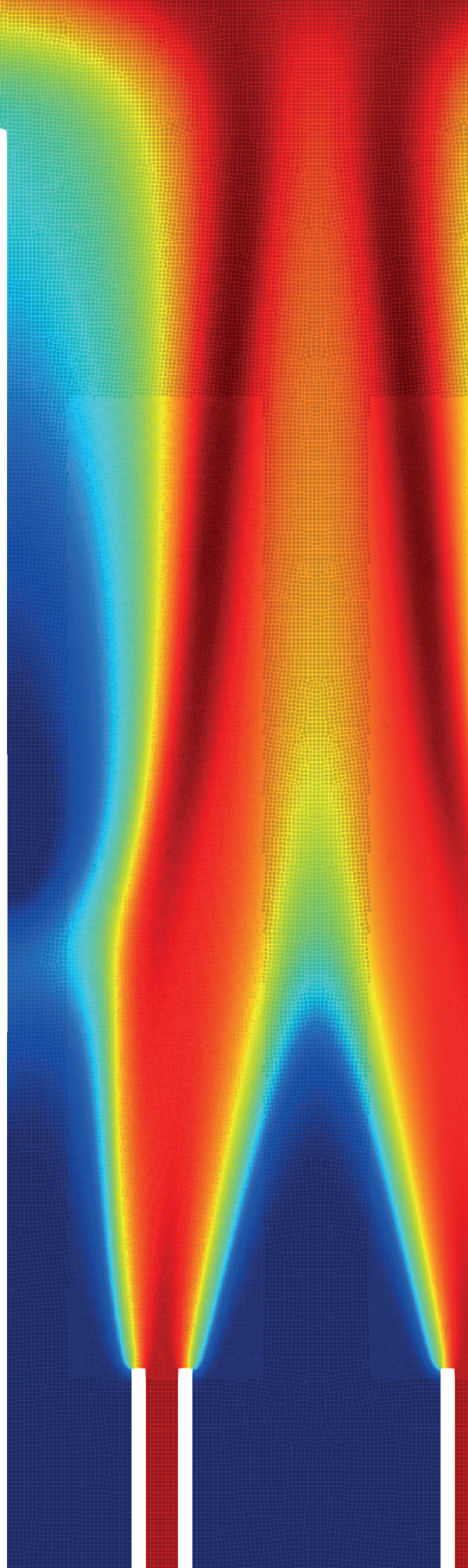


Figure 6.9: Comparison of the two models and the experimental data, total mass flow-rate

Proving Hypothesis 2: Flame quenching prevention

7



1. FLAME QUENCHING PREVENTION

In the *Currently available technology* (Section 1.1), it was mentioned the available technologies have the problem of flame quenching caused by direct impingement due to short a distance between the reaction zone (flame) and the heating object (pot).

Flame quenching is the term given to the spontaneous extinction of a flame, which is caused by a rapid reduction of the exothermic reactions, this can be caused by a deficit of branching radicals at the flame front, by flame stretching or by an balanced heat loss i.e., *heat loss > heat production* (Law, 2006). The former two are of interest here.

1.1 FLAME QUENCHING BY HEAT LOSS

This concept of rapid heat loss from the flame can be explained clearly by understanding the nature of the reaction rates, which can be characterized by the Arrhenius equation. This behavior can be seen in Figure 7.1. In this figure, the range of temperatures starts at 50 Kelvin with the purpose to show the sensitivity of the reaction rate to low temperatures. This shows that if the flame loses more heat than it produced i.e., is unbalanced negatively, then the reactions are practically stopped.

$$k(T) = BT^\alpha e^{-\frac{E_a}{RT}} \quad (\text{Eq. 7.1})$$

Where:

k is the rate constant (frequency of collisions resulting in a reaction)

T is the absolute temperature

E_a is the activation energy for the reaction

R is the universal gas constant

The problem that arises with flame quenching by unbalanced heat loss is that the hydrocarbons that are undergoing the combustion reactions are stopped and instead of fully burning, they undergo other types of reactions which occur at lower temperatures, like soot formation. Hence, a way to prevent soot and increase the efficiency is by allowing the reactions to finish and do the heat transfer only with the hot flue, and not with the flame itself. For that reason it is of interest to see if the **flame length** is altered by addition of oxygen to make the combustion in the premixed regime, instead of non-premixed, as it currently takes place in the existing technology.

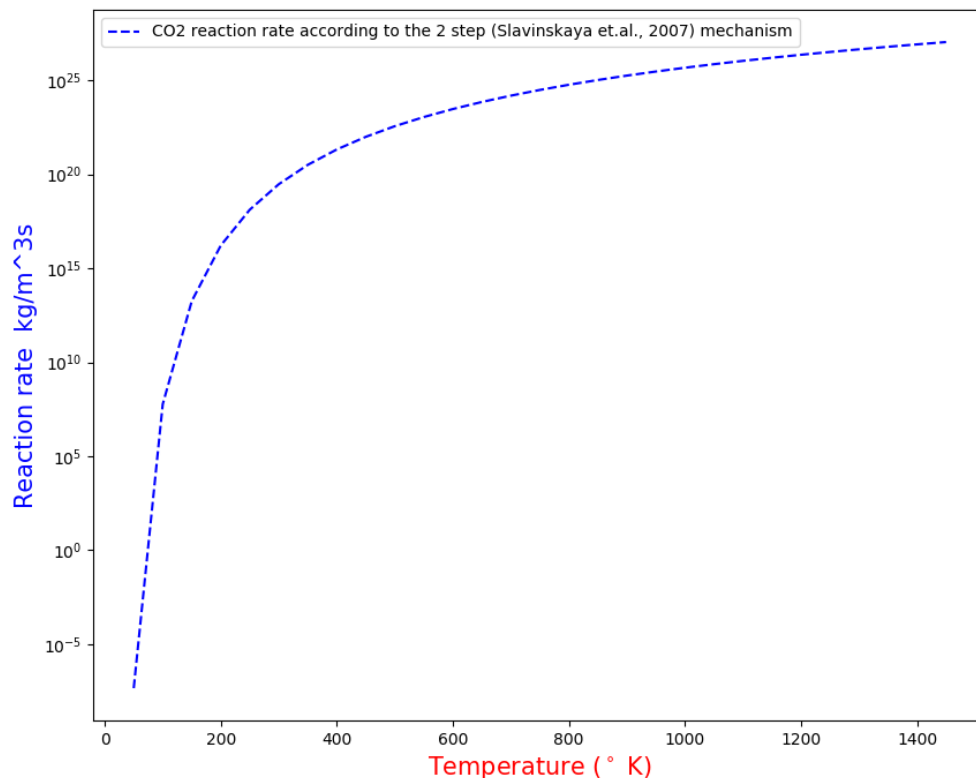


Figure 7.1: CO₂ reaction rate according to the Slavinskaya et.al., 2-step mechanism

1.2 FLAME QUENCHING BY STRETCHING

It is commonly said in literature that to have better combustion, it is required to apply the 3 *T*'s, temperature, time and turbulence. Nevertheless, just like any other generalization, it fails to address all the cases (a contradiction in itself). Turbulence does improve mixing, however, it can also disturb the flame front and cause flame quenching (Warnatz, Maas, and Dibble, 1996). It is therefore not necessarily true that turbulent combustion will lead to more complete combustions. If the combustion happens in the laminar regime, then flame quenching by stretching due to turbulence is not a problem.

Nevertheless, stretching in the laminar regime can also affect the flame front due to instabilities. This are characterized by the *Markstein* number. (Monteiro et al., 2010), (Monteiro Magalhaes, 2011), have demonstrated that the laminar flames of premixed updraft and downdraft biomass syngas and air are generally unstable, as the gradients of the flame speed vs stretch rate show positive values. Nevertheless, these gradients are small and could be negligible in an application such as the Kulkan.

2. AUXILIARY HYPOTHESIS: FEASIBLE LAMINAR FLAME SPEED

Before putting to test the hypothesis 2, it was tried to prove it false or unrealizable by testing an auxiliary hypothesis which is a necessary condition, and that has to do with the laminar flame speed of premixed syngas, which had to be in the order of $Sl \simeq 1m/s$, as this is a typical flow speed in a stove (Prapas et al., 2014).

The laminar flame speed for different syngas-mixtures was calculated using 1-Dimensional detailed chemistry simulations with the *CHEM1D* software, from the *Eindhoven University of Technology*.

First, the simulations were compared with experimental data from the literature in the conditions that the experiments were carried out. In Figure 7.2, the laminar flame speed comparison with updraft and downdraft 5 species gas compositions is presented. The error bars were set at 10% as suggested by (Oliveira et al., 2020) to be considered acceptable. Note that the difference between the updraft and downdraft syngas is the composition, as shown in Table 7.1, and the most influential in the laminar flame speed is the hydrogen fraction.

Table 7.1: Syngas Composition [% by volume] (Oliveira et al., 2020)

Gasifier type	H_2	CO	CO_2	CH_4	N_2
Updraft	11	24	9	3	53
Downdraft	17	21	13	1	48

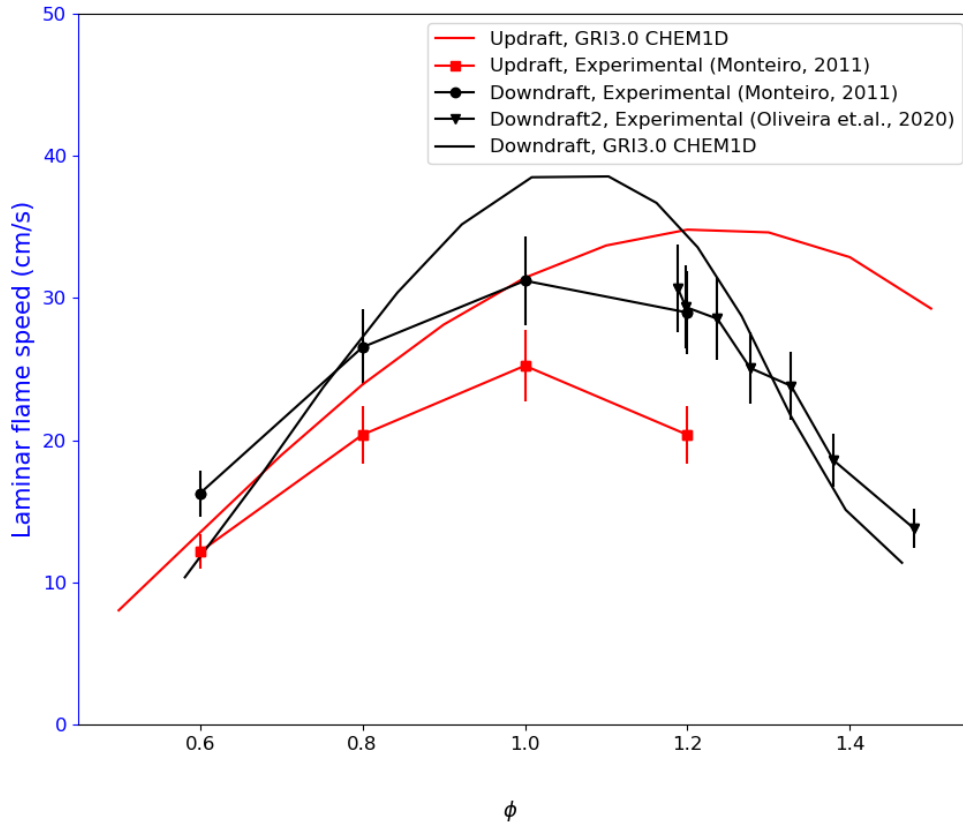


Figure 7.2: Laminar Flame Speed

It can be seen that there is good agreement for the rich side of the downdraft syngas, as well as in the lean side, but an over prediction close to the stoichiometric point. The updraft syngas shows a good agreement in the lean side, and a divergence after the stoichiometric point. It is not clear what causes the divergence in flame speed. The *CHEM1D* software has been extensively validated with experiments and can be considered to be accurate, moreover, the simulations did take into account the effect of differential diffusion i.e., non-unity Lewis numbers.

Accepting the models as sufficient to reproduce the scale of the laminar flame speed, the models were extended for higher temperatures, as in the case of the *Kulkan*, the fuel is entering the combustion chamber directly after the updraft gasifier. The simulation was performed also with varying air inlet temperature. The results are shown in Figure 7.3. The temperatures were chosen based on typical updraft gasifier exit temperature (Basu, 2010), and the air was chosen based on the results of the predicted temperature of the general model from the previous section.

It is important to mention that the exit temperature of the updraft gasifier is far from the auto-ignition temperature of the syngas, which would pose an important technical and safety problem. According to (Hagos, Aziz, and Sulaiman, 2014) the auto-ignition temperature is higher than $800K^\circ$, also supported by (Kwiatkowski, Dudyński, and Bajer, 2013).

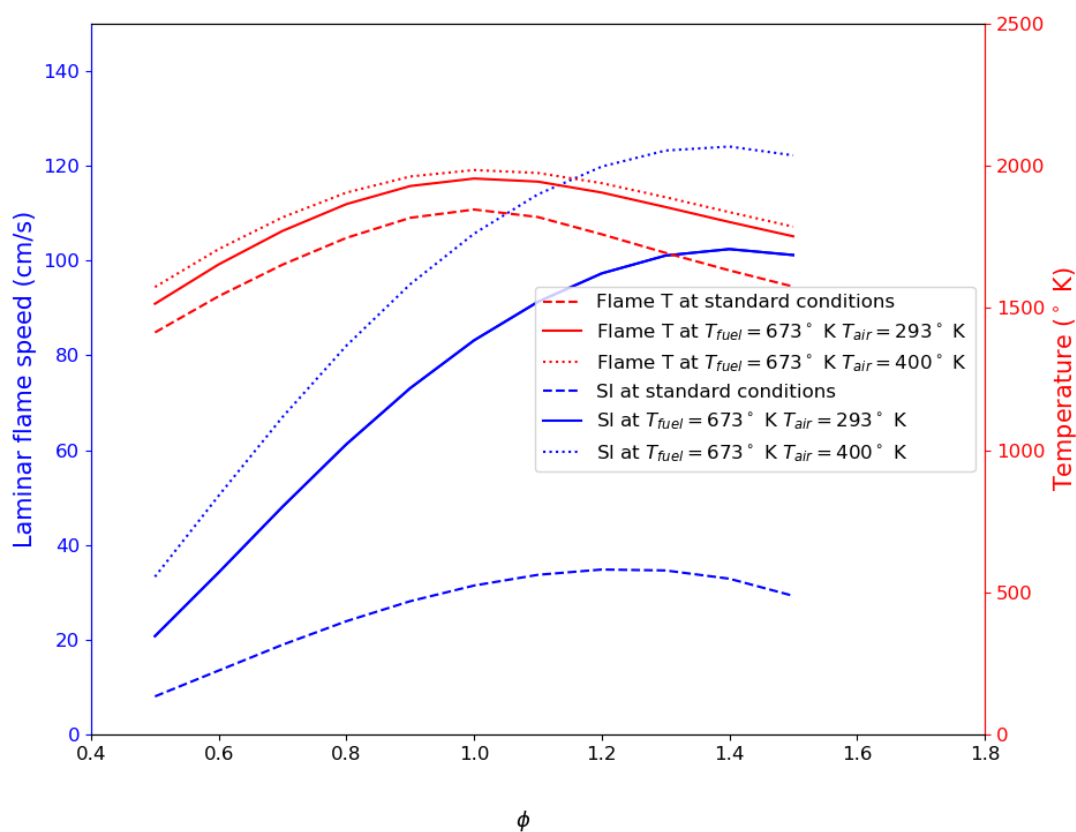


Figure 7.3: Laminar Flame Speed of updraft syngas at high inlet temperatures

As it can be observed in Figure 7.3, the maximum predicted laminar flame speed is slightly higher than $1m/s$, if it had been larger, controlling the system would have posed problems due to flashback at high speeds. However, this order of speed is readily existing in the current technology, so it does not require highly specialized equipment.

It can also be noticed that the flame speed, as well as the maximum temperature, follow a consistent trend to increase with the inlet temperature. Having high temperature is also beneficial for the flame stability, specially in not well mixed syngas compositions according to (Kwiatkowski, Dudyński, and Bajer, 2013). Putting it in other words, having low temperatures lead to flame unstabilities, and as it was mentioned before, the currently available technologies suffer from extremely high excess air, which leads to low temperatures, so current technology also suffers from flame instabilities, but this has rarely

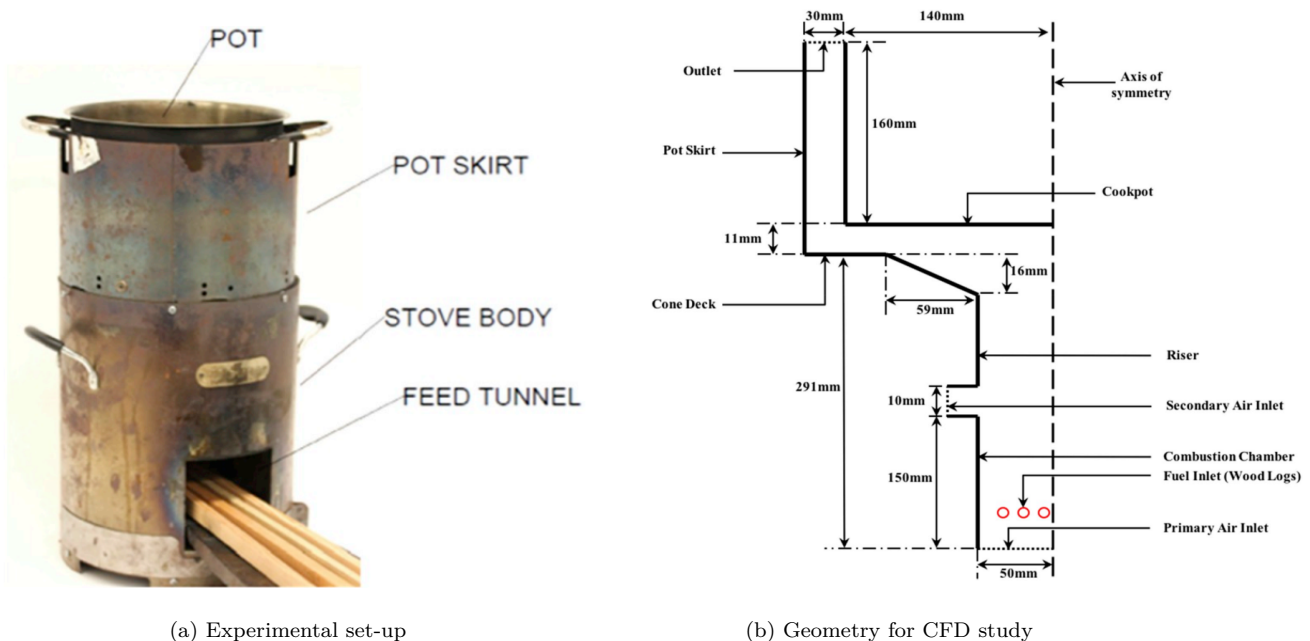
been addressed in the current literature.

Since the values of the laminar flame speed are in a manageable range, the main hypothesis was put to test, for which a more detailed CFD modeling capable of capturing more information was created.

3. 2D MODEL VALIDATION

In a recent study (Pundle et al., 2019) investigated a similar configuration as (Kshirsagar and Kalamkar, 2015) i.e., a Rocket stove, with the difference that they did a more detailed modeling using computational fluid dynamics -CFD- or reacting flow assuming axis-symmetry and later validated with experimental data, which made it an ideal reference to begin with as it had a simpler geometry than the full Kulkan rector, but still allowed to compare results to validate, and then extend.

Figure 7.4: Experimental set-up and geometry for CFD study of (Pundle et al., 2019)



Specific sub-models of the reference study:

- Turbulence: Realizable $k - \epsilon$
- Chemistry: laminar chemistry. 21-step syngas ($CO + H_2$) mechanism from (Hawkes et al., 2007)
- Radiation: discrete ordinates method, with an experimentally adjusted absorption coefficient $\alpha = 7.5$.
- Homogeneous-Heterogeneous coupling: not coupled, only homogeneous phase modeling with imposed gas composition
- Solver: STAR-CCM + (commercial. Uses volume method based)

Some of the findings reported by (Pundle et al., 2019) that are of high relevance for this study are:

1. "... the excess air is typically many times stoichiometric air during standard operating conditions and is sensitive to flow field obstructions."
2. "air entrainment, though ineffective by itself, increases turbulent mixing when used in conjunction with a central baffle but reduces thermal efficiencies due to enhanced heat transfer to the walls" ¹

¹Their claim of "ineffectiveness" should be taken with care, as the effectiveness will depend on the geometrical configuration.

3. "Lower pot support height decreases the airflow rate and increases thermal efficiency."
4. A experimentally validated CFD model which only takes into account the homogeneous reactions gave a predicted average efficiency with a difference of 1.78%, between the model and the experiments.

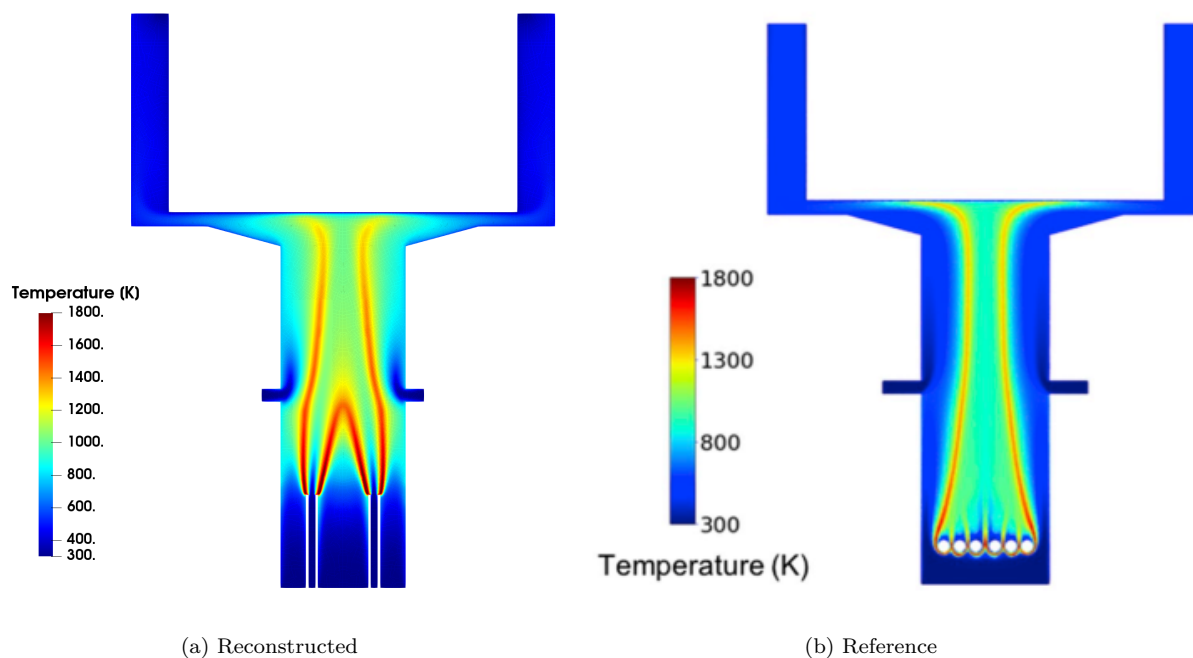
3.1 MODEL RECONSTRUCTION

The reference model was reconstructed with the commercial software *Ansys Fluent 19.2* using the *Reynolds* cluster computer at the *Energy & Process* department at *TU Delft*. Post-processing was performed using the open-sources software *Paraview* in combination with *Python*.

All the physical conditions were conserved, except the fuel inlet boundary, for which Pundle et al. do not provide sufficient information to replicate. It is mentioned that it is a *fixed mass flow inlet boundary condition*. However, from the drawings, its not clear how this is defined as it is in the middle of the domain. It seems like the flux is normal to the boundary, but this causes convergence problems, specially in the bottom of it as there is air coming in one direction and fuel going in the opposite direction. This boundary was replaced by an fuel injector, representing an annular fuel supply channel, keeping all other boundaries as in the reference, including mass-flow rates and composition.

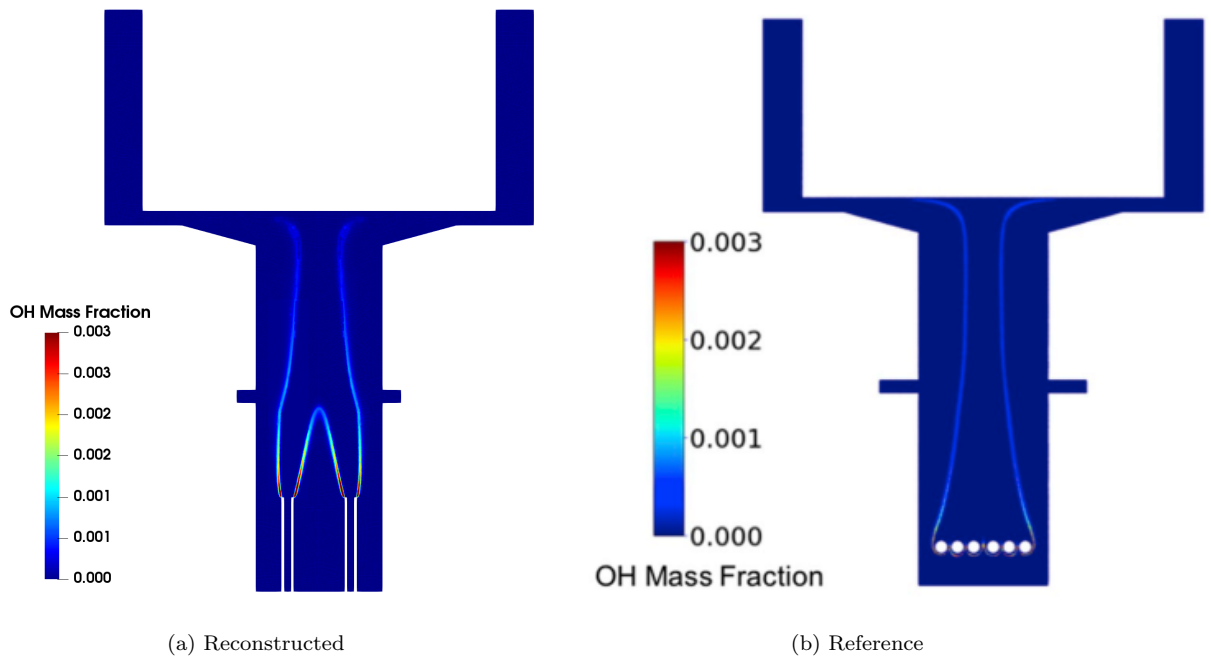
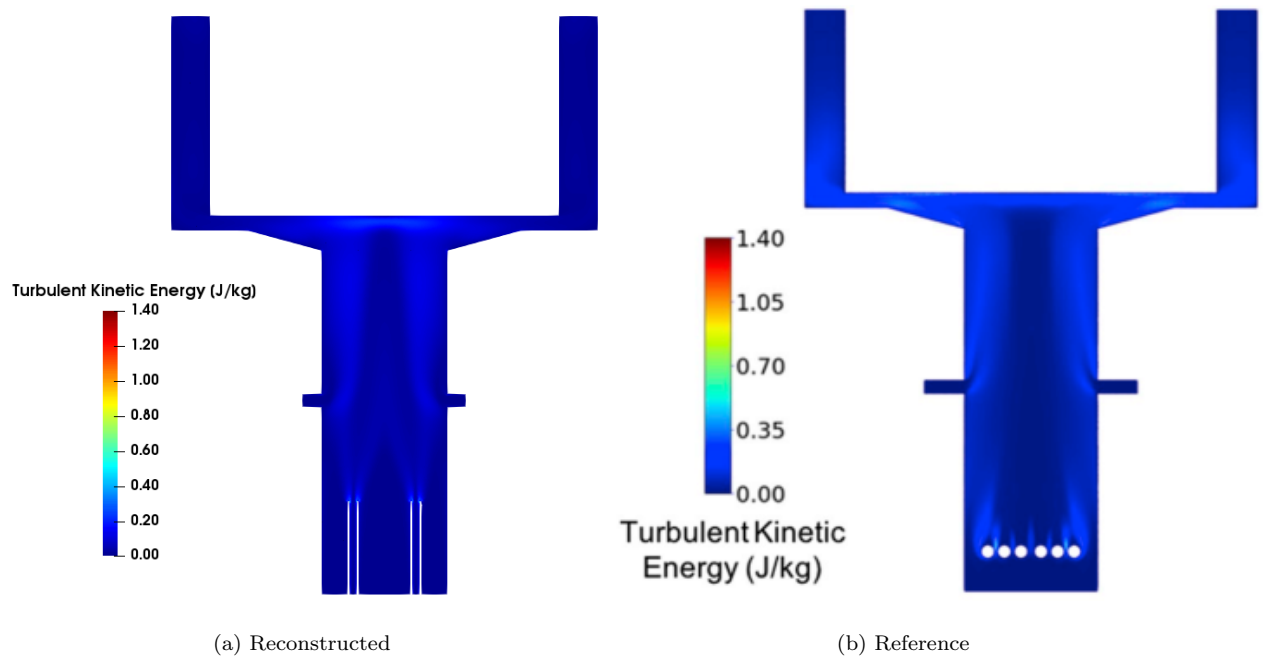
The replicated model was compared against the provided contour plots given by the author, which are depicted in Figures 7.5, 7.6 and 7.7.

Figure 7.5: Comparison between reconstructed model and (Pundle et al., 2019)



From Figure 7.5, it can be seen that the temperatures are in the same range, but the spacial profile differs because of the different burner design. The flame in the reference is longer and the tip impinges in the surface pot. On the replicated model, the flame goes further into the horizontal slit between the pot and the outer walls, this is reasonable as the fuel inlet is further into the domain. It is really important to note that the system is able fully function with open boundaries, as is the case for both the primary and secondary air-inlets, which can be seen to replicate the behavior properly. Only the fuel inlet was imposed as a mass-flow rate equivalent to $3kW$. The flame was stabilized using a heated burner tip, which enhances the ignition.

In Figure 7.6 the mass fraction of OH is shown, which indicates the zone of the highest temperature. As in the previous plot, it shows the same trend, but more concentrated, as the flame is shorter. It also

Figure 7.6: Comparison between reconstructed model and (Pundle et al., 2019)**Figure 7.7:** Comparison between reconstructed model and (Pundle et al., 2019)

looks like the OH in the reference is able to survive longer distance at the impingement region.

The Figure 7.7 shows a common central region of lower intensity, which increases as the flow is bent towards the exits. The highest regions are at the fuel inlets in both cases, and a slight increase at the secondary air inlets.

3.2 ALTERNATIVE CHEMICAL MECHANISMS

The mechanism used for the previous model validation shows to behave in an acceptable way. The contours of the main variables of importance are captured correctly, even with the differences in the fuel-inlet boundary condition. However, there have been efforts done to significantly reduce the computational expense without compromising the essential information by simplifying the chemical mechanisms. Although 21 steps is not large compared to the more complete *GRI-3.0* with 53 species and 325 reactions, or the *DLR-LS-full* with 55 species and 459 reactions; it can still be reduced.

(Alzahrani et al., 2015) did an evaluation of the accuracy of selected syngas chemical mechanisms, from which the 2-step one by (Slavinskaya, Braun-Unkloff, and Frank, 2008) was able to perform with an average error of less than 20%, "comparable to GRI mechanism... which makes it more promising compared to other reduced syngas mechanisms".

This 2-step mechanism was developed for mixtures of syngas and air at pressure of $P = 20bars$ and a temperature $T = 573K$. Yet, due to its proven accuracy and significant simplicity, it was explored in detail. For details of the comparison, see the Appendix, where the contour plots of the main variables are compared against the 21-step mechanism. In essence, the accuracy of the global 2step mechanism is formidable and in many cases, no difference was noticeable.

However, this was only for the non-premixed combustion cases, where the limiting phenomena of the reactions is the mixing rate. In premixed combustion, it was not stable as it would over-predict the reaction rates of the two reactions, and flash-back would occur. The only way of reaching stable premixed combustion was with *ad-hoc* manipulation of the pre-exponential factors, but assuming this would be realistic under different conditions seemed as a weak point, so it was not further explored for premixed combustion.

After the physics were validated against the reference by (Pundle et al., 2019), the case was further studied under pre-mixing conditions. For this, a mixture of fuel-oxygen was first studied, and then a mixture of fuel-air. Air was assumed to be 21% oxygen and 79% nitrogen.

In Figure 7.8, the three cases can be depicted, from left to right, the non-premixed, the premixed (fuel-oxygen) and the premixed (fuel-air), both for highly rich conditions of $\phi = 8.5$, to show that even a small amount of oxygen, can have a large impact in the flame length and thus quenching prevention, and more compact combustion chambers, which from the previous chapter was seen to benefit the efficiency.

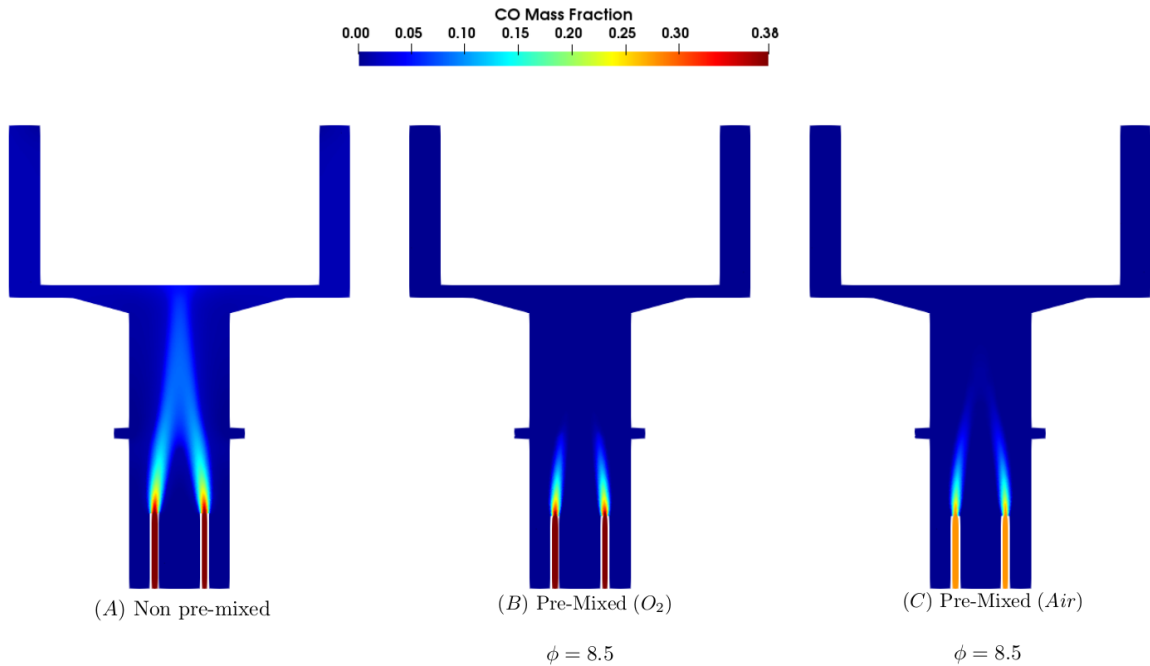


Figure 7.8: CO mass fraction for a premixed laminar flame, $\phi = 8.5$

3.3 RESULTS AND DISCUSSION

1. A 1-D detailed study of the laminar flame speed and temperature of a mixture of 5 gases, representing up-draft and downdraft syngas compositions was done using detailed chemistry, and validated against experimental data available from the literature. The updraft model is capable of reproducing the speed trend in the lean region, but over-predicts in the rich region. The model for the downdraft reproduced the speed with good accuracy in the lean and reach regions, but over-predicts close to the stoichiometric point.
2. The validated model for up-draft syngas was extended to the expected inlet conditions that the gas-fuel and air would have in the Kulkan, directly coming from the gasifier and the air pre-heater, respectively. It is shown that the higher air-temperature leads to a higher flame speed and temperature, close to the one predicted by the algebraic model (See Figure 6.8). The maximum laminar flame speed is of $1.2m/s$, with the peak at around $\phi = 1.4$. If the model is over predicting as in the validation, that means that the actual flame speed will be lower than this. As shown by (Jason Prapas, 2013), flow speeds of around $1m/s$ can be expected, so the laminar flame speed and the flow speed are close, which is a necessary condition. Thus, there was sufficient reason to further investigate the system and not discard it.
3. A 2-D CFD model was constructed and validated with the study by (Pundle et al., 2019). The physics of interest were properly replicated, with one modification of the fuel-inlet boundary condition. This model allowed to study non-premixed laminar flames with pressure boundary condition at the air inlets (in contrast with mass flow inlet boundary condition) for primary and secondary air, which showed the stability of the buoyancy driven system.
4. A 2-step chemical mechanism was validated against a more complex 21-step. It showed excellent agreement for the non-premixed case, and potential for adaptation to the premixed cases. This mechanism has great potential for more complex simulations due to its low computational cost.
5. The second hypothesis has been proven to be true. A partially premixed laminar flame can be stabilized and allow to fully develop. Even at rich mixtures of up to $\phi = 8.5$, there was a significant

reduction of the flame length, which would prevent flame quenching due to direct impingement in the pot bottom, and more compact combustion chambers, which is desired to reduce heat losses and increase efficiency, as shown in Figure 6.7.

The previous statement can be seen in Figure 7.8, the effect pre-mixing is clear. The mass fraction of the CO decays much faster in both cases. In case (C), the mass fraction of CO looks smaller than in the previous two because the mixture contains nitrogen, and the power was kept constant, which means an increase in the total mass flow and thus a higher speed, that is why the flame is slightly longer and the concentration lower at the fuel inlet pipe.

The contours of the reaction rates of the products are shown in Figures 7.9 and 7.10. It is clearly depicted that that H_2 and CO are consumed in a shorter axial distance, and that the reaction is more distributed in the premixed cases, instead of in a thin layer as in the non-premixed case. Furthermore, it can be seen in that close to the contact zone, there is a secondary reaction zone, likely due to fuel that is left unburned in that region. Another possibility is numerical diffusion due to local refinement.

A radial integration of the CO mass fraction was done as explained in Figure 7.11. The results of 250 integration lines L_i are shown in Figure 7.12, there it is depicted that at a distance of about 0.225[m], which is around 66% of the domain length where the flame exists, the CO mass fraction is virtually zero, while in the non-premixed case, it still remains close to half its initial value. Note that that both flames start at the exit of the fuel-pipe. Another remark is the slight increase in the non-premixed case, this change in the tendency is due to the change in the flow direction due to the pot bottom wall.

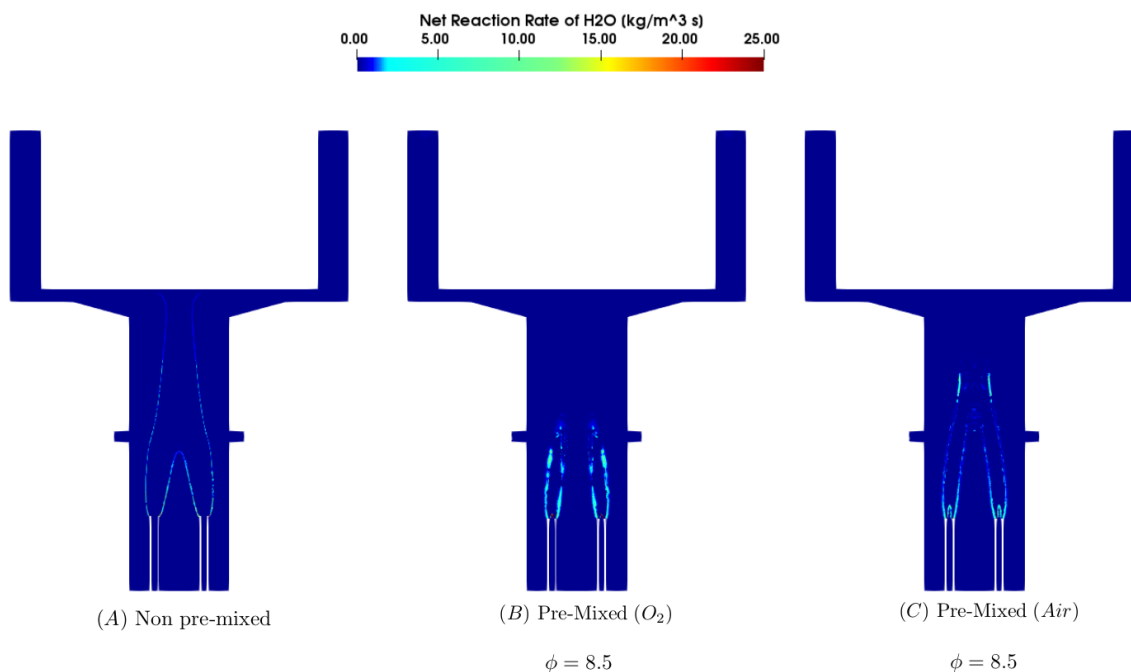


Figure 7.9: Reaction rate of H_2O for a premixed laminar flame, $\phi = 8.5$

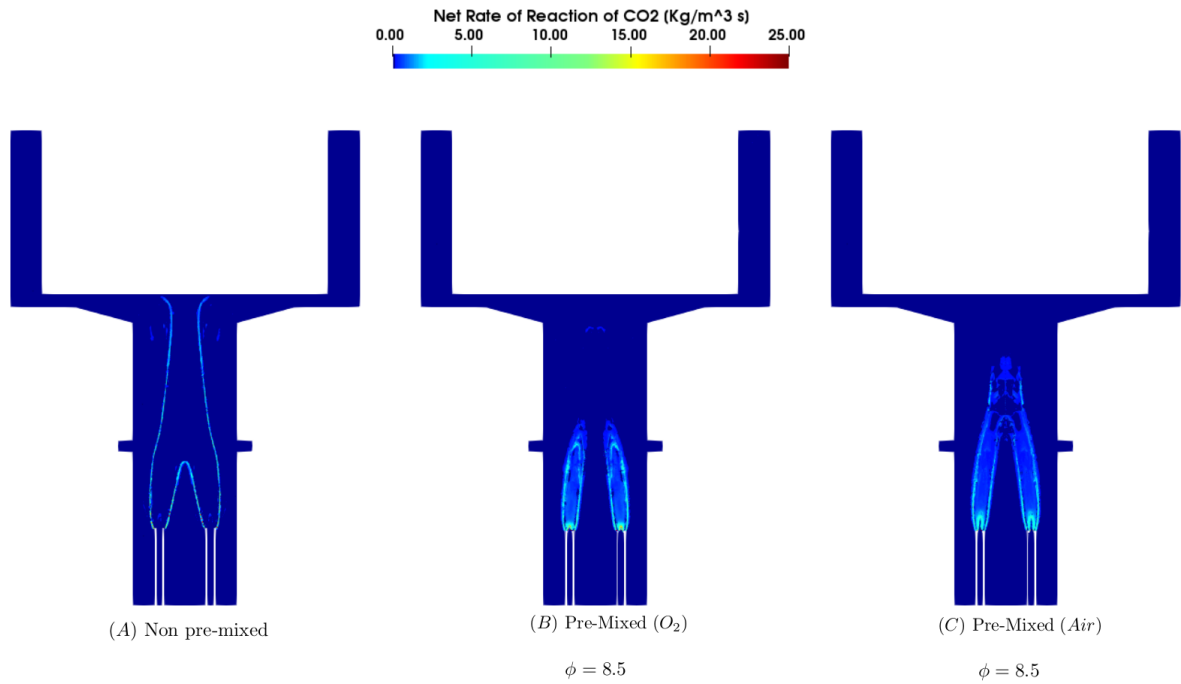


Figure 7.10: Reaction rate of CO_2 for a premixed laminar flame, $\phi = 8.5$

Radially integrated distribution

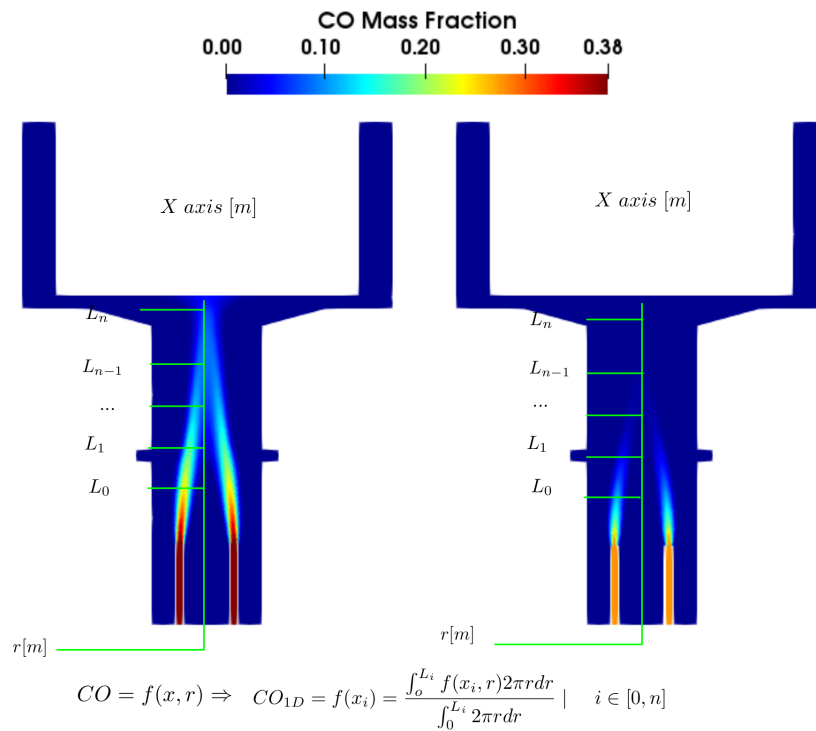


Figure 7.11: Radially integrated CO mass fraction

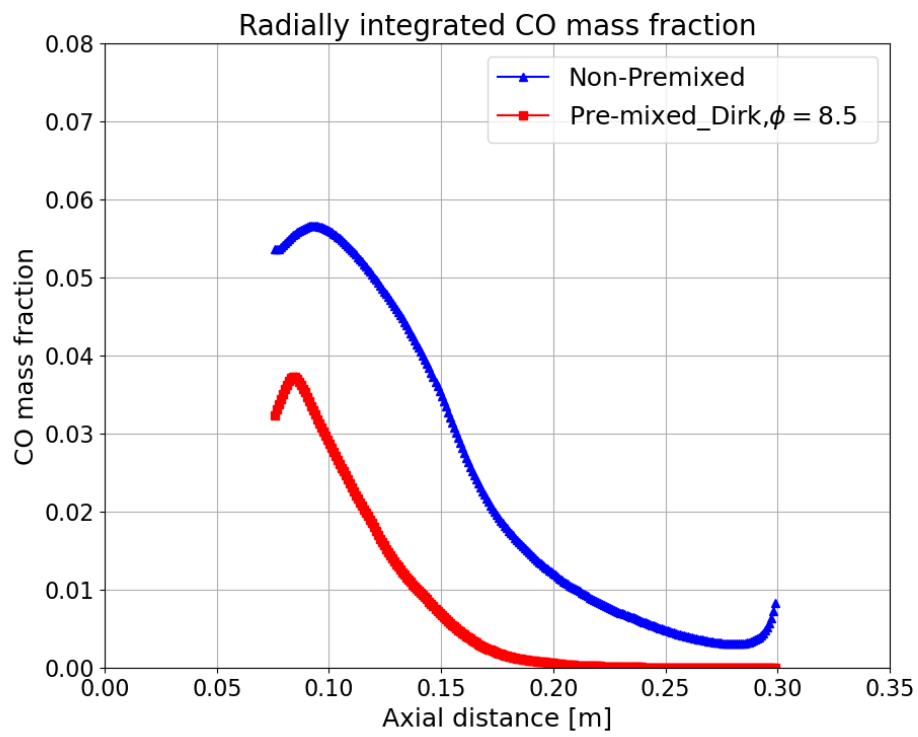
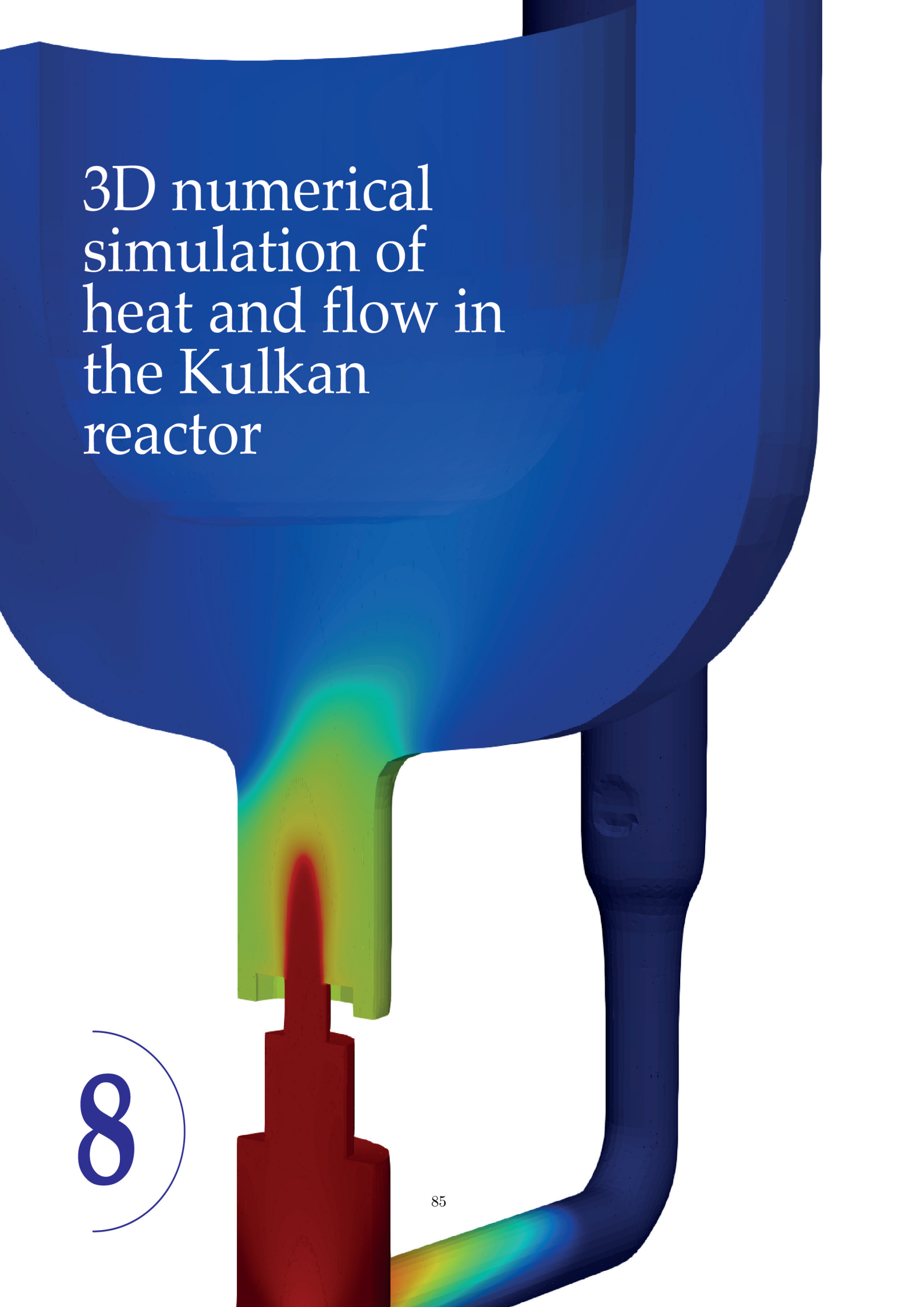


Figure 7.12: Radially integrated distribution along the axis

3D numerical simulation of heat and flow in the Kulkan reactor

8



With the hypotheses 1 and 2 proven, it was of interest to integrate them to explore the results in a more realistic scenario. Initially, it was planned to perform experiments and simulations, but due to the implications that the COVID-19 had in restrictions in indoor spaces at TUDelft, it was decided to perform more detailed simulations that could also provide essential information, at a lower expense and with ease of parametrization, hence three different 3-D studies were carried out.

1. MESH

The computational domain was created with three softwares, used for different stages of the process. The geometry was constructed in *cinema 4D*¹, then the connections were improved in *MeshMixer*², particularly the unions of the double chimney, a region of particular difficulty. Then, the meshing was done using *CF-Mesh+*³.

Three different 3-D computational domains were constructed, one for hot non-reacting flow, one for reacting flow with primary air only, and the last one for reacting flow with primary and secondary air inlets, with around $2.1 \cdot 10^6$ cells each. In Figure 8.1, the geometry and the mesh for the third are depicted, with a plane cut at $y = 0$ i.e., vertical cut through the origin, to allow all the parts to be appreciated. This geometry is the 3-D representation of the conceptual Figure 6.1.

The darker zones found between the "burner" and the "canonical pot" are local refinement zones that were done using "primitive objects". The reason why the pot is called "canonical" is because this is not intended to represent a real-life pot, but the most general one, as the real ones (and the real heat exchange configuration) should be done in the stove design process, including the cultural influence.

The flow boundary conditions for each of the patches shown are:

- **Gas-fuel inlet** = imposed constant mass flow rate for a power output of $3kW$, with the same gas composition taken from (Pundle et al., 2019), as it was extensively validated as mentioned in Chapter 7.
- **Flue-outlet** = pressure outlet to the atmosphere.
- **Air-inlet** = pressure inlet from the atmosphere.
- **All others** = walls with non-slip boundary conditions.

The burner design was inspired by the piloted non-premixed jet flame burners studied in the frame of the International Workshop on Measurement and Modeling of Turbulent Flames (TNF workshop series). The burner is shown in Figure 8.2.

¹<https://www.maxon.net/en-us/products/cinema-4d/overview/>

²<https://www.meshmixer.com/>

³<https://cfmesh.com/>

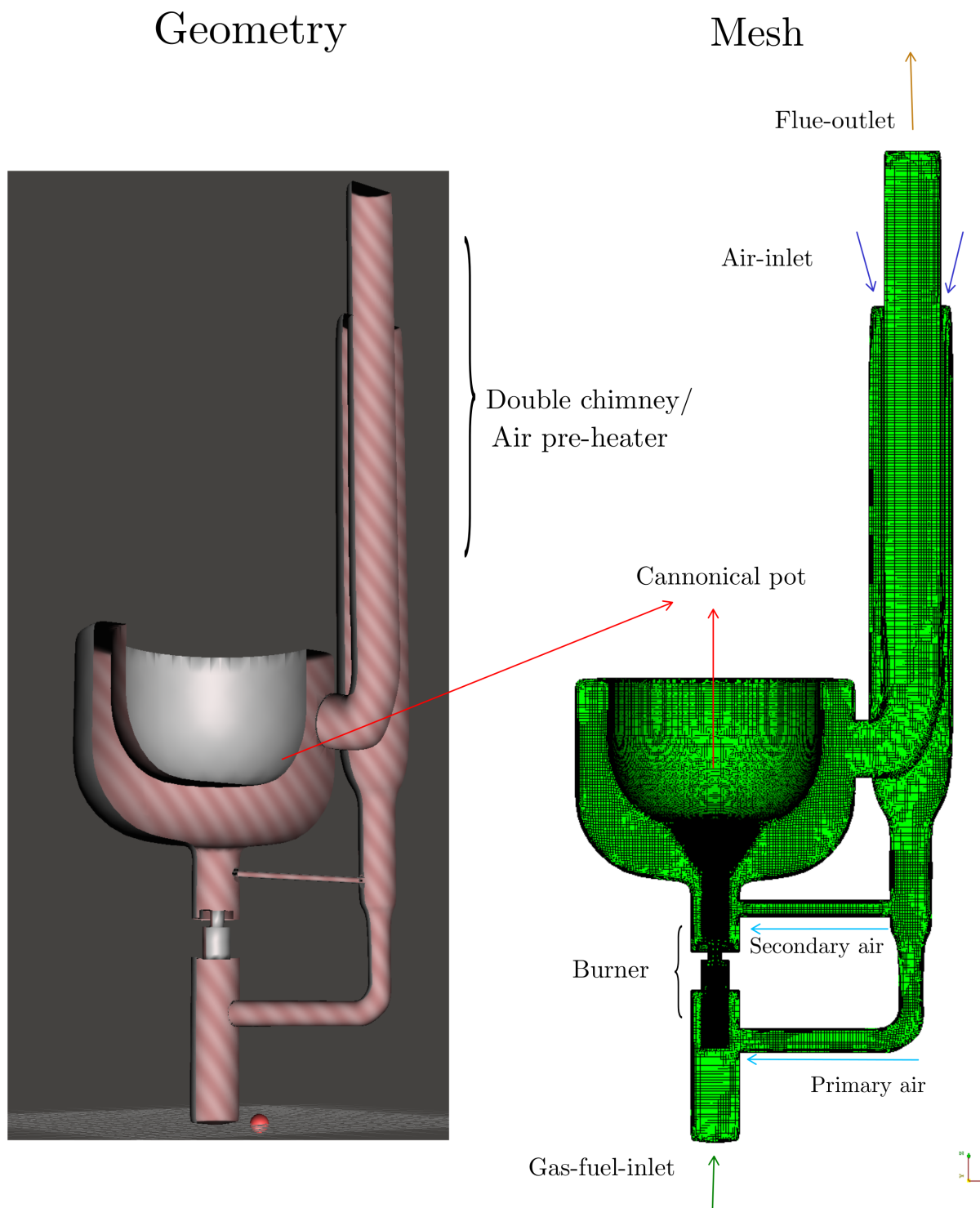
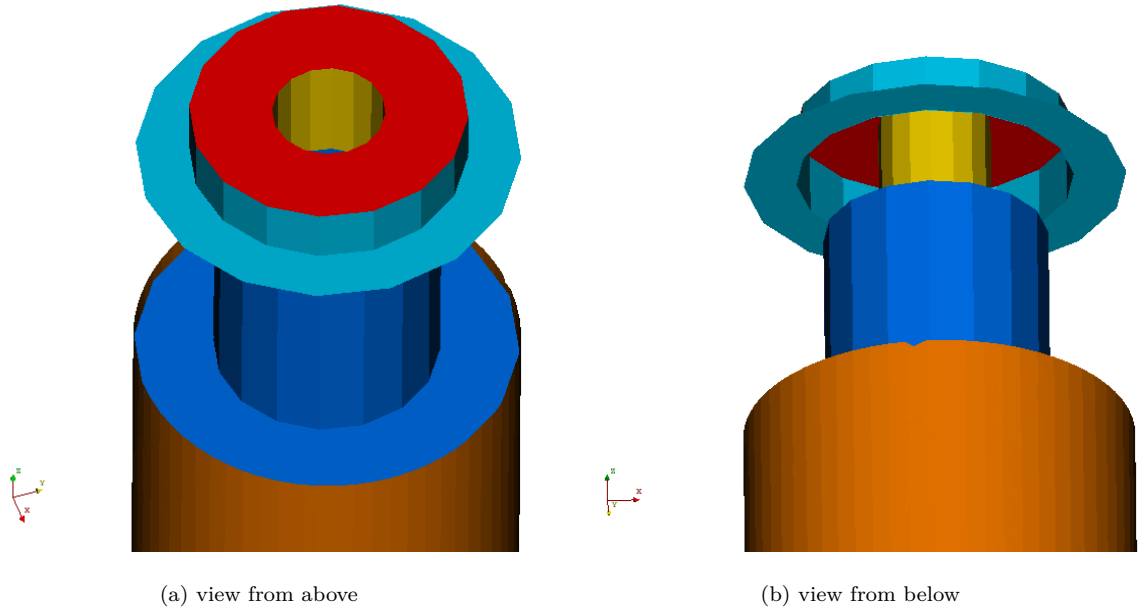


Figure 8.1: Geometry and mesh for the *Kulkan's* 3-D simulation. Plane cut at $y = 0$

Figure 8.2: Close-up views of the burner**Table 8.1:** Burner elements and their functions

Element	Color	Operation mode	Function
Burner tip	Red	Hot tip Pilot	Facilitate ignition and flame stability
Burner crown	Light-blue	Wall Open Boundary Fixed Inlet conditions	Investigate influence of different burner oxidizer conditions
Burner small contraction	Yellow	Variable temperature wall	Increase vorticity (mixing) and fuel speed to prevent flashback
Burner medium contraction	Blue	Variable temperature wall	Increase vorticity (mixing) and fuel speed to prevent flashback

The key intentions of this burner design were: flame stability, flash-back prevention, modularity of operation, accessibility from outside, and control. For which the features presented in Table 8.1 were included in the design. From top to bottom, during the 2-D studies, it was observed that to facilitate ignition and flame stability, the piloted and hot-tip techniques were highly effective, with the hot-tip being less invasive.

The bottom part of the burner crown (light blue) is intended to serve an easy to change boundary condition to operate in three modes, to investigate the influence that it would have in the entire system, and to shed light into future burner construction.

Both contractions were included to enhance mixing and increase velocity to prevent flashback. The reason why the contractions are exposed is simulate accesibility from outside, for example, to prevent

wall flash back, the yellow contraction could be cooled down. In the simulation this would be equivalent to imposing a fixed temperature at the wall, but by having the design readily accessible in concept, it facilitates future construction.

Note: In the next three sections, the three studies will be presented, and the results and discussion will be given at the end of each section, for the ease of reading, instead of at the end of the chapter, like previously.

2. NON REACTIVE FLOW SIMULATION

The first simulation to be performed was with non reactive flow, as it was computationally less expensive and would already provide valuable information of the fluid flow and the buoyant forces. Two different turbulence models were investigated, namely the *k-epsilon* and the *k-epsilon RNG*. The medium was considered to be *air*. The "gas-fuel-inlet" was set at a mass flow that that would carry an enthalpy equal to $3kW$. Note that simulations were performed without the burner as it was not necessary.

2.1 TURBULENCE MODELS: *K-EPSILON* VS *K-EPSILON RNG*

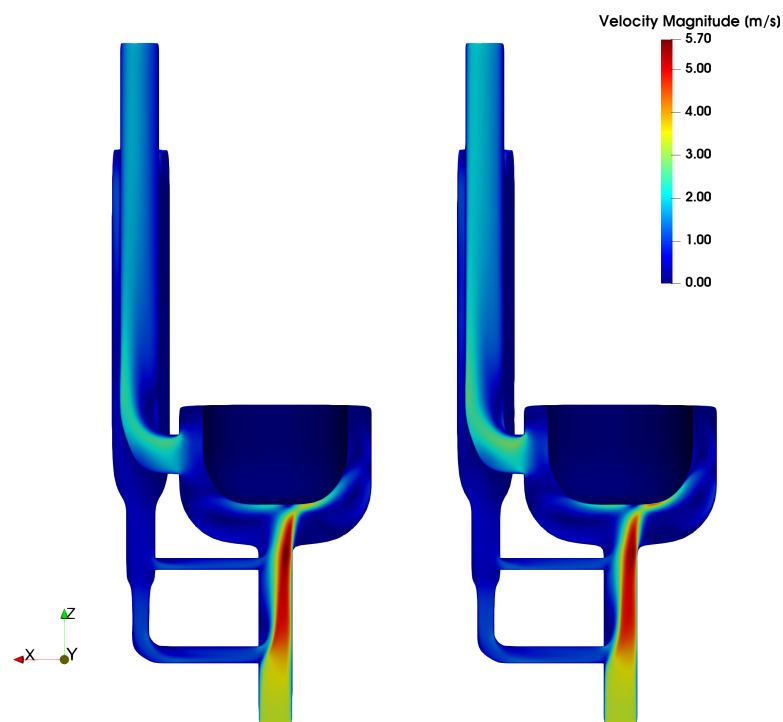


Figure 8.3: 3-D contour plot of velocity magnitude. Plane cut $y = 0$
k-epsilon (left) vs *k-epsilon RNG* (right)

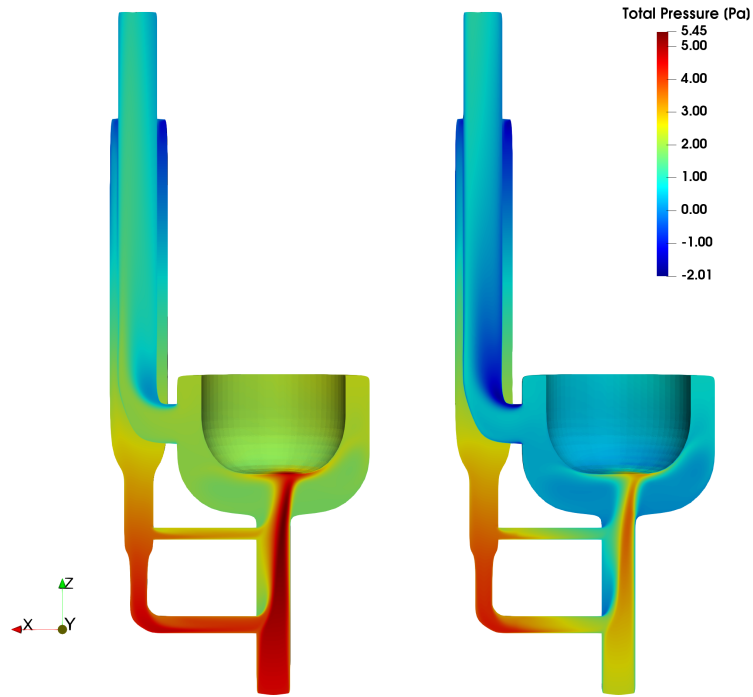


Figure 8.4: 3-D contour plot of total pressure. Plane cut $y = 0$
k-epsilon (left) vs *k-epsilon RNG* (right)

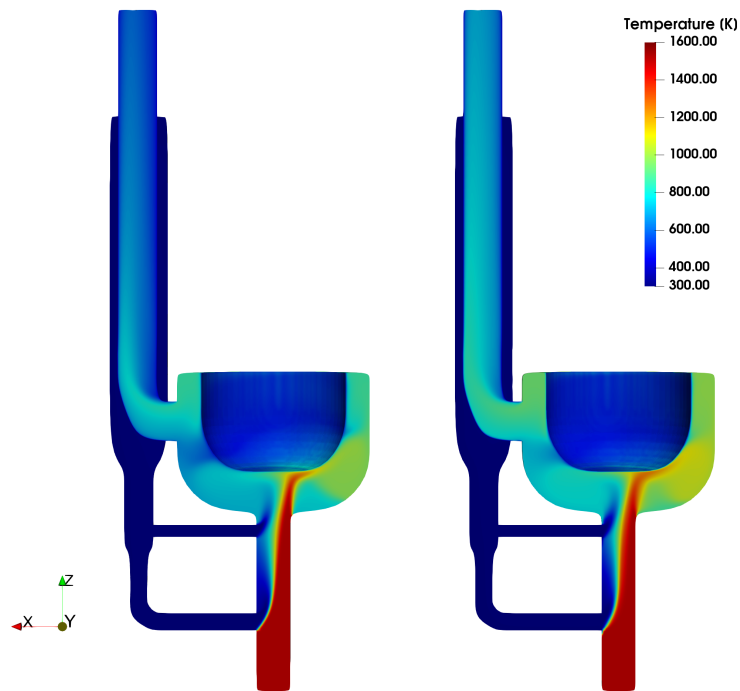


Figure 8.5: 3-D contour plot of static temperature. Plane cut $y = 0$
k-epsilon (left) vs *k-epsilon RNG* (right)

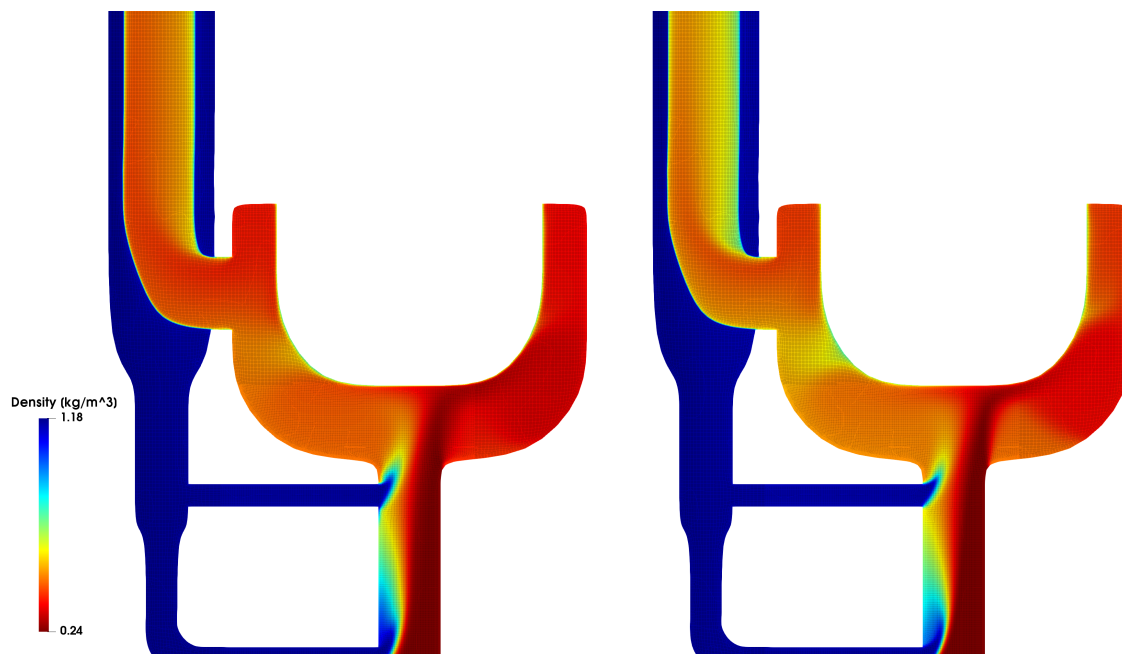


Figure 8.6: Flat contour plot of density. Plane cut $y = 0$
k-epsilon (left) vs *k-epsilon RNG* (right)

From Figure 8.3 it can be seen that both the models describe the physics with great similarity. There are not substantial differences in the velocity magnitude field, except for the inner chimney, where the RNG model predicts a higher speed. Another region of higher velocity is to right (based on the picture) of the stagnation point at the pot bottom. The higher velocity at the chimney likely results from the different wall treatment given by the RNG model.

The total pressure gives notably different results. The RNG model predicts a maximum pressure which is around 40% less than the counter part. This difference is better explained by taking into account Figure 8.5, where the temperature field can be seen to also differ in the inner chimney region. This phenomena can be explained by the wall interactions. In the RNG model, the wall treatment is better, which results in better the heat transfer between the fluid and the wall. To support this claim, a zoomed in contour plot of the density is shown in Figure 8.6.

The mesh was plotted together with the density contour to show the more abrupt change close to the bottom pot with a fixed temperature of $373K$ (resembling boiling water and an infinitely thin wall). Its clear that this is the region of relevance, as in the previous regions there is virtually no difference (except for a small difference at the "primary air" jet). Hence, it is the heat exchange and thus reduction of density of the hot air that causes the reduction in speed, temperature and pressure.

2.2 EFFECT OF HOT-CHIMNEY WALL

The goal of this study was to understand what is the influence of a "hot inner chimney wall", which resembles the behavior of the air pre-heater. A Dirichlet boundary condition with $T = 500K$ was used, this value approximated from the predicted by the algebraic model as the mean value of the 5 chimney section. All the simulations carried out in this section used the *k-epsilon RNG* model, as it provides better information of the flow behavior close to the walls. This also shows the importance of having refined boundary layers.

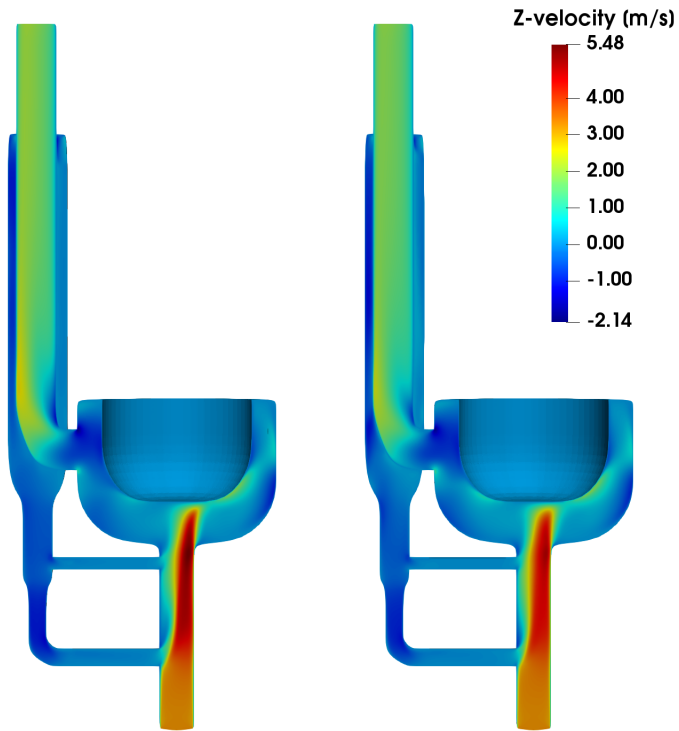


Figure 8.7: 3-D contour plot of \hat{z} velocity. Plane cut $y = 0$
cold wall (left) vs *hot wall* (right)

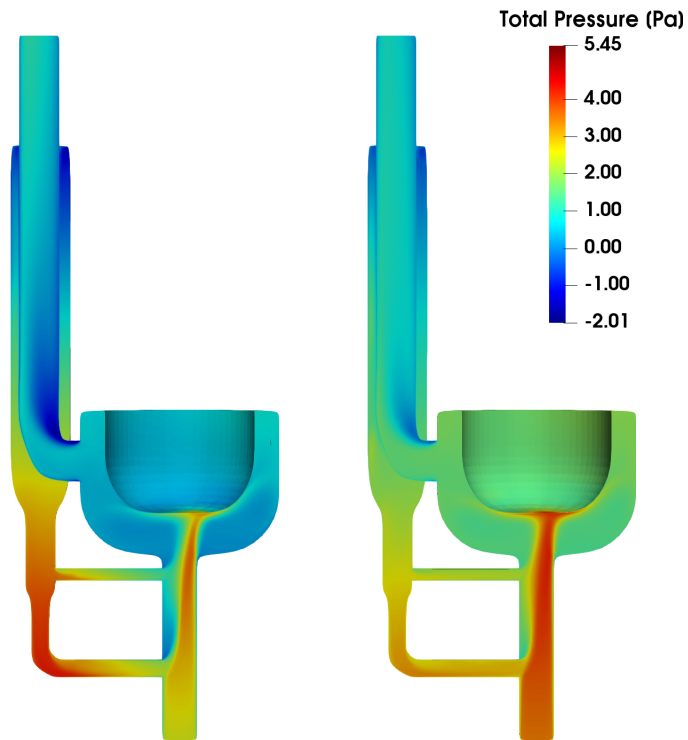


Figure 8.8: 3-D contour plot of total pressure. Plane cut $y = 0$
cold wall (left) vs *hot wall* (right)

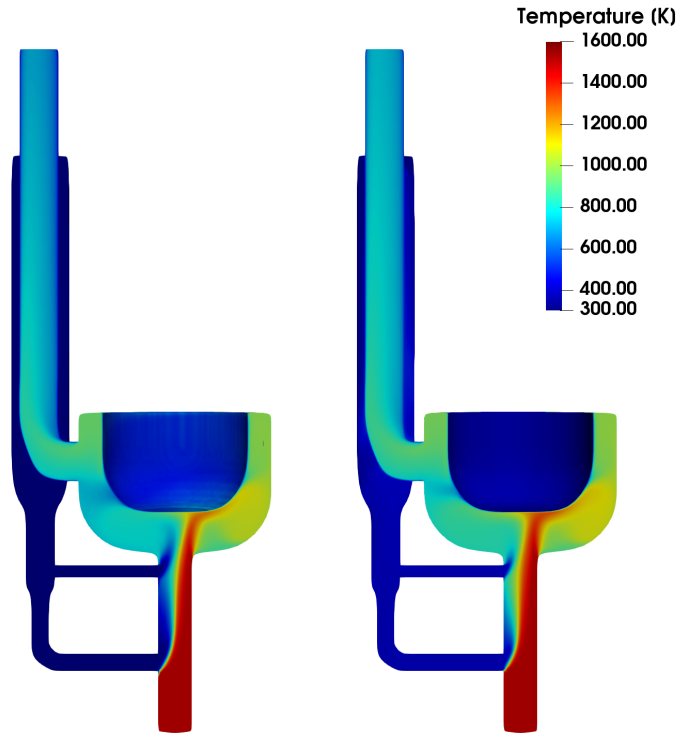


Figure 8.9: 3-D contour plot of static temperature. Plane cut $y = 0$
cold wall (left) vs hot wall (right)

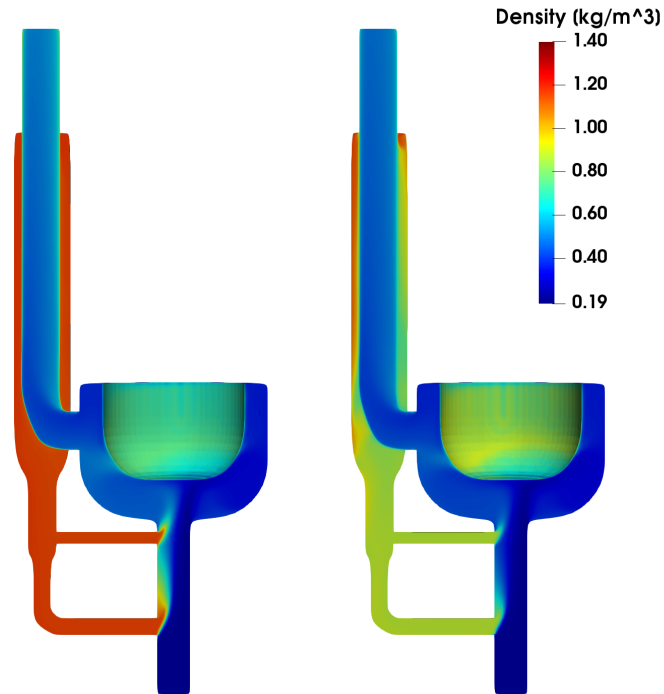


Figure 8.10: 3-D contour plot of density. Plane cut $y = 0$
cold wall (left) vs hot wall (right)

The effect of the hot wall on the \hat{z} velocity is not high, except there is a small reduction after the mixing between the hot-flow and the primary and secondary air. The biggest impact is on the pressure,

as seen in Figure 8.8. The pressure difference between the inlet and the outlet is noticable, which already brings to picture the importance of the pressure drops in the system to ensure proper functioning. Also, there is higher pressure in the system, overall, which is expected as the density of the gas (See Figure 8.10) is considerable lower i.e., higher temperature (See 8.9).

3. REACTIVE FLOW SIMULATION

Two cases were studied with reactive flow, one with primary and secondary air air-inlets, and one without secondary air-inlet. The differences will be discussed ahead.

All the simulations were for steady state, carried out using the less computationally expensive standard *k-epsilon* model, as the *k-epsilon RNG* was too expensive given the cluster capabilities available.

The combustion was modeled using the *Eddy dissipation concept -EDC-*, with the 24 – step chemical mechanism by (Hawkes et al., 2007) used in the 2-D simulations was used, because the simpler 2 – step mechanism was not suited for the pre-mixed case, as explained before. The radiation was modeled using the *Discrete ordinates method* with an absorption coefficient of $\alpha = 7.5m^{-1}$ as proposed by (Pundle et al., 2019).

3.1 SYSTEM WITH A SECONDARY AIR-INLET

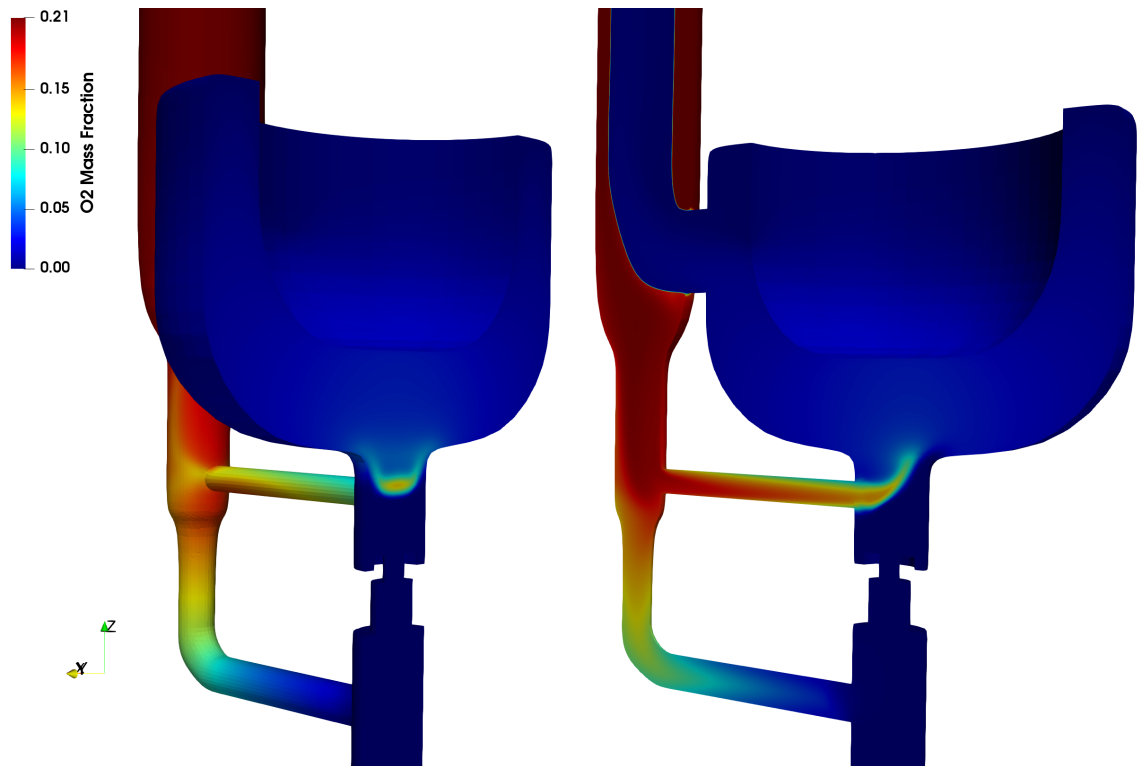


Figure 8.11: 3-D Contour plot of O₂ Mass Fraction. Plane cuts $y = 0$ and $x = 0$

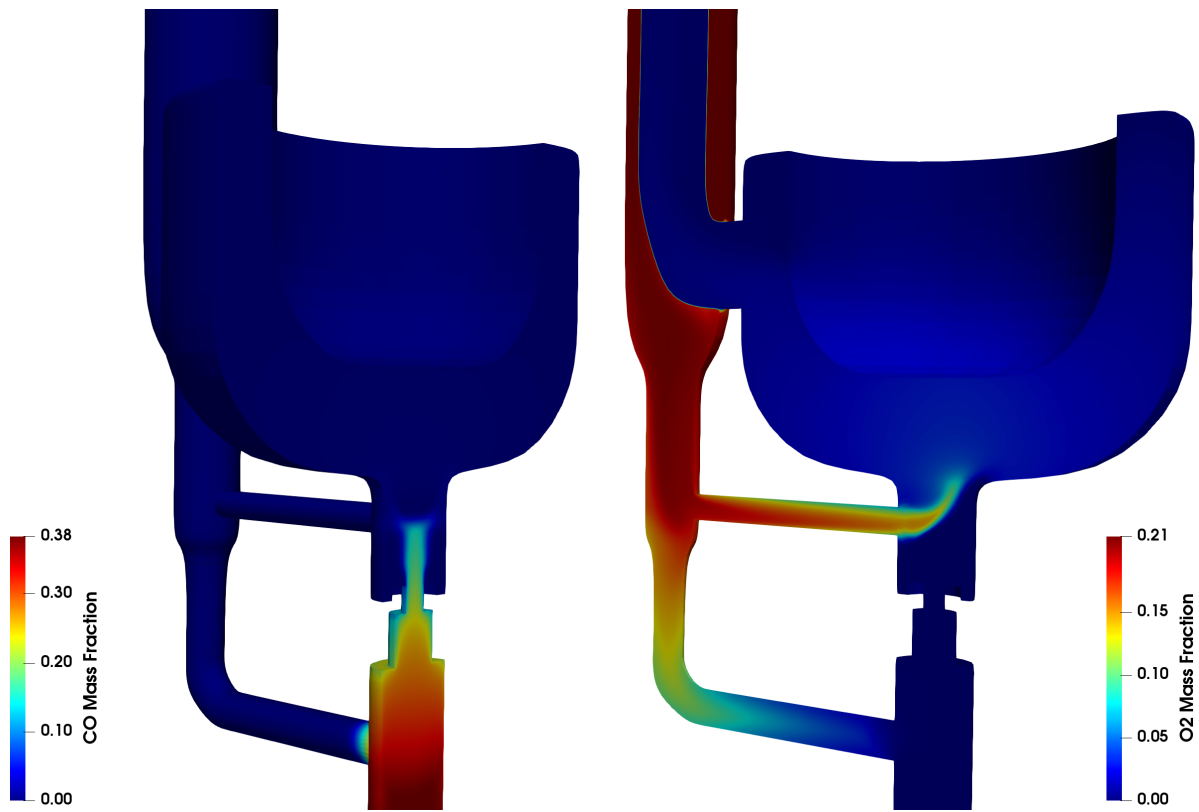


Figure 8.12: 3-D Contour plot of CO and O_2 Mass Fraction. Plane cuts $y = 0$ and $x = 0$

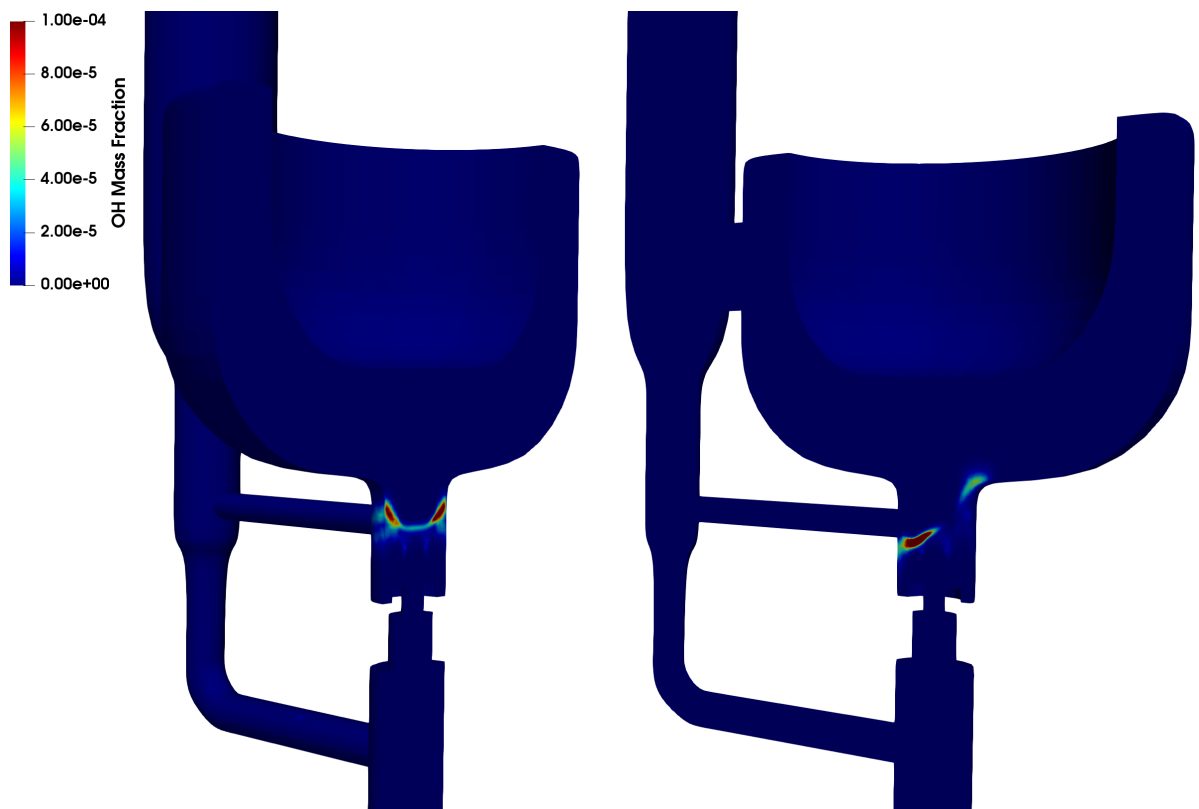


Figure 8.13: 3-D Contour plot of OH Mass Fraction. Plane cuts $y = 0$ and $x = 0$

From this study, it can be noticed that the flow path (injection angle and shape) are extremely important for the behaviour of the combustion. From Figure 8.11, it can be seen that most of the air goes through the "secondary air" pipe, and very much smaller proportion goes to the "primary", this is because the flow path that the secondary pipe offers is of much less resistance than the primary air, mainly due to the dynamic pressure created by the incoming fuel and the burner pressure drop, which is very significant.

This creates a mainly non-premixed flame behaviour, as can be seen in Figure 8.12. There, the two orthogonal jets of CO -left- and O_2 -right-, create a counter diffusion flame, with very defined reaction zones, which can be seen in Figure 8.13, where profiles of OH are shown.

The foreseeable problems from this configuration is that the fuel can go in the undesirable direction i.e., via the primary air pipe, and escape through the annular chimney. This calls the attention for future design improvements which take into account the direction, pressure drops and security checks.

3.2 SYSTEM WITH PRIMARY AIR ONLY

To overcome the problem of the fuel flowing in the undesirable direction, a system with only primary air was designed.

This system was capable of holding a laminar partially pre-mixed flame, as can be seen in Figures 8.14, 8.15 and 8.16. In the first one, the temperature contour clearly denotes the laminar flame where immediately after, the peak temperature is reached. This was a piloted flame with hot CO_2 and H_2O , similar results were obtained with a hot burner tip, with the only difference being higher temperatures in the piloted flame.

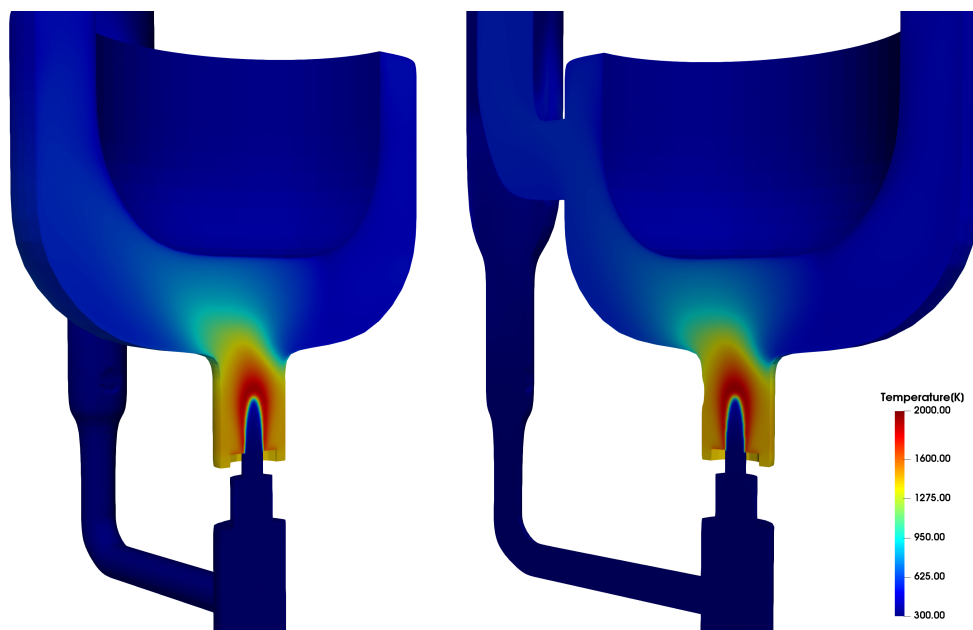


Figure 8.14: 3-D Contour plot of temperature. Plane cuts $y = 0$ and $x = 0$

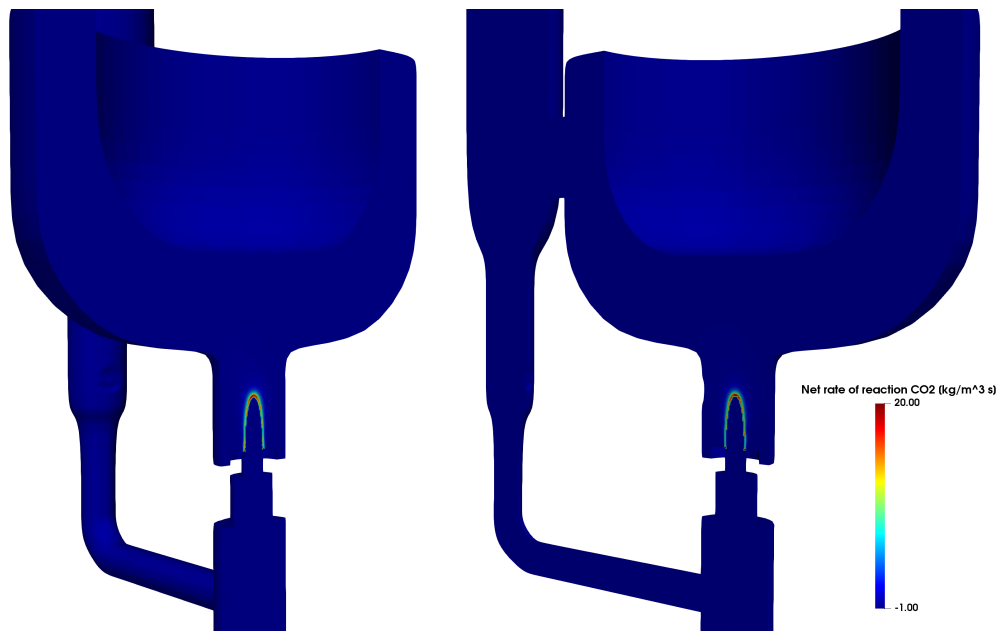


Figure 8.15: 3-D Contour plot of CO_2 reaction rate. Plane cuts $y = 0$ and $x = 0$

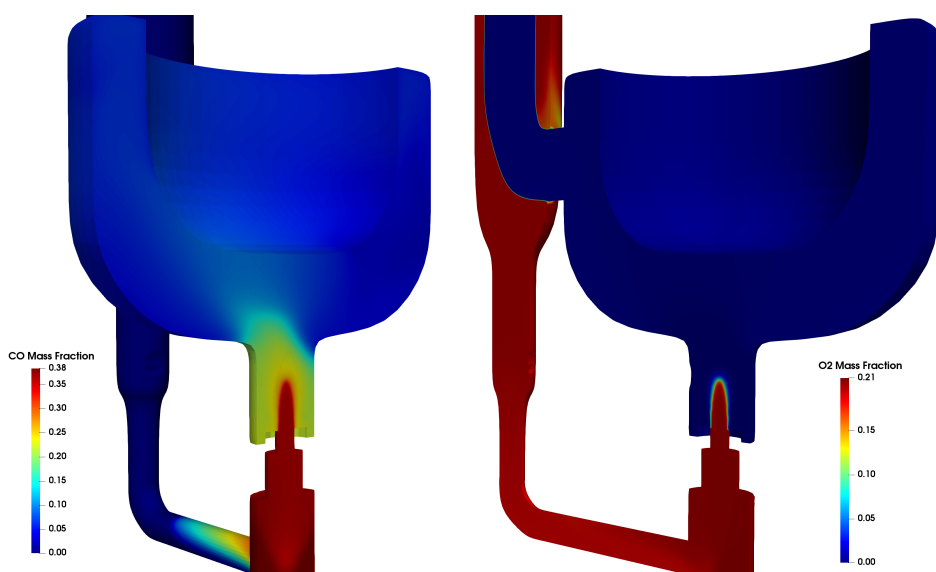


Figure 8.16: 3-D Contour plot O_2 and CO mass fractions. Plane cuts $y = 0$ and $x = 0$

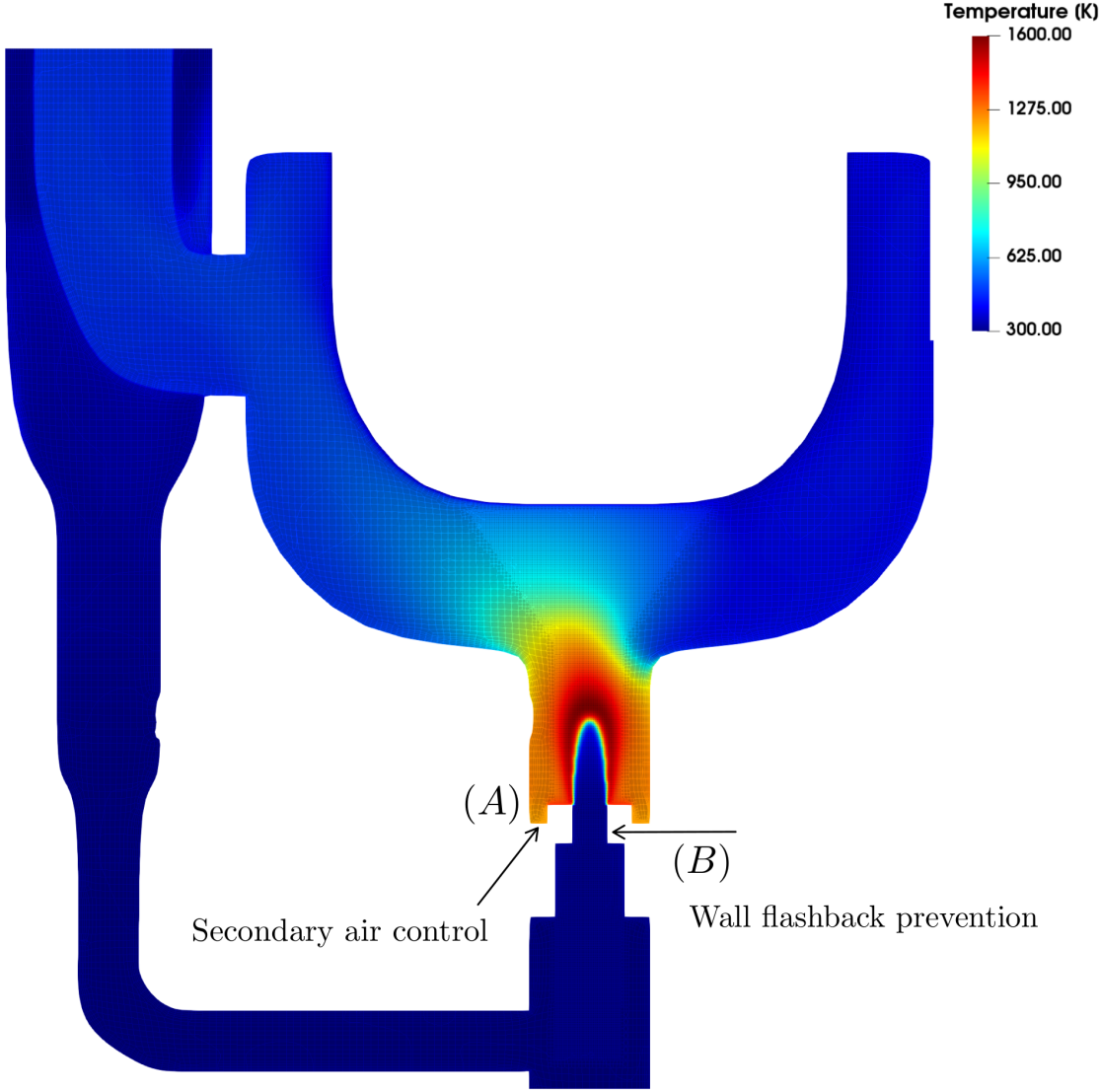


Figure 8.17: Close up of the temperature at the burner. Plane cuts $y = 0$ and $x = 0$

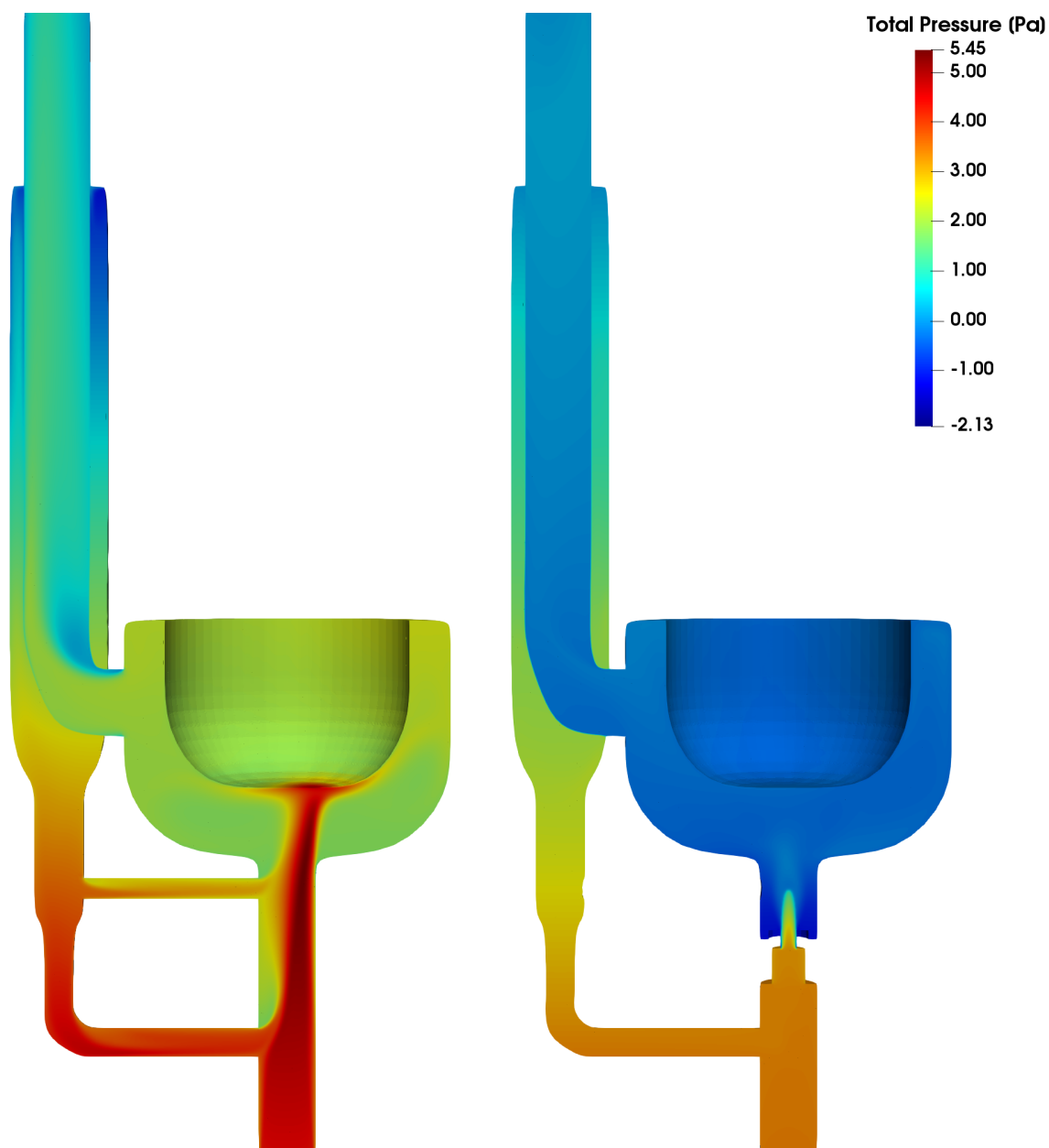


Figure 8.18: Pressure drop of non-reactive versus reactive flow simulations. Plane cuts at $y = 0$

To better show the premixed laminar flame stabilized in the burner, the reaction rate of CO_2 is presented in Figure 8.15. The symmetry of the flame denotes stability and a very well defined reaction zone, expected from laminar flames.

Figure 8.16 provides key information that must be taken into account in the design process of the burner. Here, it is clear that there is not sufficient oxidizer (air), in the system, as the O_2 fraction is completely depleted after the flame front. However, there is CO that "survives" the flame front, denoting incomplete combustion. Furthermore, there is fraction of the fuel flowing in the undesired direction, which might be caused by insufficient drag at the chimney, which in turn might be caused by the insufficient amount of oxidizer, once again, showing the coupling of the system. Note that this solution did not fully converge. Allowing the solution to iterate further leads to fuel flowing in the wrong direction.

The most important lessons from this study is the importance of the pressure drop along the burner as can be seen in Figure 8.18. This completely modifies the fluid flow and since this is a natural draft driven system, the pressure drops along it are determinant for the correct functioning.

This simulations already shed light in the importance of burner design, the one presented here was capable of stabilizing a flame, and allows for future studies with simple variations of the conditions which can allow for different combustion behaviors, which could also be used in reality. For example, the bottom annular region (*A*) in Figure 8.17 can have simple holes to provide secondary air for complete combustion, and slowly be closed to increase the resistance and make the draft of the inner chimney pull air via the pre-heater. Another possibility is to exercise control over the temperature in the second contraction (*B*) in the same Figure, to prevent wall flash back.

Lastly, it is desired to make a emphasis in the importance of the pressure drop calculations in order to ensure proper functioning of the system, its clear that the burner and the air connections are essential, as can be seen in Figure 8.18. In the design here, its clear that having straight 90 degrees air inlets is not the best option, alternative ways which make use of flow entrainment and difficulty for backward flow could be better solutions.

Despite the problem caused by the pressure drop across the burner, this first proof of concept readily sheds light into the direction to follow. It is able to meet the criteria used for its design, in such that it is able to stabilize a pre-mixed laminar flame, does not show flash-back propensity at the conditions tested, allows modular operability as the boundary conditions are easily modified e.g., (hot tip, open-boundaries in the bottom annular region, cold contraction wall, among other). In addition, this burner can serve as an initial model for experiments as the previously mentioned features can be implemented in practice. For example, by adding small air-openings in region (*A*) (Figure 8.17) to provide control over secondary air or by cooling down the region (*B*) to prevent wall flash back.

Argumentation
on the
hypothesis 3:
Alkali fly-ash
prevention



9

1. ALTERNATIVE MEASURE OF THE HARMFULNESS

As it was explained in section 2, the essential elements of the health problem caused by biomass combustion emissions comes are the emitted molecule size, number, composition and exposure time. The current way of quantifying the "harmfulness" or "cleanness" of the technologies fails to address those elements, as it only incorporates the amount of emitted mass. It is of utmost importance to measure the such properties with care, specially as it has been recently pointed out that high efficiency combustion generates more harmful and higher number of particles (even if the overall mass decreases).

Therefore, a new way of measuring the harmfulness of the emissions is proposed as follows.

$$H_i = f(Y, T_i, d, t) \quad (\text{Eq. 9.1})$$

Where:

H = "harmfulness" of species "i"

Y_i = dosage, measured in the form of density e.g., ppm or $\nu\text{grams}/m^3$

T_i = toxicity of the species "i"

d = penetration depth

t = exposure time

It is not known what the actual mathematical relationship of the "harmfulness" is to the other variables, so it was assumed to be linear as a starting point, which should then be evaluated with real-world data. The study by (Borgmann, Norwood, and Dixon, 2004) can be a starting point.

2. ULTRA-FINE PARTICLE PREVENTION

The ultra fine alkali fly-ash particles are generated by evaporation of the metals contained in the fuel bed, this is caused by high temperatures. And then they are entrained by the flow which goes through the fuel bed. Hence, the two main parameters which determine the generation and advection are the temperature and flow.

It has been proven by (Oberberger et al., 2017) that, by primary measures, the alkali fly ash can be minimized by up to 2 orders of magnitude. The principle on which their large scale gasifier-combustor works is based on a flow path modification. In this design, the particles which are mostly released at the fuel-bed given the high temperature (solid combustion front), now have to go through the upper (colder) pyrolysis and drying layers, this reduced the flow speed, and thus entrainment, and allows adsorption to occur. Hence the ash is released at the bottom and is not entrained as fly ash.

Based on this same principle, this Kulkan has been designed to have 3 reaction zones instead of 1 or 2 as the current technologies do. The first reaction zone (from bottom to top), is where the solid phase combustion occurs, here the heat for the gasification process is generated. This is the region where the alkali particles are mostly generated, as it is a high temperature region with gas phase temperatures of $T > 1500K$ in presence of the embed alkali particles.

In the second reaction zone is where most of the fuel is found, and this is the fuel that undergoes a thermochemical conversion of solid into mostly gas (syngas), at a lower temperature $T \simeq 1100$, thus already at lower temperatures than in regular combustion devices.

Furthermore, by having the fuel bed on top of the reaction zone (bottom lit), instead of of below the flame (top lit -see Figure 3.5-), the bed increases the flow resistance, thus reducing the flow speed and the shear stress that would cause particles to detach from the fuel bed.

The total skin friction drag, is determined as:

$$F = \int_{\partial\Omega} \frac{1}{2} \rho u^2 C_f d(\partial\Omega) \quad (\text{Eq. 9.2})$$

2. Ultra-fine particle prevention

Moreover, by having more flow resistances e.g., the burner and the air pre-heater which adds a pressure in the opposite direction to the flow and reduces the draft by cooling the flue, the overall flow speed in the system is reduced.

By combining both previously mentioned measures, the temperature at the larger part of the fuel bed is reduced, as well as the skin friction which causes the entrainment, hence an overall reduction of the alkali fly ash should be expected.

Conclusions



10

1. The current economic-development system based on fossil fuels must be radically changed. This paradigm, along with the fossil fuel economy that powers its workings, has already contributed to the extinctions of nearly 60% of all animal species since 1970 and is endangering the rest, including human beings. The model has threatened the very stability of our climate. While we know we must stop emitting green house gases as soon as possible, we are locked in a contradictory system (See Figures 2.1 2.2) that can only be overcome by creating a new development model that allows the fair and democratic allocation of resources, respects the knowledge and dignity of all peoples, and makes materially possible the successful implementation of the universal human rights. (See Chapter 2). The creation and distribution of technologies that give people the ability to meet their own needs without harming their own health, the stability of their communities and the ecosystems upon which they depend is the first step towards restoring balance – both for world climate and world justice.
2. Low-efficiency biomass burning technologies in the form of open fires and woodstoves are the main source of energy for nearly one third of the global population. The deforestation, indoor pollution and constant labor are required to tend these fires. Their use destroys quality of life, damages the environment, and kills millions prematurely every year. The technologies, programs and evaluation protocols which have attempted to solve this problem have not met real life requirements, often simply due to contradiction between technical-cultural, designer-user features. Evidence of this failure to listen, learn and respect the voices of those who would use the technology was seen in the unsuccessful attempts of large initiatives to replace traditional technologies, the poor understanding of the ultra-fine emissions, and the lack of optimization of the thermochemical processes that take place during the combustion of biomass (See Chapter 3 for details).
3. Available biomass cooking technologies (both traditional and high-end) are highly polluting, have poor control over the combustion process, have excessive air intake, quench the flames against walls, lose nearly 40% of the heat by the flue gas, and nearly 30% through the body. The top-tier stoves that report the highest efficiencies rely on biomass pellets which are hardly available in rural communities, produce more toxic and deeper penetration ultra-fine alkali particles, use of electric fans, and fuel-feeding mechanisms that often clash with the customs. In addition, there is limited data on the true-impact of these technologies, as more than 90% of the evaluations limit themselves to the most basic and lab-conditioned protocols, incapable of capturing the real-life user experience and thus fail to replace the traditional technologies (See 3 for details).
4. Replacing biomass as the main source of energy of people living in developing countries is unrealistic. The solution is to improve its use through a fundamental understanding of the way physics and culture work in tandem. This proposal is unique in this way, as it makes a conceptual separation between a reactor based on physics and a stove containing culture. The Kulkan treats both with dedicated attention. The result is a novel reactor concept and three different combustion regimes fundamentally based in three hypotheses tested using numerical studies and validated with experimental data from the literature. (See Chapter 4 for details).
5. Out of the hundreds of studies on thermochemical conversion of biomass, only a handful is dedicated to technologies of people living in poverty. Even less have been done using computational fluid dynamics, hence, there is a not much distributed knowledge on the modeling of such devices. Moreover, the existing ones have mostly been limited to description of the phenomena, not to transformation of it with optimization purposes. Therefore, there is a still much space for future research using more detailed mathematical modeling.
6. The first hypothesis, named *Heat recovery by and air pre-heater*, was tested using a validated algebraic system of 46 non-linear equations coupling the heat and mass flows in the system. The combustion chamber was modeled as a *perfectly stirred reactor*, discretizing the system in zones, using empirical correlations for the heat-transfer and adding the novel features of a chimney/air pre-heater which was modeled as a plug-flow concentric pipes heat exchanger. After calculating the thermal efficiency of thousands of different geometrical configurations, the optimal limits was found at around [60 – 65%] which is between 4 – 8 times higher than that of traditional

technologies and 25% higher than the most efficient ever reported, proving the hypothesis to be true (See Chapter 6 for details).

7. The second hypothesis, named *Premixed laminar flame* had a sub-hypothesis which served as a necessary condition for the operability range of the flow-speed and flash-back limits. This was tested using computational fluid dynamics -CFD- of reacting flow in 1-D. This allowed to estimate the range of expected laminar flame for a gas-fuel constituted by 5 species, simulating the syngas coming from an up-draft biomass gasifier obtained from experimental data available from literature. The calculations were performed for varying stoichiometric ratios, and inlet temperatures for the air and oxidizer. The results showed that the expected velocities for all configurations are in the range of $[0.8 - 1.2]m/s$ which are reasonable speeds that the flow can experience in naturally draft driven flows, which support the idea of the system functioning without auxiliary equipment, and in flash-back safe region, thus fulfilling the operability condition (See 7 for details).
8. With the necessary condition fulfilled, the second hypothesis was tested using an asymmetric 2-D CFD model. This model allowed to explore the length of a premixed and non premixed burner stabilized laminar flame. The results show a sharp decrease of the flame axial length by roughly the half, even at highly rich mixtures of $\phi = 8.5$. This was measured by comparing mass fraction contours, reaction rates and by calculating the radially integrated mass fraction of the slowest reacting species i.e., *CO*. Thus, proving that the second hypothesis is true, and that pre-mixing the fuel before burning should be done in order to reach more complete combustion, prevent flame quenching and having more compact combustion chambers, which minimizes losses (See Chapter 7 for details).
9. A 3-D model of the *Kulkan* was constructed for non-reacting flow, reacting flow with primary and secondary air, and only primary air. The simulations show that the system can work and the it is of utmost importance to calculate the pressure drop across the entire system, specially the burner during the design phase. A first burner was proposed which proved to stabilize the flame successfully in *hot-tip* and *piloted* modes, it also allows future studies by making it easy to modify the boundary conditions to test out different behaviors of the system e.g., secondary air control by opening to the environment at the bottom of the burner (See Chapter 8 for details).
10. The current understanding of the emissions from biomass cooking technologies is rather poor. Both in terms of fundamental knowledge of the formation of the particles and in the way in which they are measured, This impacts the definition of “clean” technology. Arguments related the generation at the fuel-bed and the entrainment by the flow are presented, which are intended to minimize the particles by use of a fuel bed designed to produce lower temperature and lower flow speeds. (See Chapter 9 for details).
11. The *Kulkan*, a novel biomass reactor addressing the people’s needs for renewable energy in the developing world has been conceived, analyzed and tested numerically. The reactor has reached the highest efficiency ever reported with regards to heat recovery and optimization of physical phenomena via geometry optimization. This shows that there is a way to satisfy the energy needs of people living poverty by using the locally available energy resources in a highly efficient manner. The *Kulkan* is a contribution to a new, truly sustainable and just development model.

Recommendations

11

1. The concept of the *Kulkan* reactor has been demonstrated with high detailed mathematical models. The future work must be its construction and testing including the gasifier. It should starting at a lab and as soon as stable combustion is reached, then it must be tested under real-life conditions. Followed up by a *Community Based Participatory Research* project to incorporate the cultural aspects and make it into a stove, so it can actually improve the life quality of people and reduce the environmental impact.
2. All the models constructed here were for steady state conditions. It would be valuable to obtain transient curves of power ($\dot{Q}(t)$) from typical conditions, as well as gas compositions ($X_i(t)$) for updraft gasifiers feed in a semi-continuous way. These two parameters would be essential to extend the models presented here, primarily to see simulate the behavior of the *Kulkan* under such conditions, and to determine the stability limits of its functioning.
3. Further investigate the behavior of the *Kulkan*. In Chapter 8, a first design of a burner that allows different operational behaviour was presented, and the importance of the pressure drop across the system was highlighted. It is recommended valuable to further investigate this burner by varying the different boundary conditions that were presented in Table 8.1. Also, it is recommended to find the limiting pressure drops that can be allowed in the system, to find the best geometry of the primary and secondary air connections.
4. The previous recommendation can be combined with the algebraic model presented in Chapter 6, which has the advantage of being highly flexible given its modularity, and does not require large computational capacity. In this model, a general equation to include the discharge coefficient was presented, for which different empirically determined *loss coefficients* for e.g., a new burner or air-inlet, can be added to determine if the proper behavior of system is feasible or not, without having to entirely build the system or performing complex 3D simulations, unless its necessary.
5. The global two step mechanism by (Slavinskaya, Braun-Unkhoff, and Frank, 2008) proved to give substantial computational cost reductions while maintaining the accuracy of the main variables under non-premixed conditions. Further adapting this mechanism for pre-mixed conditions would be highly valuable, and therefore it is recommended.
6. Most of the studies on CFD of cooking technology limit themselves to the standard $k - \epsilon$ turbulence model. Which is in most cases sufficient due to the low Reynolds number. However, the *RNG* recommended by (Scharler et al., 2020) has significant differences in the prediction of the heat transfer in the *Kulkan* reactor (see Chapter 8), hence, it is recommended to explore which one is better suited.
7. An list of arguments for the third hypothesis were presented. Since the mathematical models related to emission are not suited for the system presented here, hence, it is recommended to test study this hypothesis further by experimental methods, and also to develop a new measuring method for the harmfulness of the emissions from high efficiency biomass combustion.
8. The detailed simulations presented here were restricted to homogeneous phase reactions. In the Appendix, the essential equations information, references and equations for the heterogeneous reactions are compiled to ease the future work on this topic, as it is recommended to explore the combination of both phases.
9. It is also highly interesting to explore the limits of the arguments presented by (Chanphavong and Zainal, 2019) and (Sedighi and Salarian, 2017), regarding the independence of the combustion properties of the syngas coming from different biomass sources. It was noticed that the composition and hydrogen fraction varies by the type of gasifier, which affects the laminar flame speed, and thus burner design. There are plenty of studies on the effect of different biomass parameters

in the syngas composition, and it would be valuable to know the range of operability, based on the possible fuel properties.

- 10.** A call for a new development model has been proposed, in order to tackle the existential crisis that the current poses to all complex life forms. This new development model should prioritize the use of locally available renewable energy resources, managed in a democratic way. An example of how to do this was presented here, focusing on one of the basic needs that one third of the world population, access to clean renewable energy for cooking and heating. It is recommended to follow this approach to reach higher scales of energy and power for example, to reach higher needs satisfaction, sustainably, for example by following the Figure 2.3.

Appendix



12

1. SOLID PHASE THERMOCHEMICAL CONVERSION OF BIOMASS

This section is intended to provide complement the Chapter 5, which provided all the essential equations that govern the thermochemical conversion of syngas coming from biomass. Here, the phenomena that takes place in the solid phase is explained, and the mathematics to model it are presented, with the intention of providing all the necessary components for future studies.

1.1 DRYING

Within the wood particles, there is water in three forms: free liquid in the cell lumen, held by capillary forces, water vapor in the cell in thermodynamic equilibrium with the liquid water and bound or hygroscopic water bounded to the wood structure via hydrogen bonds. (Mehrabian Bardar, 2013).

When the wood is exposed to the incoming heat, its temperature starts to rise, and with it the saturation pressure of the water vapor increases. Thus increasing the diffusion of water across the cell pores. If the vapor pressure exceeds the external pressure, then the convection mechanism overtakes diffusion. As water vapor leaves the cell, the liquid water starts to evaporate and once no more free water is left, the bounded water starts to evaporate and once this one is depleted the temperature starts to raise since no more latent heat can be taken (idem).

The models for the drying phase can be divided into three categories: kinetic rate model, thermal models, and equilibrium models.

The **kinetic rate** models assume the evaporation to be a reaction from *wet biomass* \rightarrow *dry biomass* governed by a reaction rate:

$$\dot{m}_{evp} = A \cdot \exp\left(\frac{-E_a}{RT}\right) \rho_s Y_w \quad (\text{Eq. A.1})$$

Where A is the pre-exponential factor, E_a is the activation energy, both are determined experimentally and depend on the conditions of the fuel. R is the ideal gas constant, T is the absolute temperature, ρ_s is the solid density and Y_w is the mass fraction of water.

The **thermal model** assumes that the drying begins when the temperature reaches the evaporation temperature and ends when there is no more water, when pyrolysis starts. It is modeled with a piecewise function:

$$\begin{aligned} \dot{m}_{evp} &= 0 & \text{for } T_s < T_{evp} \\ \dot{m}_{evp} &= \frac{(T_g - T_{evp}) \rho_s c_p}{H_{evp} \delta t} & \text{for } T_s \geq T_{evp} \end{aligned} \quad (\text{Eq. A.2})$$

The **thermal equilibrium** approach is a combination of the previous two which assumes that water vapor and liquid are in equilibrium and coupled by mass and heat transfer by the following equations.

$$\begin{aligned} \dot{m}_{evp} &= S_a D_w (c_{w,s} - c_{w,g}) & \text{for } T_s < T_{evp} \\ \dot{m}_{evp} &= \frac{Q_{cr}}{H_{evp}} & \text{for } T_s \geq T_{evp} \end{aligned} \quad (\text{Eq. A.3})$$

With:

$$Q_{cr} = S_a (h_s (T_g - T_s) + \varepsilon_b \sigma_b (T_{env}^4 - T_s^4)) \quad (\text{Eq. A.4})$$

Where S_a is the surface area, D_w is the mass transfer coefficient at the solid-gas interface, $c_{w,s}$ and $c_{w,g}$ are the water concentrations in the solid and gas phase, respectively. Q_{cr} is the total heat transfer by convection and radiation between both phases, h_s is the convective heat transfer, ε_b is the emissivity σ_b is the Stefan-Boltzmann constant, T_{env} and T_s are the environmental and surface temperature, respectively.

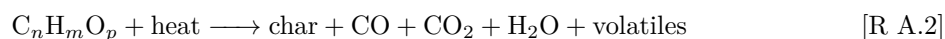
1.2 TORREFACTION

If biomass is heated to higher temperatures than those needed for total evaporation of the water, then some chemical reactions start to take place. These reactions lead to higher carbon content and lower oxygen content. This process is called torrefaction and takes place in the absence of oxygen, in the temperature range of 200 – 300°C (Basu, 2010).

The reason why it is limited to 300°C is because at higher temperature (and atmospheric pressure), extensive devolatilization and carbonization of polymers would take place, as well as loss of lignin, which are undesirable as torrefaction is used as a pre-treatment process to increase the energy density of the fuel (by reducing its water, oxygen content and volatiles).

It can be characterized by the following reaction.

Torrefaction:



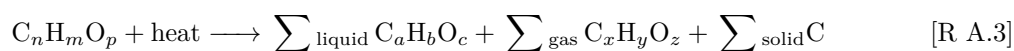
1.3 PYROLYSIS

It is the process in which large hydrocarbon molecules are broken into simpler (shorter) molecules by addition of heat, up to higher temperatures than torrefaction. It takes place between 300 – 650°C (Basu, 2010) in total absence of oxidizers or in a limited amount. Some of those shorter hydrocarbons can undergo another break up into even smaller hydrocarbons via secondary reactions. During these reactions, gas and tar species leave the solid array of carbon. (Basu, 2010), (Mehrabian Bardar, 2013).

The products of pyrolysis can be categorized in three (Dernbecher et al., 2019):

- **solid fraction or char** which is maximized at lower temperatures, low heating rates, high pressure and thermally thick particles, high lignin, moisture, and inorganics content
- **liquid fraction or condensable volatiles at room temperature** which is maximized at high heating rates and low residence time ($t < 2s$) and medium temperatures (500°C)
- **gas fraction**, composed of a highly heterogeneous mixture of organic and inorganic gases including, primary oxygenates, secondary hydrocarbons and tertiary compounds (Milne, Evans, and Abatzoglou, 1998)

Pyrolysis:



Although these reactions seem somewhat simple, in reality, it is not possible to determine what are all the reactions that happen, as there are countless intermediate reactions happening. Nevertheless, serious effort has been put in developing chemical mechanisms to model the pyrolysis, one of the most accurate and used models is that proposed by (Ranzi et al., 2008), with 10,934 reactions and 327 species.

Besides the inherent complexity of the chemical reactions that, the phenomena is also affected by the temperature at which the pyrolysis takes place, the biomass composition, the heating rate, the shape of the particles, among other variables.

1.4 GASIFICATION

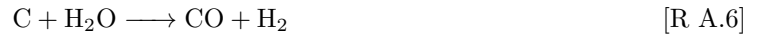
If sufficient heat is supplied to the system to continue to thermochemically decompose the biomass passed the endothermic drying and pyrolysis reactions, then the leftover char will start to react with a gasifying agent (e.g., air, or steam) and partially react to form mostly carbon monoxide. This partial oxidation produces 72% less heat than what would be produced in complete combustion (Basu, 2010). Thus most of the energy that was contained in the bonds of the solid carbon, remains in the form of gaseous carbon monoxide.



The modeling of the gasification reactions is even more complex than pyrolysis, because heterogeneous reactions take place, and the multiphase nature broadens the modes through which matter and energy are transferred. Mehrabian Bardar summarizes the reaction in the following steps:

1. Transport of oxidizing/gasifying agent to the particle surface
2. Diffusion through the ash layer
3. Adsorption on the reaction surface
4. Chemical reaction
5. Desorption of products from the surface
6. Diffusion of products through the ash layer
7. Transport of products from the particle surface back to the environment

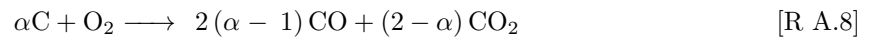
The typical overall reactions used to model the char gasification are:



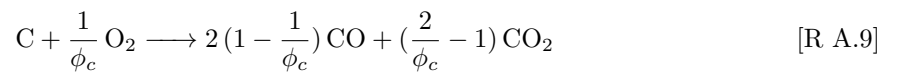
1.5 SOLID PHASE COMBUSTION

Combustion is the final stage of the thermochemical process. It takes place in two ways, in the solid and gas phases. The first one is the most complex and not very well understood. Modeling approaches are surface reactions or solid-gas interface reactions divided in three: shrinking core, shrinking sphere and shrinking density.

(Mehrabian Bardar, 2013) developed a model which was experimentally validated using a 1-step reaction scheme for the surface reactions.



Or with more detail as:



Where:

$$\phi_c = \frac{\frac{1}{rc}}{\frac{1}{2} + \frac{1}{rc}}$$

$$rc = \frac{CO}{CO_2} = \alpha \cdot \exp\left(-\frac{\beta}{T_s}\right)$$

CO/CO_2 is the ratio at the temperature T_s of the solid. α and β are determined experimentally. (See (Dernbecher et al., 2019) for further details).

When the reactions are not considered at the surface of the char but in the interior interface, a two step reaction as shown in R A.10 is preferred, and the solid-gas interaction can modeled as a shrinking particles, a shrinking sphere or shrinking density. For which diffusion of heat and mass play a key role and the *Biot* and *Thiele* numbers determine the type of model (See (De Jong and Van Ommen, 2014) for further details).



These overall reactions reach states determined by thermodynamics, and the rate at which they happen is determined by the chemical kinetics. Nevertheless, these reactions do not represent the real chemical reactions, as there are intermediate steps that are better captured by elementary reactions which conform a chemical mechanism (Mehrabian Bardar, 2013).

1.6 MODELING APPROACH FOR THE "FUEL BED" PROCESSES

The modeling of biomass thermochemical conversion in a reactor begins with the fuel-bed, as it provides the inlet information for the gas phase in the free board. The approaches can be categorized in four (Dernbecher et al., 2019):

- Empirical bed model
- Separate bed model (zero to three dimensions)
- Discrete particle method based bed model
- Porous medium model

In the **empirical bed model**, the composition of the syngas is determined experimentally and used as an inlet boundary condition for the gas-phase simulation. In the second one, the heterogeneous and homogeneous regions are simulated separately. They can be coupled via mass or heat transfer.

The **zero dimensional** model is the one based on thermodynamic equilibrium or chemical reaction kinetics considering a perfectly stirred tank with no temperature nor concentration gradients, and the reactions are the only responsible for the conversion.

The **one dimensional** models take into account gradients along one spacial coordinate and the different thermochemical processes explained in Sec. 2 are modeled in this domain and the results used as inlet boundary conditions for the gas phase.

The **two dimensional** models are mainly used for moving grate furnaces, where the volatile composition varies along the grate. Hence the two dimensions are the fuel height and the length of the grate. The bed itself has been modeled as moving sub-domains or porous media (Kær, 2005), (Van Der Lans et al., 2000).

The **three dimensional** models are rare, only two have been done according to (Dernbecher et al., 2019, p.40). Both are based on porous media and thermally thick particles.

The **discrete particle method -DPM-** is used for simulated beds composed of pellets or wood chips. The particles are modeled as Lagrangian and the thermal conversion of each particle is simulated. An example of such simulation is the study by (Mahmoudi et al., 2015) with an Eulerian-Lagrangian approach, Eulerian for the fluid flow. They validated their results and found good agreement with experiments.

The **porous medium** approach allows to directly simulate the solid-gas interaction, which is not clearly understood and thus poses difficulties for simulations. In this approach, each cell contains a fraction of solid and gas defined by the porosity, and they interchange heat and mass, this is usually referred as Euler-Euler approach. A remarkable difference between this approach and the others is that no difference is made between the solid phase and gas phase reactions, as both belong to the same domain (idem).

1.7 CRITERIA FOR THE BEST FIT MODEL

Before the starting the modeling, some initial calculations can provide useful information to determine the best fit model. The dimensionless numbers of Biot, Péclet, Damköhler and the Thiele modulus can provide some insight.

The Biot number (Eq. A.5) can indicate if the particles can be considered thermally thin ($Bi < 0.2$) or thick. The Damköhler numbers (Eq. A.6), which compares the reaction rate to the convective (first number) and diffusive mass transfer rates (second number) determines if the reactions occur in a large zone as in a perfectly stirred tank reactor ($Da < 1$), or if the flame front moves along with the bed ($Da > 1$). The Péclet (Eq. A.8) number compares the diffusion and the mass transfer, which is relevant particularly for moving grate reactors. When $Pe \gg 1$, then Da_1 is adequate. The Thiele modulus (Eq. A.9) compares the kinetic rate to the diffusion timescale for reactions of order 1, for $Th < 1$ the shrinking core regime is applicable and for $Th > 1$ a reacting core is better fit.

$$Bi = \frac{h_{rad}L}{k} \quad (\text{Eq. A.5})$$

Where h_{rad} is the convective and radiative heat transfer coefficient, L is the characteristic length scale and k is the thermal conductivity.

$$Da_1 = \frac{S_{Y_{i,g}}l_B}{u} \quad (\text{Eq. A.6})$$

$$Da_2 = \frac{S_{Y_{i,g}}l_B^2}{D} \quad (\text{Eq. A.7})$$

Where $S_{Y_{i,g}}$ is the source term of the mass fraction of the gaseous species, l_B is the characteristic length scale of the packed bed, u is the flow speed and D is the diffusion coefficient.

$$Pe = \frac{l_B \cdot u}{D} \quad (\text{Eq. A.8})$$

Where l_B is the characteristic length scale of the packed bed, u is the flow bulk velocity and D is the diffusion coefficient.

$$Th = l_p \sqrt{\frac{k}{D_p r}} \quad (\text{Eq. A.9})$$

Where l_p is the characteristic length scale of the particle, k is the conductive heat transfer coefficient, D_p is the diffusion coefficient and r is the hydraulic radius.

2. 2D CHEMICAL MECHANISM COMPARISON

As it was mentioned in Chapter 7, two chemical mechanisms were compared for the 2-D axis-symmetric simulations, namely the one by (Hawkes et al., 2007) used and compared with experimental data by (Pundle et al., 2019) and the one by (Slavinskaya, Braun-Unkhoff, and Frank, 2008), recommended after the extensive study and comparison by (Alzahrani et al., 2015). Here, contours of the main variables are presented. They provide almost the same results, except for the reaction rates, which do not change drastically the behavior of the system, as the system is diffusion dominated because its non-premixed.

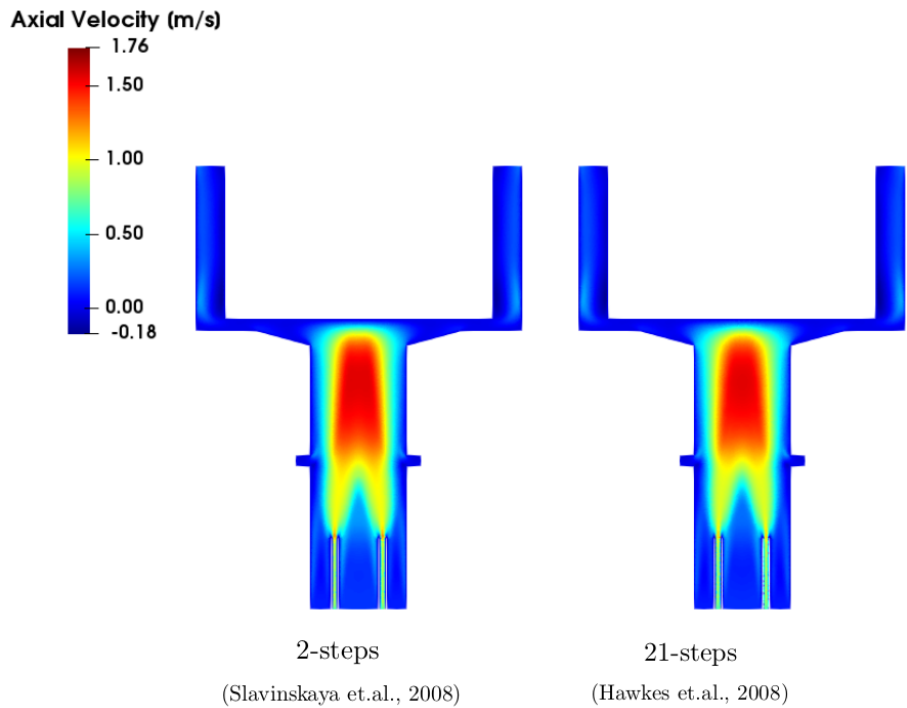


Figure A.1: Axial Velocity

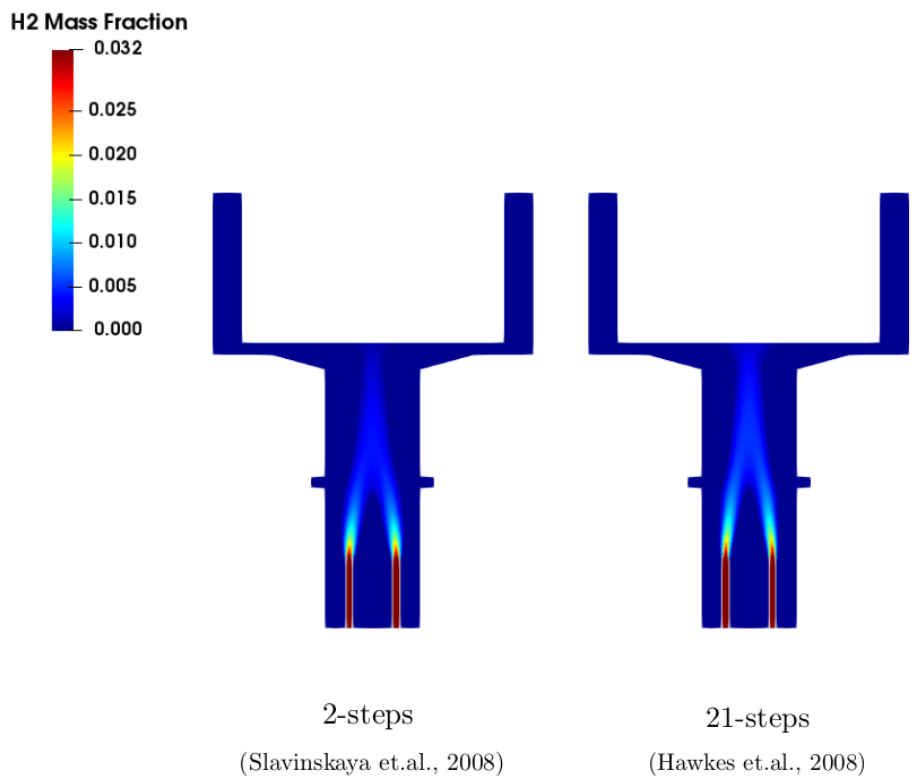


Figure A.2: Hydrogen mass fraction

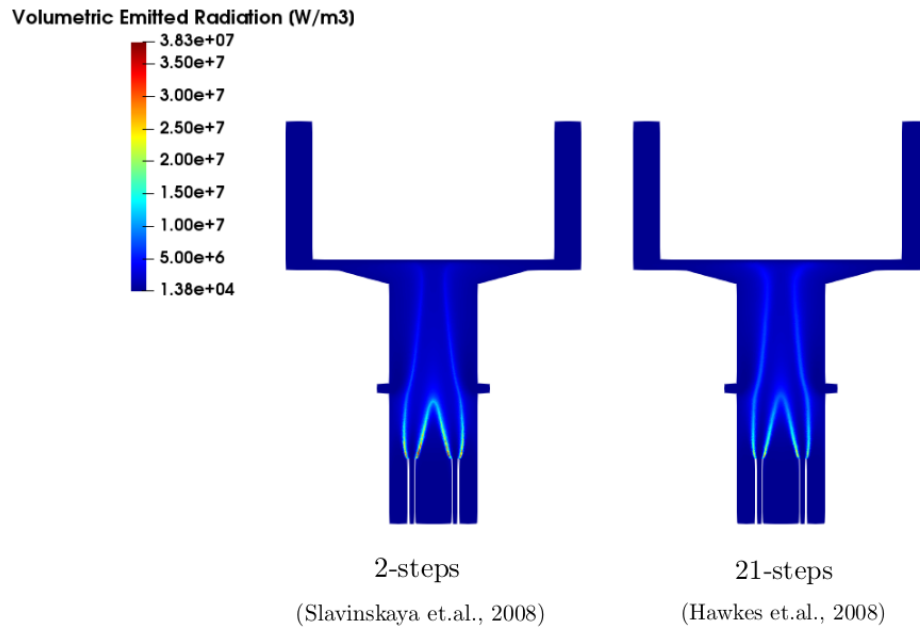
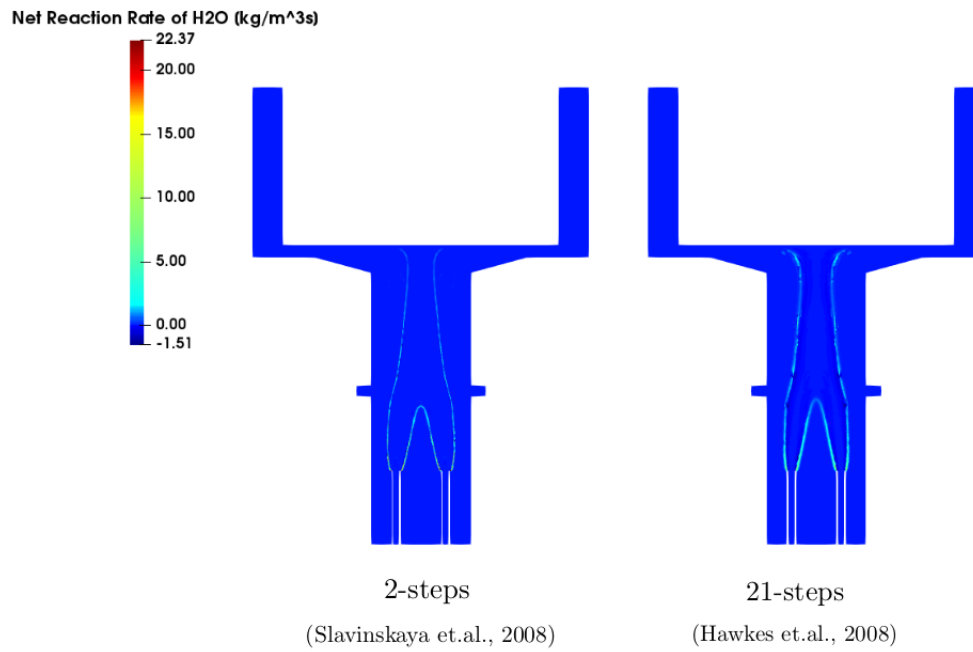


Figure A.3: Volumetric emitted radiation

Figure A.4: H₂O reaction rate

3. ALTERNATIVE TURBULENCE AND COMBUSTION MODELS

As mentioned in Chapter 5, most of the CFD studies have limited themselves to the standard $k - \epsilon$ turbulence model and the *Eddy dissipation concept* for the chemistry. These models have proved to be sufficiently accurate to represent the variables of importance in the literature, mostly due to the low Reynolds number seen in the systems treated here. Despite that, there is a notable difference with the *RNG*, as can already be depicted in the following graphs.

The effect of the laminar chemistry model and the EDC is negligible. It only had impact in the computational costs. Where the EDC was substantially less demanding.

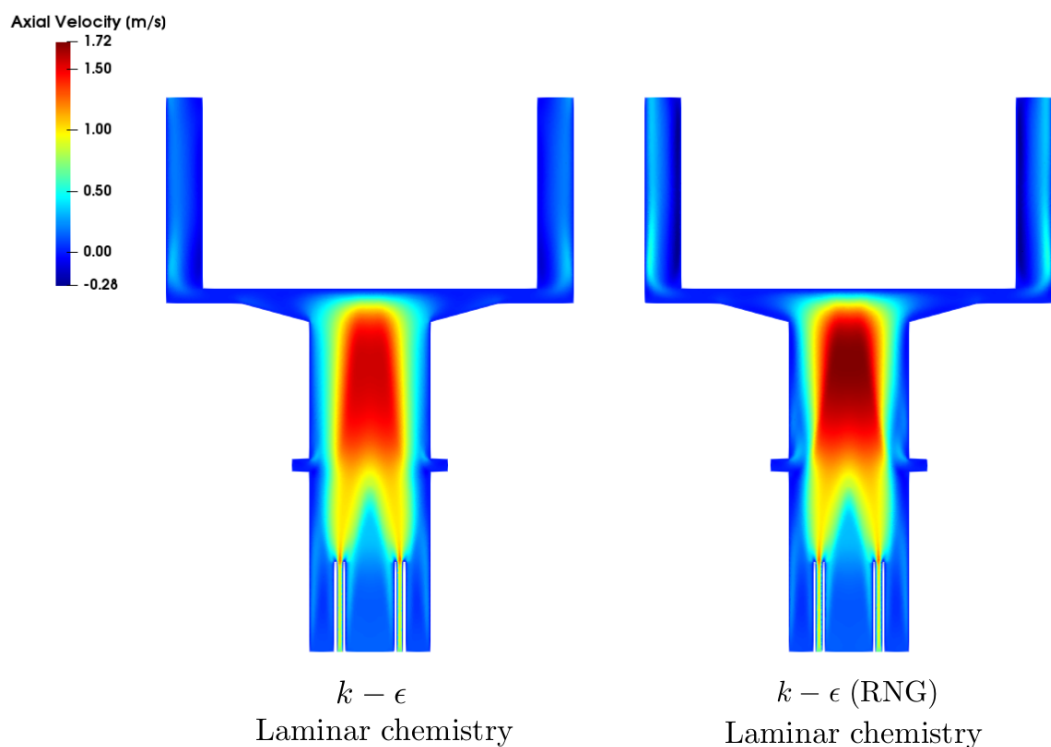


Figure A.5: Axial velocity

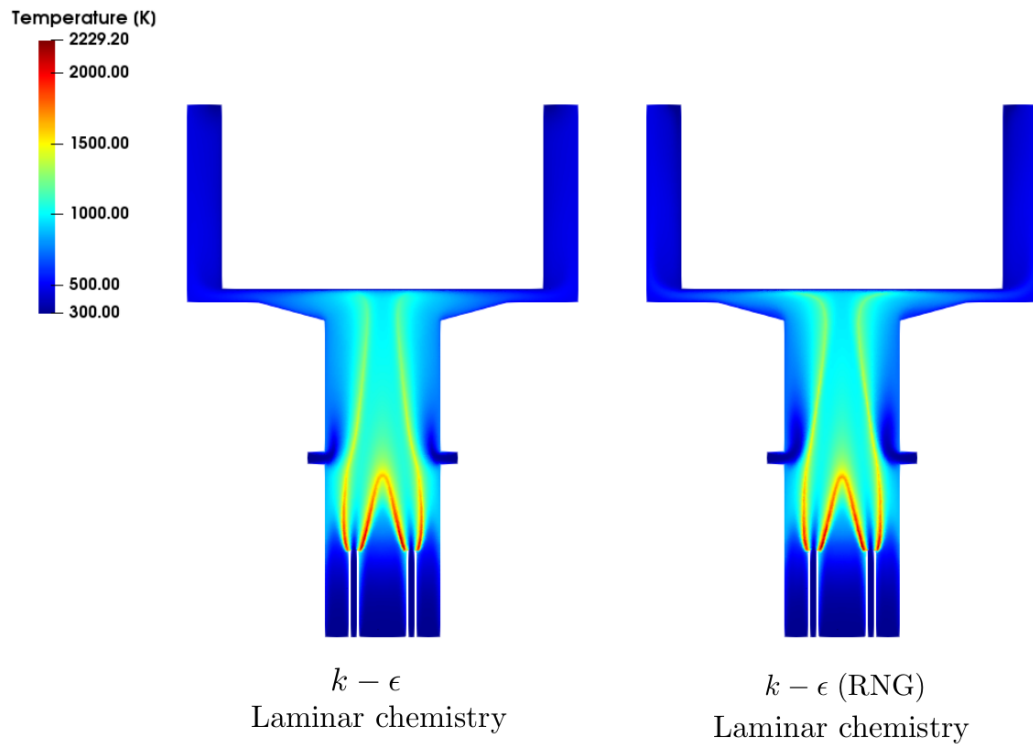


Figure A.6: Temperature

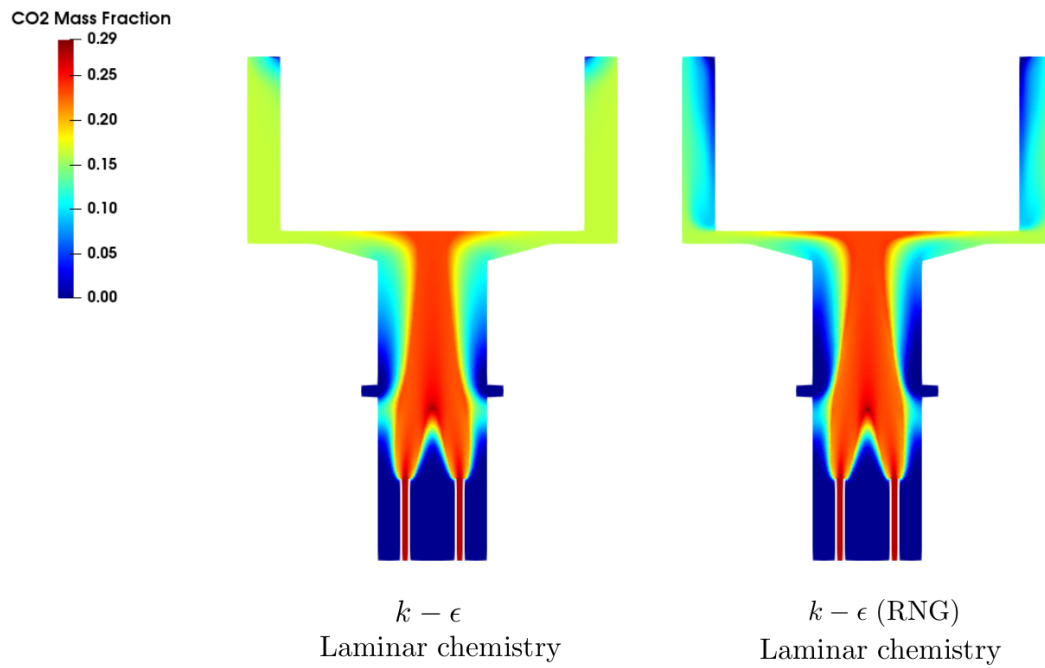


Figure A.7: CO2 Mass fraction

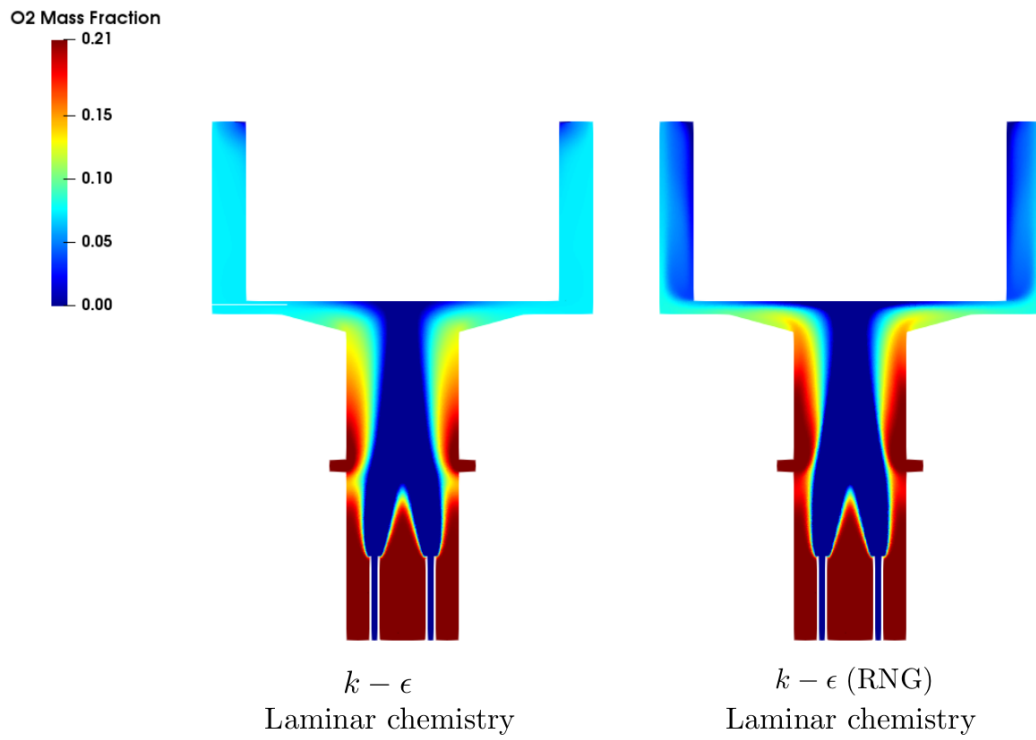


Figure A.8: O2 Mass Fraction

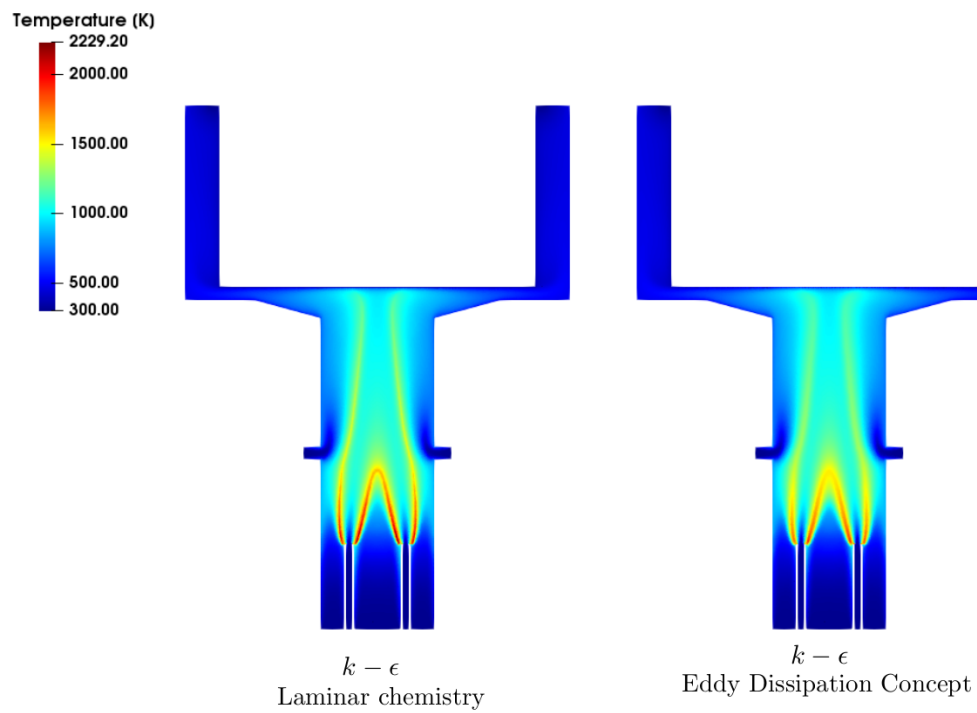


Figure A.9: Temperature

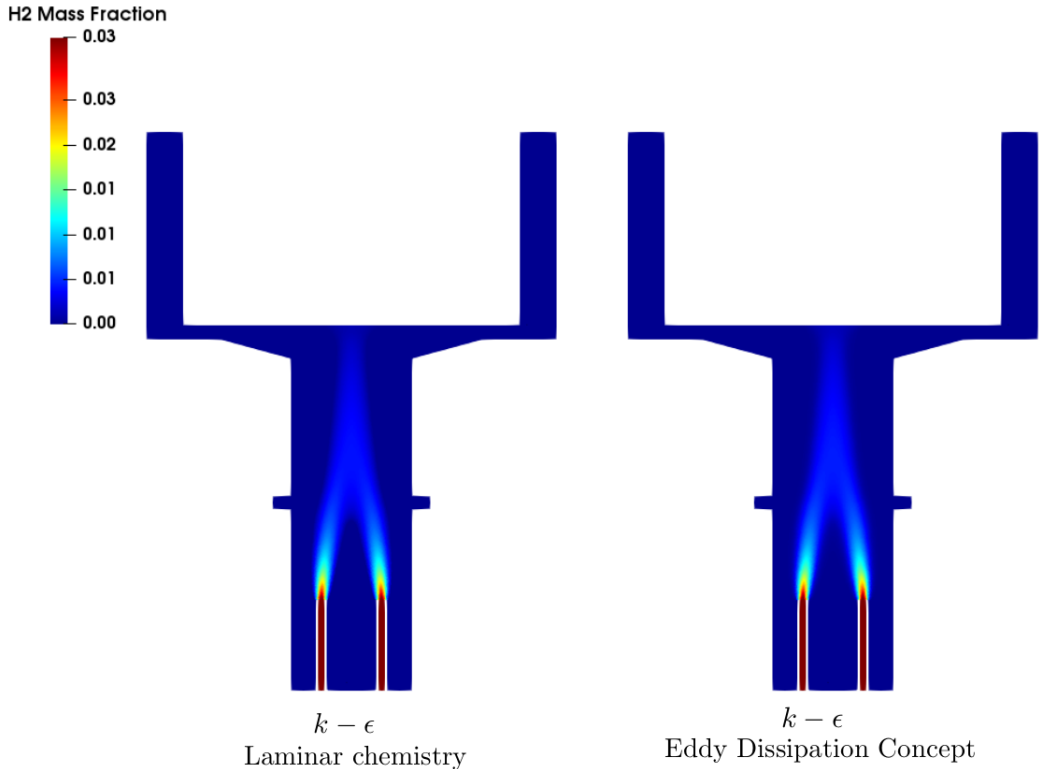


Figure A.10: H2 Mass Fraction

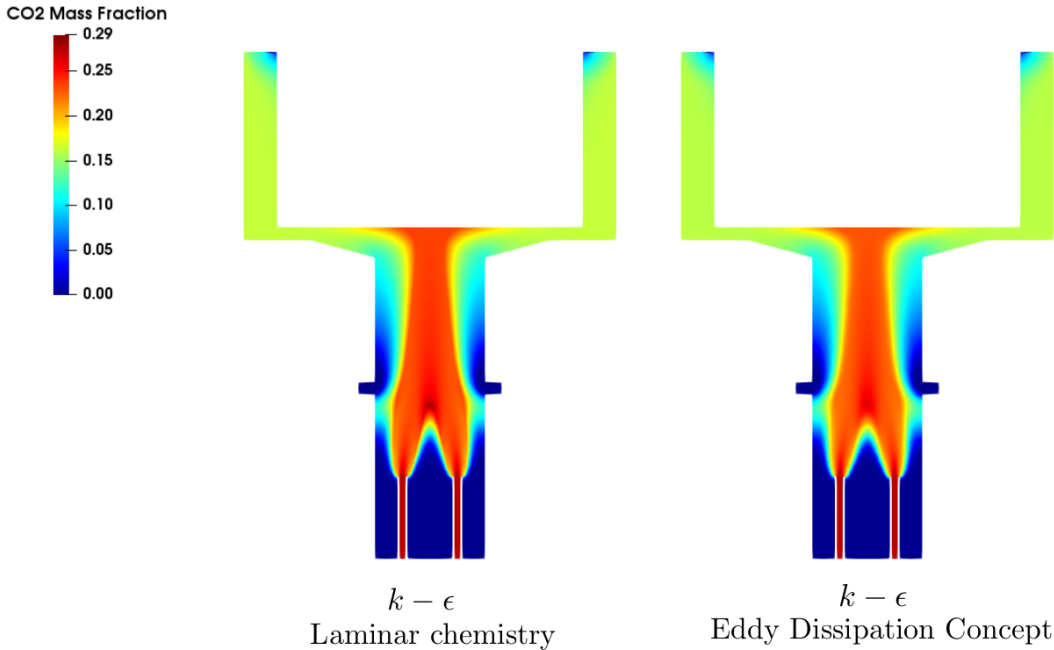


Figure A.11: CO2 Mass Fraction

4. CHEMICAL MECHANISMS

4.1 2 STEPS GLOBAL SYNGAS MECHANISM

For details of the origin of the mechanism and the validation, see (Slavinskaya, Braun-Unkhoff, and Frank, 2008). Note that the original paper has a typo in each of the exponents of the "pre-exponential factor". The original paper has $10E - 7$ and $20.15E - 8$, but this lacks physical meaning as simulations with this values predic a dissociation of water into hydrogen and oxigen at atmospheric conditions, which is unrealistic. The behaviour with the corrected values is realistic and in surprising agreement with the 21 steps mechanism by (Hawkes et al., 2007).

```

! =====
! * Slavinskaya, Braun-Unkhoff & Frank 2008 syngas global mech *
! =====
!
! ----- Compiled in Chemkin format by Diego Quan -----
!
ELEMENTS
O H N C
END
SPECIES
H2 O2 H2O CO CO2 N2
END

REACTIONS
!----- R 1 -----
2H2+O2=>2H2O          10.8E7      6.1      40547.7
FORD/H2 2.0/
!----- R 2 -----
CO+O2+H2=>CO2+H2O      20.15E8      5.9      25529.5
FORD /O2 1.0/
FORD /CO 1.4/
END

```

4.2 21 STEPS SKELETAL SYNGAS MECHANISM

11 species, 21 reations syngas skeletal mechanisms by (Hawkes et al., 2007). For details of the origin of the mechanism, see the reference. The thermodynamic data is included in the original attached files from the reference.

```

ELEMENTS
C H O N
END

SPECIES
H2 O2 O OH H2O H HO2 CO CO2 HCO N2
END

REACTIONS

! ***** H2-O2 Chain Reactions *****

! Hessler, J. Phys. Chem. A, 102:4517 (1998)
H+O2=O+OH          3.547e+15 -0.406 1.6599E+4

! Sutherland et al., 21st Symposium, p. 929 (1986)
O+H2=H+OH          0.508E+05 2.67 0.629E+04

```

```

! Michael and Sutherland, J. Phys. Chem. 92:3853 (1988)
H2+OH=H2O+H      0.216E+09 1.51 0.343E+04

! Sutherland et al., 23rd Symposium, p. 51 (1990)
O+H2O=OH+OH      2.97e+06 2.02 1.34e+4

! ***** H2-O2 Dissociation Reactions *****

! Tsang and Hampson, J. Phys. Chem. Ref. Data, 15:1087 (1986)
H2+M=H+H+M      4.577E+19 -1.40 1.0438E+05
  H2/2.5/ H2O/12/
  CO/1.9/ CO2/3.8/

! Tsang and Hampson, J. Phys. Chem. Ref. Data, 15:1087 (1986)
O+O+M=O2+M      6.165E+15 -0.50 0.000E+00
  H2/2.5/ H2O/12/
  CO/1.9/ CO2/3.8/

! Tsang and Hampson, J. Phys. Chem. Ref. Data, 15:1087 (1986)
O+H+M=OH+M      4.714E+18 -1.00 0.000E+00
  H2/2.5/ H2O/12/
  CO/1.9/ CO2/3.8/

! Tsang and Hampson, J. Phys. Chem. Ref. Data, 15:1087 (1986)
!H+OH+M=H2O+M  2.212E+22 -2.00 0.000E+00
H+OH+M=H2O+M    3.800E+22 -2.00 0.000E+00
  H2/2.5/ H2O/12/
  CO/1.9/ CO2/3.8/

!***** Formation and Consumption of HO2*****

! Cobos et al., J. Phys. Chem. 89:342 (1985) for kinf
! Michael, et al., J. Phys. Chem. A, 106:5297 (2002) for k0

!*****
! MAIN BATH GAS IS N2 (comment this reaction otherwise)
!
H+O2(+M)=HO2(+M) 1.475E+12 0.60 0.00E+00
  LOW/6.366E+20 -1.72 5.248E+02/
  TROE/0.8 1E-30 1E+30/
  H2/2.0/ H2O/11./ O2/0.78/ CO/1.9/ CO2/3.8/

! Tsang and Hampson, J. Phys. Chem. Ref. Data, 15:1087 (1986) [modified]
HO2+H=H2+O2      1.66E+13 0.00 0.823E+03

! Tsang and Hampson, J. Phys. Chem. Ref. Data, 15:1087 (1986) [modified]
HO2+H=OH+OH      7.079E+13 0.00 2.95E+02

! Baulch et al., J. Phys. Chem. Ref Data, 21:411 (1992)
HO2+O=O2+OH      0.325E+14 0.00 0.00E+00

! Keyser, J. Phys. Chem. 92:1193 (1988)
HO2+OH=H2O+O2    2.890E+13 0.00 -4.970E+02

!***** CO/HCO REACTIONS *****

! Troe, 15th Symposium
CO+O(+M)=CO2(+M) 1.80E+10 0.00 2384.

```

4. Chemical mechanisms

```
! Fit of Westmoreland, AiChe J., 1986, rel. to N2 - Tim adjusted from MTA's
! rate constant, which was rel to Ar.
  LOW/1.55E+24 -2.79 4191./
  H2/2.5/ H2O/12/ CO/1.9/ CO2/3.8/

! Tsang and Hampson, JPC Ref. Data, 15:1087 (1986)
CO+O2=CO2+O      0.253E+13 0.00 0.477E+05

! This rate constant is modified per an updated value for H02+H02=H2O2+OH
CO+H02=CO2+OH    3.01E+13 0.00 2.30E+04

! This study (2004) by matching literature experiment results
CO+OH=CO2+H      2.229E+05 1.89 -1158.7

! This study (2004) by matching literature experiment results
HCO+M=H+CO+M     4.7485E+11 0.659 1.4874E+04
H2/2.5/ H2O/6/ CO/1.9/ CO2/3.8/

! Timonen et al., JPC, 92:651 (1988)
HCO+O2=CO+HO2    0.758E+13 0.00 0.410E+03

! Timonen et al., JPC, 91:692 (1987)
HCO+H=CO+H2      0.723E+14 0.00 0.000E+00

! All reactions from Tsang and Hampson, JPC Ref. Data, 15:1087 (1986)
HCO + O = CO2 + H      3.000E+13 0.00 0.000E+00

END
```

Bibliography

1. Agenbrood, Joshua et al. (2011a). “A simplified model for understanding natural convection driven biomass cooking stoves-Part 1: Setup and baseline validation”. In: *Energy for Sustainable Development* 15.2, pp. 160–168. ISSN: 09730826. DOI: [10.1016/j.esd.2011.04.004](https://doi.org/10.1016/j.esd.2011.04.004). URL: <http://dx.doi.org/10.1016/j.esd.2011.04.004>.
2. — (2011b). “A simplified model for understanding natural convection driven biomass cooking stoves-Part 2: With cook piece operation and the dimensionless form”. In: *Energy for Sustainable Development* 15.2, pp. 169–175. ISSN: 09730826. DOI: [10.1016/j.esd.2011.04.002](https://doi.org/10.1016/j.esd.2011.04.002). URL: <http://dx.doi.org/10.1016/j.esd.2011.04.002>.
3. Al Jazeera News (2018). *IPCC concludes Paris accord is not enough to limit global warming*. URL: <https://www.aljazeera.com/news/2018/10/ipcc-climate-change-report-paris-climate-accord-181009134051255.html>.
4. Alzahrani, Fahad M. et al. (2015). “Evaluation of the accuracy of selected syngas chemical mechanisms”. In: *Journal of Energy Resources Technology, Transactions of the ASME* 137.4, pp. 1–13. ISSN: 15288994. DOI: [10.1115/1.4029860](https://doi.org/10.1115/1.4029860).
5. Arora, Pooja, Suresh Jain, and Kamna Sachdeva (2013). “Physical characterization of particulate matter emitted from wood combustion in improved and traditional cookstoves”. In: *Energy for Sustainable Development* 17.5, pp. 497–503. ISSN: 09730826. DOI: [10.1016/j.esd.2013.06.003](https://doi.org/10.1016/j.esd.2013.06.003). URL: <http://dx.doi.org/10.1016/j.esd.2013.06.003>.
6. Bailis, Rob, Kirk R Smith, and Rufus Edwards (2007). *Kitchen Performance Test (KPT)*. Tech. rep. Household Energy and Health Programme, Shell Foundation.
7. Baillis, Rob (2004). *Controlled Cookint Tests (CCT)*. Tech. rep. Household Energy and Health Programme, Shell Foundation.
8. Ballard-Tremeer, G. and H. H. Jawurek (1996). “Comparison of five rural, wood-burning cooking devices: Efficiencies and emissions”. In: *Biomass and Bioenergy* 11.5, pp. 419–430. ISSN: 09619534. DOI: [10.1016/S0961-9534\(96\)00040-2](https://doi.org/10.1016/S0961-9534(96)00040-2).
9. Basu, Prabir (2010). *Biomass gasification and pyrolysis: practical design and theory*. Academic press.
10. Berkeley Air Monitoring Group and Global Alliance for Clean Cookstoves (2012). *Stove Performance Inventory Report*. Tech. rep. October. Berkeley Air Monitoring Group and Global Alliance for Clean Cookstoves, pp. 1–37. URL: http://cleancookstoves.org/resources%7B%5C_%7Dfiles/stove-performance-inventory-pdf.pdf.
11. Berrueta, Víctor M., Rufus D. Edwards, and Omar R. Masera (2008). “Energy performance of wood-burning cookstoves in Michoacan, Mexico”. In: *Renewable Energy* 33.5, pp. 859–870. ISSN: 09601481. DOI: [10.1016/j.renene.2007.04.016](https://doi.org/10.1016/j.renene.2007.04.016).
12. Bologa, A., H.-R. Paur, and R. Koerber (n.d.). *Electrostatic Precipitator of Fine Particles from Biomass Combustion Facilities*. URL: www.ki.edu.
13. Bonan, Jacopo, Stefano Pareglio, and Massimo Tavoni (2017). “Access to modern energy: A review of barriers, drivers and impacts”. In: *Environment and Development Economics* 22.5, pp. 491–516. ISSN: 14694395. DOI: [10.1017/S1355770X17000201](https://doi.org/10.1017/S1355770X17000201).
14. Bond, T. C. et al. (June 2013). “Bounding the role of black carbon in the climate system: A scientific assessment”. In: *Journal of Geophysical Research Atmospheres* 118.11, pp. 5380–5552. ISSN: 21698996. DOI: [10.1002/jgrd.50171](https://doi.org/10.1002/jgrd.50171). URL: <http://doi.wiley.com/10.1002/jgrd.50171>.

15. Borgmann, U., W. P. Norwood, and D. G. Dixon (Oct. 2004). “Re-evaluation of metal bioaccumulation and chronic toxicity in *Hyalella azteca* using saturation curves and the biotic ligand model”. In: *Environmental Pollution* 131.3, pp. 469–484. ISSN: 02697491. DOI: [10.1016/j.envpol.2004.02.010](https://doi.org/10.1016/j.envpol.2004.02.010).
16. Bridgwater, A. V. (May 1995). *The technical and economic feasibility of biomass gasification for power generation*. DOI: [10.1016/0016-2361\(95\)00001-L](https://doi.org/10.1016/0016-2361(95)00001-L).
17. Bryden, Mark et al. (2005). *Design principles for wood burning cook stoves*. Aprovecho Research Center.
18. Burnham, Alan K (2010). *Estimating the Heat of Formation of Foodstuffs and Biomass*. Tech. rep. Lawrence Livermore National Lab.(LLNL), Livermore, CA (United States).
19. Cable, Matthew (2009). “An evaluation of turbulence models for the numerical study of forced and natural convective flow in Atria”. PhD thesis. Queen’s University.
20. Cambridge English Dictionary (2020). *DEVELOPMENT* | meaning in the Cambridge English Dictionary. URL: <https://dictionary.cambridge.org/dictionary/english/development> (visited on 02/23/2020).
21. Carbone, Francesco et al. (2016). “The Whirl Cookstove: A Novel Development for Clean Biomass Burning”. In: *Combustion Science and Technology* 188.4-5, pp. 594–610. ISSN: 1563521X. DOI: [10.1080/00102202.2016.1139364](https://doi.org/10.1080/00102202.2016.1139364).
22. Champion, Wyatt M. and Andrew P. Grieshop (2019). “Pellet-Fed Gasifier Stoves Approach Gas-Stove Like Performance during in-Home Use in Rwanda”. In: *Environmental Science and Technology* 53.11, pp. 6570–6579. ISSN: 15205851. DOI: [10.1021/acs.est.9b00009](https://doi.org/10.1021/acs.est.9b00009).
23. Chanphavong, Lemthong and Z. A. Zainal (2019). “Characterization and challenge of development of producer gas fuel combustor: A review”. In: *Journal of the Energy Institute* 92.5, pp. 1577–1590. ISSN: 17460220. DOI: [10.1016/j.joei.2018.07.016](https://doi.org/10.1016/j.joei.2018.07.016). URL: <https://doi.org/10.1016/j.joei.2018.07.016>.
24. Chomiak, J., J. P. Longwell, and A. F. Sarofim (1989). “Combustion of low calorific value gases; Problems and prospects”. In: *Progress in Energy and Combustion Science* 15.2, pp. 109–129. ISSN: 03601285. DOI: [10.1016/0360-1285\(89\)90012-9](https://doi.org/10.1016/0360-1285(89)90012-9).
25. *Clean Cooking Alliance* (2020). URL: <https://www.cleancookingalliance.org/impact-areas/environment/index.html> (visited on 02/23/2020).
26. Committee, W B T Technical et al. (2014). *The Water Boiling Test: Version 4.2. 3*.
27. Costa, Luí s, Diego Rybski, and Jürgen P Kropp (2011). “A human development framework for CO2 reductions”. In: *PloS one* 6.12.
28. Daniel David, Miller-Lionberg (2011). “A FINE RESOLUTION CFD SIMULATION APPROACH FOR BIOMASS COOK STOVE DEVELOPMENT”. Master of Science Thesis. Colorado State University.
29. De Jong, Wiebren and J Ruud Van Ommen (2014). *Biomass as a sustainable energy source for the future: Fundamentals of conversion processes*. John Wiley & Sons.
30. Defoort, Morgan (2015). *Achieving Tier 4 Emissions and Efficiency in Biomass Cookstoves*. Tech. rep. Energy Institute, Colorado State University.
31. Dernbecher, Andrea et al. (2019). *Review on modelling approaches based on computational fluid dynamics for biomass combustion systems: Focus on fixed bed and moving grate systems*. Vol. 9. 1. Biomass Conversion and Biorefinery, pp. 129–182. ISBN: 1339901900. DOI: [10.1007/s13399-019-00370-z](https://doi.org/10.1007/s13399-019-00370-z).

32. Dilger, Marco et al. (2016). “Toxicity of wood smoke particles in human A549 lung epithelial cells: the role of PAHs, soot and zinc”. In: *Archives of Toxicology* 90.12, pp. 3029–3044. ISSN: 14320738. DOI: [10.1007/s00204-016-1659-1](https://doi.org/10.1007/s00204-016-1659-1).
33. FAO (2019). *Wood Energy*. URL: <http://www.fao.org/forestry/energy/en/> (visited on 02/24/2020).
34. Galgano, Antonio and Colomba Di Blasi (2006). “Coupling a CFD code with a solid-phase combustion model”. In: *Progress in Computational Fluid Dynamics* 6.4-5, pp. 287–302. ISSN: 14684349. DOI: [10.1504/PCFD.2006.010037](https://doi.org/10.1504/PCFD.2006.010037).
35. Garland, Charity et al. (2017). “Black carbon cookstove emissions: A field assessment of 19 stove/fuel combinations”. In: *Atmospheric Environment* 169, pp. 140–149. ISSN: 18732844. DOI: [10.1016/j.atmosenv.2017.08.040](https://doi.org/10.1016/j.atmosenv.2017.08.040). URL: <https://doi.org/10.1016/j.atmosenv.2017.08.040>.
36. Gifford, Mary Louise (2010). “A Global Review of Improved Cookstove Programs”. In: *Salzburg - Energy Reform Conference 2010*, pp. 2–31.
37. Google Dictionary (2018). *Economic Growth*. Ed. by Google. URL: <https://bit.ly/2DNMtIr>.
38. Groom, Nichola (2019). *Weaning U.S. power sector off fossil fuels would cost USD 4.7 trillion, study*. Ed. by Reuters. URL: <https://www.reuters.com/article/us-usa-carbon-report/weaning-u-s-power-sector-off-fossil-fuels-would-cost-4-7-trillion-study-idUSKCN1TSOGX>.
39. Grooten, Monique, R E A Almond, et al. (2018). “Living planet report-2018: aiming higher.” In: *Living planet report-2018: aiming higher*.
40. Hagos, Ftwi Yohaness, A. Rashid A. Aziz, and Shaharin Anwar Sulaiman (2014). “Trends of syngas as a fuel in internal combustion engines”. In: *Advances in Mechanical Engineering* 2014. ISSN: 16878132. DOI: [10.1155/2014/401587](https://doi.org/10.1155/2014/401587).
41. Happo, Mikko S. et al. (2013). “Pulmonary inflammation and tissue damage in the mouse lung after exposure to PM samples from biomass heating appliances of old and modern technologies”. In: *Science of the Total Environment* 443, pp. 256–266. ISSN: 00489697. DOI: [10.1016/j.scitotenv.2012.11.004](https://doi.org/10.1016/j.scitotenv.2012.11.004). URL: <http://dx.doi.org/10.1016/j.scitotenv.2012.11.004>.
42. Hawkes, Evatt R. et al. (2007). “Scalar mixing in direct numerical simulations of temporally evolving plane jet flames with skeletal CO/H₂ kinetics”. In: *Proceedings of the Combustion Institute* 31 I.1, pp. 1633–1640. ISSN: 15407489. DOI: [10.1016/j.proci.2006.08.079](https://doi.org/10.1016/j.proci.2006.08.079).
43. Hertzberg, Tommy and Per Blomqvist (2003). “Particles from fires - A screening of common materials found in buildings”. In: *Fire and Materials* 27.6, pp. 295–314. ISSN: 03080501. DOI: [10.1002/fam.837](https://doi.org/10.1002/fam.837).
44. Huff, Ryan D., Chris Carlsten, and Jeremy A. Hirota (2019). “An update on immunologic mechanisms in the respiratory mucosa in response to air pollutants”. In: *Journal of Allergy and Clinical Immunology* 143.6, pp. 1989–2001. ISSN: 10976825. DOI: [10.1016/j.jaci.2019.04.012](https://doi.org/10.1016/j.jaci.2019.04.012). URL: <https://doi.org/10.1016/j.jaci.2019.04.012>.
45. Husain, Zakir et al. (2019). “Computational Fluid Dynamics Study of Biomass Cook Stove - Part 1: Hydrodynamics and Homogeneous Combustion”. In: *Industrial and Engineering Chemistry Research*. ISSN: 15205045. DOI: [10.1021/acs.iecr.9b03181](https://doi.org/10.1021/acs.iecr.9b03181).
46. International, Amnesty (2010). *Deadly Delivery: The Maternal Health Care Crisis In the USA*. Amnesty International Publications.
47. International Energy Agency (2019). *SDG7: Data and Projections*. Flashship Report. IEA. URL: <https://www.iea.org/reports/sdg7-data-and-projections/access-to-clean-cooking>.
48. International Monetary Fund (2012). *Statistics on the Growth of the Global Domestic Gross Product (GDP) from 2003 to 2012*. URL: <https://www.statista.com/statistics/273951/growth-of-the-global-gross-domestic-product-gdp/>.

49. Intra, Panich, Pravitt Limueadphai, and Nakorn Tippayawong (2010). “Particulate emission reduction from biomass burning in small combustion systems with a multiple tubular electrostatic precipitator”. In: *Particulate Science and Technology* 28.6, pp. 547–565. ISSN: 02726351. DOI: [10.1080/02726351003758444](https://doi.org/10.1080/02726351003758444).
50. IPCC (2018). *Summary for Policymakers*. Tech. rep. 9, pp. 1689–1699. DOI: [10.1017/CB09781107415324.004](https://doi.org/10.1017/CB09781107415324.004). arXiv: [arXiv:1011.1669v3](https://arxiv.org/abs/1011.1669v3).
51. ISO (2018). *INTERNATIONAL STANDARD ISO 19867-1, Clean cookstoves and clean cooking solutions - Harmonized laboratory test protocols -*.
52. Jetter, James et al. (2012). “Pollutant emissions and energy efficiency under controlled conditions for household biomass cookstoves and implications for metrics useful in setting international test standards”. In: *Environmental Science and Technology* 46.19, pp. 10827–10834. ISSN: 0013936X. DOI: [10.1021/es301693f](https://doi.org/10.1021/es301693f).
53. Jeuland, Marc A. and Subhrendu K. Pattanayak (2012). “Benefits and costs of improved cookstoves: Assessing the implications of variability in health, forest and climate impacts”. In: *PLoS ONE* 7.2. ISSN: 19326203. DOI: [10.1371/journal.pone.0030338](https://doi.org/10.1371/journal.pone.0030338).
54. Johnson, Michael et al. (2014). *WHO Indoor Air Quality Guidelines: household Fuel Combustion - Review 3: Model for linking household energy use with indoor air quality*. Tech. rep. World Health Organization, pp. 1–29.
55. Juhasz, Antonia (2013). *Why the war in Iraq was fought for Bil Oil*. Ed. by CNN. URL: <https://edition.cnn.com/2013/03/19/opinion/iraq-war-oil-juhasz/index.html>.
56. Kær, Søren K. (Mar. 2005). “Straw combustion on slow-moving grates - A comparison of model predictions with experimental data”. In: *Biomass and Bioenergy* 28.3, pp. 307–320. ISSN: 09619534. DOI: [10.1016/j.biombioe.2004.08.017](https://doi.org/10.1016/j.biombioe.2004.08.017).
57. Kan, JJIM van, A Segal, and F J Vermolen (2005). *Numerical methods in scientific computing*. VSSD. ISBN: 90-71301-50-8.
58. Karl, Jürgen (2014). “Biomass heat pipe reformer-design and performance of an indirectly heated steam gasifier”. In: *Biomass Conversion and Biorefinery* 4.1, pp. 1–14. ISSN: 21906823. DOI: [10.1007/s13399-013-0102-6](https://doi.org/10.1007/s13399-013-0102-6).
59. Kelz, J et al. (2010). “Pm Emissions From Old and Modern Biomass Combustion Systems and Their Health Effects”. In: *18th European Biomass Conference and Exhibition May 2010*, pp. 1231–1243.
60. Knight, M et al. (2017). “Saving lives, improving mothers’ care: lessons learned to inform future maternity care from the UK and Ireland confidential enquiries into maternal deaths and morbidity 2009-2012”. In.
61. Kshirsagar, Milind P. and Vilas R. Kalamkar (2015). “A mathematical tool for predicting thermal performance of natural draft biomass cookstoves and identification of a new operational parameter”. In: *Energy* 93, pp. 188–201. ISSN: 03605442. DOI: [10.1016/j.energy.2015.09.015](https://doi.org/10.1016/j.energy.2015.09.015). URL: <http://dx.doi.org/10.1016/j.energy.2015.09.015>.
62. Kwiatkowski, Kamil, Marek Dudyński, and Konrad Bajer (2013). “Combustion of low-calorific waste biomass syngas”. In: *Flow, Turbulence and Combustion* 91.4, pp. 749–772. ISSN: 13866184. DOI: [10.1007/s10494-013-9473-9](https://doi.org/10.1007/s10494-013-9473-9).
63. Law, Chung K. (2006). *Combustion Physics*. Cambridge University Press, p. 714. ISBN: 9780521870528.
64. Leskinen, J. et al. (2014). “Fine particle emissions in three different combustion conditions of a wood chip-fired appliance - Particulate physico-chemical properties and induced cell death”. In: *Atmospheric Environment* 86, pp. 129–139. ISSN: 13522310. DOI: [10.1016/j.atmosenv.2013.12.012](https://doi.org/10.1016/j.atmosenv.2013.12.012). URL: <http://dx.doi.org/10.1016/j.atmosenv.2013.12.012>.

65. LeVeque, Randall J et al. (2002). *Finite volume methods for hyperbolic problems*. Vol. 31. Cambridge university press.
66. Lind, Terttaliisa et al. (2003). “Electrostatic precipitator collection efficiency and trace element emissions from co-combustion of biomass and recovered fuel in fluidized-bed combustion”. In: *Environmental Science and Technology* 37.12, pp. 2842–2846. ISSN: 0013936X. DOI: [10.1021/es026314z](https://doi.org/10.1021/es026314z).
67. MacCarty, N et al. (2007). “Laboratory comparison of the global-warming potential of six categories of biomass cooking stoves”. In: *Aprovecho Research Center* September, p. 26. URL: http://farm-check.com/lcs/docs/Global%7B%5C_%7Dwarming%7B%5C_%7Dfull%7B%5C_%7D9-6-07.pdf.
68. MacCarty, Nordica, Damon Ogle, et al. (2008). “A laboratory comparison of the global warming impact of five major types of biomass cooking stoves”. In: *Energy for sustainable development* 12.2, pp. 56–65.
69. MacCarty, Nordica, Dean Still, and Damon Ogle (2010). “Fuel use and emissions performance of fifty cooking stoves in the laboratory and related benchmarks of performance”. In: *Energy for Sustainable Development* 14.3, pp. 161–171. ISSN: 09730826. DOI: [10.1016/j.esd.2010.06.002](https://doi.org/10.1016/j.esd.2010.06.002). URL: <http://dx.doi.org/10.1016/j.esd.2010.06.002>.
70. Maccarty, Nordica et al. (2008). “Assessing Cook Stove Performance: Field and Lab Studies of Three Rocket Stoves Comparing the Open Fire and Traditional Stoves in Tamil Nadu, India on Measures of Time to Cook, Fuel Use, Total Emissions, and Indoor Air Pollution”. In: *Indoor Air*, pp. 1–18.
71. MacCarty, Nordica A. and Kenneth M. Bryden (2015). “Modeling of household biomass cookstoves: A review”. In: *Energy for Sustainable Development* 26, pp. 1–13. ISSN: 23524669. DOI: [10.1016/j.esd.2015.02.001](https://doi.org/10.1016/j.esd.2015.02.001). URL: <http://dx.doi.org/10.1016/j.esd.2015.02.001>.
72. MacCarty, Nordica A. and Kenneth Mark Bryden (2016). “An integrated systems model for energy services in rural developing communities”. In: *Energy* 113, pp. 536–557. ISSN: 03605442. DOI: [10.1016/j.energy.2016.06.145](https://doi.org/10.1016/j.energy.2016.06.145). URL: <http://dx.doi.org/10.1016/j.energy.2016.06.145>.
73. Mahmoudi, Amir Houshang et al. (2015). “An experimental and numerical study of wood combustion in a fixed bed using Euler-Lagrange approach (XDEM)”. In: *Fuel* 150, pp. 573–582. ISSN: 00162361. DOI: [10.1016/j.fuel.2015.02.008](https://doi.org/10.1016/j.fuel.2015.02.008). URL: <http://dx.doi.org/10.1016/j.fuel.2015.02.008>.
74. Marchese, J. Anthony et al. (2018). *ACHIEVING TIER 4 E MISSIONS IN BIOMASS COOKSTOVES, Final Technical Report, DOE Award Number DE-EE006086*. Tech. rep. Colorado State University.
75. Masson-Delmotte, Valerie et al. (2018). “IPCC, 2018: Summary for policymakers”. In: *Global warming of 1.5 C* 1.
76. McCracken, John P. and Kirk R. Smith (1998). “Emissions and efficiency of improved woodburning cookstoves in highland Guatemala”. In: *Environment International* 24.7, pp. 739–747. ISSN: 18736750. DOI: [10.1016/S0160-4120\(98\)00062-2](https://doi.org/10.1016/S0160-4120(98)00062-2).
77. Mehetre, Sonam A et al. (2017). “Improved biomass cookstoves for sustainable development: A review”. In: *Renewable and Sustainable Energy Reviews* 73, pp. 672–687.
78. Mehrabian Bardar, R. (2013). “CFD Simulation of the Thermal Conversion of Solid Biomass in Packed Bed Furnaces by Ramin Mehrabian Bardar”. PhD thesis. Graz University of Technology.
79. Mental Health Foundation (2018). *Suicide*. URL: <https://www.mentalhealth.org.uk/a-to-z/s/suicide>.

80. Migliavacca, Gabriele et al. (2014). “Reduction of pm emissions from biomass combustion appliances: Evaluation of efficiency of electrostatic precipitators”. In: *Chemical Engineering Transactions* 37, pp. 25–30. ISSN: 22839216. DOI: [10.3303/CET1437005](https://doi.org/10.3303/CET1437005).
81. Milne, Thomas A, Robert J Evans, and N Abatzoglou (1998). *Biomass gasifier”Tars”: their nature, formation, and conversion*. Tech. rep. National Renewable Energy Laboratory, Golden, CO (US).
82. Mitchell, E. J.S. et al. (2019). “Pollutant Emissions from Improved Cookstoves of the Type Used in Sub-Saharan Africa”. In: *Combustion Science and Technology* 0.0, pp. 1–21. ISSN: 1563521X. DOI: [10.1080/00102202.2019.1614922](https://doi.org/10.1080/00102202.2019.1614922). URL: <https://doi.org/10.1080/00102202.2019.1614922>.
83. Monteiro, Eliseu et al. (2010). “Laminar burning velocities and Markstein numbers of syngas-air mixtures”. In: *Fuel* 89.8, pp. 1985–1991. ISSN: 00162361. DOI: [10.1016/j.fuel.2009.11.008](https://doi.org/10.1016/j.fuel.2009.11.008). URL: <http://dx.doi.org/10.1016/j.fuel.2009.11.008>.
84. Monteiro Magalhaes, Eliseu (2011). “Combustion Study of Mixtures Resulting From a Gasification Process of Forest Biomass”. In: June, p. 233.
85. Moses, Nicholas D. and Nordica A. MacCarty (2019). “What makes a cookstove usable? Trials of a usability testing protocol in Uganda, Guatemala, and the United States”. In: *Energy Research and Social Science* 52.June 2018, pp. 221–235. ISSN: 22146296. DOI: [10.1016/j.erss.2019.02.002](https://doi.org/10.1016/j.erss.2019.02.002). URL: <https://doi.org/10.1016/j.erss.2019.02.002>.
86. Moses, Nicholas D., Mohammad H. Pakravan, and Nordica A. MacCarty (2019). “Development of a practical evaluation for cookstove usability”. In: *Energy for Sustainable Development* 48, pp. 154–163. ISSN: 23524669. DOI: [10.1016/j.esd.2018.12.003](https://doi.org/10.1016/j.esd.2018.12.003). URL: <https://doi.org/10.1016/j.esd.2018.12.003>.
87. NASA (1999). *NASA thermodynamic files*. URL: <http://combustion.berkeley.edu/gri-mech/version30/files30/thermo30.dat> (visited on 10/16/2020).
88. Nations, United (1948). *Universal Declaration of Human Rights*. URL: <https://www.un.org/en/universal-declaration-human-rights/> (visited on 10/23/2020).
89. Nieuwstadt, Frans T M, Bendiks J Boersma, and Jerry Westerweel (2016). *Turbulence: introduction to theory and applications of turbulent flows*. Springer. ISBN: 9783319315973.
90. Nina Martin (2017). *U.S. Has The Worst Rate of Maternal Deaths In The Developed World : NPR*. URL: <https://www.npr.org/2017/05/12/528098789/u-s-has-the-worst-rate-of-maternal-deaths-in-the-developed-world?t=1603415331174> (visited on 10/23/2020).
91. Obernberger, Ingwald et al. (2017). “Strategies and technologies towards zero emission biomass combustion by primary measures”. In: *Energy Procedia* 120, pp. 681–688. ISSN: 18766102. DOI: [10.1016/j.egypro.2017.07.184](https://doi.org/10.1016/j.egypro.2017.07.184). URL: <http://dx.doi.org/10.1016/j.egypro.2017.07.184>.
92. Oliveira, Guthman Palandi et al. (2020). “Experimental laminar burning velocity of syngas from fixed-bed downdraft biomass gasifiers”. In: *Renewable Energy* 153, pp. 1251–1260. ISSN: 18790682. DOI: [10.1016/j.renene.2020.02.083](https://doi.org/10.1016/j.renene.2020.02.083). URL: <https://doi.org/10.1016/j.renene.2020.02.083>.
93. Orange, C L, M Defoort, and B Willson (2012). “Energy for Sustainable Development In fl uence of testing parameters on biomass stove performance and development of an improved testing protocol”. In: *Energy for Sustainable Development* 16.1, pp. 3–12. ISSN: 0973-0826. DOI: [10.1016/j.esd.2011.10.008](https://doi.org/10.1016/j.esd.2011.10.008). URL: <http://dx.doi.org/10.1016/j.esd.2011.10.008>.
94. Paasonen, Pauli et al. (2016). “Continental anthropogenic primary particle number emissions”. In: *Atmospheric Chemistry and Physics* 16.11, pp. 6823–6840. ISSN: 16807324. DOI: [10.5194/acp-16-6823-2016](https://doi.org/10.5194/acp-16-6823-2016).
95. Pande, Rohan R., Milind P. Kshirsagar, and Vilas R. Kalamkar (2018). “Experimental and CFD analysis to study the effect of inlet area ratio in a natural draft biomass cookstove”. In: *Environment, Development and Sustainability* 0123456789. ISSN: 15732975. DOI: [10.1007/s10668-018-0269-x](https://doi.org/10.1007/s10668-018-0269-x). URL: <https://doi.org/10.1007/s10668-018-0269-x>.

96. Poinso, Thierry and Denis Veynante (2005). *Theoretical and numerical combustion*. RT Edwards, Inc.
97. Poláčik, Jan et al. (2018). “Particulate matter produced by micro-scale biomass combustion in an oxygen-lean atmosphere”. In: *Energies* 11.12. ISSN: 19961073. DOI: [10.3390/en11123359](https://doi.org/10.3390/en11123359).
98. Population Reference Bureau (2016). *Suicide Replaces Homicide as Second-Leading Cause of Death Among U.S. Teenagers*. Ed. by Beth Jarosz Alicia Vanorman. URL: <https://www.prb.org/suicide-replaces-homicide-second-leading-cause-death-among-us-teens/>.
99. Prapas, J et al. (2014). “Influence of chimneys on combustion characteristics of buoyantly driven biomass stoves”. In: *Energy for Sustainable Development* 23, pp. 286–293. ISSN: 23524669. DOI: [10.1016/j.esd.2014.08.007](https://doi.org/10.1016/j.esd.2014.08.007). URL: <http://dx.doi.org/10.1016/j.esd.2014.08.007>.
100. Prapas, Jason (2013). “Toward the Understanding and Optimization of Chimneys for Buoyantly Driven Biomass Stoves”. In.
101. Pundle, Anamol et al. (2019). “Predicting and analyzing the performance of biomass-burning natural draft rocket cookstoves using computational fluid dynamics”. In: *Biomass and Bioenergy* 131. ISSN: 18732909. DOI: [10.1016/j.biombioe.2019.105402](https://doi.org/10.1016/j.biombioe.2019.105402).
102. Quackenbush, Casey (2019). “The Worlds Top 26 Billionaires Now Own as Much as the Poorest 3.8 Billion, Says Oxfam”. In: *TIME*.
103. Quan-Reyes, Diego, Avishek Goel, and Victor Mora (2020). “Performance Evaluation of Biomass Cookstoves in Rural Guatemala”. In: *Conference Paper in the World Sustainable Energy Days*.
104. Ragland, Kenneth W and Kenneth M Bryden (2011). *Combustion engineering*. CRC press.
105. Ranzi, Eliseo et al. (2008). “Chemical kinetics of biomass pyrolysis”. In: *Energy and Fuels* 22.6, pp. 4292–4300. ISSN: 08870624. DOI: [10.1021/ef800551t](https://doi.org/10.1021/ef800551t).
106. Reed, T B and Ronal Larson (1997). “A wood-gas stove for developing countries”. In: *Developments in thermochemical biomass conversion*. Springer, pp. 985–993.
107. Roden, Christoph A. et al. (2009). “Laboratory and field investigations of particulate and carbon monoxide emissions from traditional and improved cookstoves”. In: *Atmospheric Environment* 43.6, pp. 1170–1181. ISSN: 13522310. DOI: [10.1016/j.atmosenv.2008.05.041](https://doi.org/10.1016/j.atmosenv.2008.05.041). URL: <http://dx.doi.org/10.1016/j.atmosenv.2008.05.041>.
108. *Lecture notes for the AE4262 Combustion for Propulsion and Power Systems, Delft University of Technology* (2020).
109. Roth, Christa (2011). “Micro gasification: cooking with gas from biomass”. In: *GIZ HERA Poverty-oriented Basic Energy Service*.
110. Ruiz-Mercado, Ilse et al. (2011). “Adoption and sustained use of improved cookstoves”. In: *Energy Policy* 39.12, pp. 7557–7566. ISSN: 03014215. DOI: [10.1016/j.enpol.2011.03.028](https://doi.org/10.1016/j.enpol.2011.03.028). URL: <http://dx.doi.org/10.1016/j.enpol.2011.03.028>.
111. Scarlat, N et al. (2019). “Brief on biomass for energy in the European Union”. In: *European Commission’s Knowledge Centre for Bioeconomy*.
112. Scharler, Robert et al. (2020). “Transient CFD simulation of wood log combustion in stoves”. In: *Renewable Energy* 145, pp. 651–662. ISSN: 18790682. DOI: [10.1016/j.renene.2019.06.053](https://doi.org/10.1016/j.renene.2019.06.053).
113. Sedighi, Mohammadreza and Hesamoddin Salarian (2017). “A comprehensive review of technical aspects of biomass cookstoves”. In: *Renewable and Sustainable Energy Reviews* 70, pp. 656–665.
114. Shah, Rahul and A. W. Date (2011). “Steady-state thermochemical model of a wood-burning cook-stove”. In: *Combustion Science and Technology* 183.4, pp. 321–346. ISSN: 00102202. DOI: [10.1080/00102202.2010.516617](https://doi.org/10.1080/00102202.2010.516617).

115. Shen, Guofeng et al. (2017). “A Laboratory Comparison of Emission Factors, Number Size Distributions, and Morphology of Ultrafine Particles from 11 Different Household Cookstove-Fuel Systems”. In: *Environmental Science and Technology* 51.11, pp. 6522–6532. ISSN: 15205851. DOI: [10.1021/acs.est.6b05928](https://doi.org/10.1021/acs.est.6b05928).
116. Simon, Gregory L. et al. (2014). “Current debates and future research needs in the clean cookstove sector”. In: *Energy for Sustainable Development* 20.1, pp. 49–57. ISSN: 09730826. DOI: [10.1016/j.esd.2014.02.006](https://doi.org/10.1016/j.esd.2014.02.006). URL: <http://dx.doi.org/10.1016/j.esd.2014.02.006>.
117. Sippula, Olli (2010). “Fine Particle Formation and Emissions in Biomass Combustion”. Dissertation. University of Eastern Finland, p. 68. ISBN: 9789525822144. URL: <http://www.atm.helsinki.fi/FAAR/reportseries/rs-108.pdf>.
118. Slavinskaya, N., M. Braun-Unkhoff, and P. Frank (2008). “Reduced reaction mechanisms for methane and syngas combustion in gas turbines”. In: *Journal of Engineering for Gas Turbines and Power* 130.2. ISSN: 07424795. DOI: [10.1115/1.2719258](https://doi.org/10.1115/1.2719258).
119. Sovacool, Benjamin K. (2012). “The political economy of energy poverty: A review of key challenges”. In: *Energy for Sustainable Development* 16.3, pp. 272–282. ISSN: 09730826. DOI: [10.1016/j.esd.2012.05.006](https://doi.org/10.1016/j.esd.2012.05.006). URL: <http://dx.doi.org/10.1016/j.esd.2012.05.006>.
120. Still, Dean K. et al. (2018). “Laboratory experiments regarding the use of filtration and retained heat to reduce particulate matter emissions from biomass cooking”. In: *Energy for Sustainable Development* 42, pp. 129–135. ISSN: 09730826. DOI: [10.1016/j.esd.2017.09.011](https://doi.org/10.1016/j.esd.2017.09.011). URL: <https://doi.org/10.1016/j.esd.2017.09.011>.
121. Stockholm International Peace Research Institute (2018). *Military expenditure*. Ed. by The World Bank. URL: <https://data.worldbank.org/indicator/MS.MIL.XPND.CD?end=2018%7B%5C%7Dstart=1960%7B%5C%7Dview=chart>.
122. Talukder, Sabera, Sanghyeon Park, and Juan Rivas-Davila (2017). “A portable electrostatic precipitator to reduce respiratory death in rural environments”. In: *2017 IEEE 18th Workshop on Control and Modeling for Power Electronics, COMPEL 2017*. DOI: [10.1109/COMPEL.2017.8013316](https://doi.org/10.1109/COMPEL.2017.8013316).
123. Thakur, M., C. P. van Schayck, and E. A. Boudewijns (2019). “Improved cookstoves in low-resource settings: a spur to successful implementation strategies”. In: *npj Primary Care Respiratory Medicine* 29.1, pp. 23–25. ISSN: 20551010. DOI: [10.1038/s41533-019-0148-4](https://doi.org/10.1038/s41533-019-0148-4). URL: <http://dx.doi.org/10.1038/s41533-019-0148-4>.
124. Thakur, Megha et al. (2018). “Impact of improved cookstoves on women’s and child health in low and middle income countries: A systematic review and meta-analysis”. In: *Thorax*, pp. 1–15. ISSN: 14683296. DOI: [10.1136/thoraxjnl-2017-210952](https://doi.org/10.1136/thoraxjnl-2017-210952).
125. The World Bank (2014). *CO2 emissions (metric tons per capita)*. URL: <https://data.worldbank.org/indicator/EN.ATM.CO2E.PC>.
126. — (2018). “Nearly Half the World Lives on Less than \$5.50 a Day”. In: *The World Bank Press Release -2019/044/DEC-GPV -*.
127. Torvela, Tiina (2015). “Fine Particle Formation in Biomass Morphological Features and Toxicity”. PhD thesis. University of Eastern Finland. ISBN: 9789527091128.
128. Tryner, Jessica, John Volckens, and Anthony J Marchese (2018). “Effects of operational mode on particle size and number emissions from a biomass gasifier cookstove”. In: *Aerosol Science and Technology* 52.1, pp. 87–97. ISSN: 15217388. DOI: [10.1080/02786826.2017.1380779](https://doi.org/10.1080/02786826.2017.1380779). URL: <https://doi.org/10.1080/02786826.2017.1380779>.
129. Urmee, Tania and Samuel Gyamfi (2014). “A review of improved Cookstove technologies and programs”. In: *Renewable and Sustainable Energy Reviews* 33, pp. 625–635.

130. Uski, O. et al. (2014). “Different toxic mechanisms are activated by emission PM depending on combustion efficiency”. In: *Atmospheric Environment* 89, pp. 623–632. ISSN: 18732844. DOI: [10.1016/j.atmosenv.2014.02.036](https://doi.org/10.1016/j.atmosenv.2014.02.036). URL: <http://dx.doi.org/10.1016/j.atmosenv.2014.02.036>.
131. Uski, Oskari J. et al. (2012). “Acute systemic and lung inflammation in C57Bl/6J mice after intratracheal aspiration of particulate matter from small-scale biomass combustion appliances based on old and modern technologies”. In: *Inhalation Toxicology* 24.14, pp. 952–965. ISSN: 08958378. DOI: [10.3109/08958378.2012.742172](https://doi.org/10.3109/08958378.2012.742172).
132. Van Der Lans, R. P. et al. (Sept. 2000). “Modelling and experiments of straw combustion in a grate furnace”. In: *Biomass and Bioenergy* 19.3, pp. 199–208. ISSN: 09619534. DOI: [10.1016/S0961-9534\(00\)00033-7](https://doi.org/10.1016/S0961-9534(00)00033-7).
133. Venkata Ramana, Putti et al. (2015). “The State of the Global Clean and Improved Cooking Sector”. In: *ESMAP and GACC*, pp. 1–179. DOI: [007/15](https://doi.org/10.1016/j.esmap.2015.07.001). URL: <https://openknowledge.worldbank.org/bitstream/handle/10986/21878/96499.pdf>.
134. Viana, Helder Filipe dos Santos et al. (2018). “Evaluation of the physical, chemical and thermal properties of Portuguese maritime pine biomass”. In: *Sustainability (Switzerland)* 10.8. ISSN: 20711050. DOI: [10.3390/su10082877](https://doi.org/10.3390/su10082877).
135. Warnatz, Jurgen, Ulrich Maas, and Robert W Dibble (1996). *Combustion: Physical and Chemical Fundamentals, Modeling and Simulation, Experiments, Pollutant Formation*. 2nd. Springer.
136. Warren, Katie (2020). “Jeff Bezos is facing backlash for Amazon’s donation of only \$690,000 to Australian wildfire recovery. Here are 11 mind-blowing facts that show just how wealthy the CEO really is”. In: *Business Insider*.
137. Watson Institute for International and Public Affairs (2020). *Costs of War*. Ed. by Steven Aftergood. URL: <https://watson.brown.edu/costsofwar/costs/economic>.
138. Wesseling, Pieter (2009). *Principles of computational fluid dynamics*. Vol. 29. Springer Science & Business Media.
139. Wilson, D. L. et al. (2016). “Avoided emissions of a fuel-efficient biomass cookstove dwarf embodied emissions”. In: *Development Engineering* 1, pp. 45–52. ISSN: 23527285. DOI: [10.1016/j.deveng.2016.01.001](https://doi.org/10.1016/j.deveng.2016.01.001). URL: <http://dx.doi.org/10.1016/j.deveng.2016.01.001>.
140. Yuntanwi, Ernestine A.T. et al. (2008). “Laboratory study of the effects of moisture content on heat transfer and combustion efficiency of three biomass cook stoves”. In: *Energy for Sustainable Development* 12.2, pp. 66–77. ISSN: 09730826. DOI: [10.1016/S0973-0826\(08\)60430-5](https://doi.org/10.1016/S0973-0826(08)60430-5). URL: [http://dx.doi.org/10.1016/S0973-0826\(08\)60430-5](http://dx.doi.org/10.1016/S0973-0826(08)60430-5).
141. Zuckerman, N. and N. Lior (2006). *Jet impingement heat transfer: Physics, correlations, and numerical modeling*. Vol. 39. C. Elsevier Masson SAS, pp. 565–631. DOI: [10.1016/S0065-2717\(06\)39006-5](https://doi.org/10.1016/S0065-2717(06)39006-5). URL: [http://dx.doi.org/10.1016/S0065-2717\(06\)39006-5](http://dx.doi.org/10.1016/S0065-2717(06)39006-5).